DROUGHT AND FLASH FLOODS RISK ASSESSMENT METHODOLOGY

by

Manuel Andrés Díaz Loaiza

Supervisor:

Prof. Dr. Allen Bateman Pinzón

Co-supervisor:

Dr. Vicente de Medina Iglesias

PhD. Thesis

Technical University of Catalonia – BarcelonaTech (UPC)

Grup D'Investigació en Modelització Integral de Conques i Transport de Sediments

Funded by:

Barcelona

July 2015

Abstract

Floods and Drought are some of the most catastrophic natural disasters for humanity. Risk management science has grown in the last years and allows us to assess the risk and the possible benefits if some specific measures are implemented (e.g. mitigation / adaptation measures). A methodology for Non-Structural Measures (NSM) implementation in risk assessment has been developed for flood event management. Likewise, an uncertainty analysis has been done in order to identify the variation of the possible results in the risk assessment. An analysis has been done based on the Expected Annual Damage (EAD) to determine the optimal return period of design of a structural measure. A new indicator has been proposed based on this analysis: The Optimal Expected Annual Damage indicator (OEAD).

For drought events, a new methodology has been developed in order to relate quantitative potential economic losses for rainfed crops with "*Meteorological Drought"* assessed through the Self Calibrated Palmer Drought Severity Index (SC-PDSI). The vulnerability of crops is assessed considering two seasons: the sowing and the harvesting seasons which could be the representative time interval for the phenological development of crops. Several statistical distribution functions have been implemented in order to find related return periods for phenological time intervals of the different types of crops (Sowing and Harvesting). The calibration of the model is done through statistical data information of crop production and crop area in the case study area.

Preface

The present document includes the results of 2 European projects related with Flood and Drought risk assessment: the SUFRI project funded by the CRUE Era-Net and developed from 2009 to 2011; and MEDDMAN project funded by the European Union Framework Package 6 (FP6), started in 2006 and finished during 2010. The gathered interesting results are presented in Chapters 3, 4 and 5 which have already the form of journal article. Chapters 3 and 4 have been submitted to peer reviews journal about flood risk assessment and reason why some pages are somehow shared. Chapter 5 will intend to be submitted soon to the Water Resources Research journal.

Acknowledgements

Once I reach this point I was considering make a short acknowledgments, but thinking in the amount of time I used to develop my thesis and also in the fact that one of the lessons learned is precisely that "there is always time for everything", I will try to remember all the people who have most influenced me and helped over the years. I hope no one is left out of this list and if so, do not think I do not be grateful.

First, I would like to say thanks to my family: my mother, my father, my brother, Beppe and Diana. I am really thankful to life for being sharing all these years with them, and especially because they are an example of persistence and perseverance. Family, just only say thank you for everything you have gave me. I love you very much.

In the UPC, at first, I have to say thank you to my supervisor Allen Bateman, which served me as a guide during these years of Doctorate. Thanks for your help and for gave me lessons of life. To my co-supervisor, Vicente Medina, that was always at the right moment to give me a smile, and for teaching me the most important thing in life: “friends”.

In the research group GITS, many people had passed, but the truth is that I have really good memories from all of them. GITS, thank you for the countless bbq. To my office mates: Francesco, Alberto, Anna, Ana, Cristina and Khaled, thank you for the support and lunch together. In the department of DEHMA: Anais, Belén, Rodrigo, Hans, Gonzalo, Jackson, Xavi, Sergi and Francisco, thank you. In the UPC: Felipe, Olver, Jordi, Romeo, Carlos, Mabel,

Mauricio Tapias and Guillaume and professors: Daniel Sempere, Juan Pedro Martin Vide and Marcel Hurlimann, thank you very much.

To the Erasmus students, Daniela, Arthur, Maartin, Guillaume, Phillip, Alex, Clara, Manu, Shibone, Daniel Walsh (thanks for correcting my bad English), Iona, Diego Zambrano, Malgo, Diego Gomez, Gabriel, Judy, Tom, and Nikeh Booister (for supporting me and likewise help with English).

To Barcelona, and the incredible people I had meet with unbelievable experiences. Special thanks to: Daniel, Kat Kleim, Herman, Ingrid, Chus, Daniela, José, Ruben, Aisha, Jean Paul, Elitza, Sandra, Azucena, Pamela, Felipe (Pipe), Olver, Marcela, Tatiana Ramirez, my second brother Leonardo Guayara, Ruth, Alessandra, Adriana Barba, Mireia, Laura (thanks for your support and free psychiatry sessions), Isma, Parra, Ivan and Diego (ARENA combo). To family de Pourcq: Luc, Jacqueline, Jan, Karel and especially to Katrien, for all these years of friendship (the surrealistic conversation and jokes made me more tolerable this long way in the Phd).

In Colombia, to all my family and uncles thank you very much for the support and especially to the memory of my grandparents (Miguel, Mercedes and Camilo) and to my grandmother Abigail. To my neighborhood and university friends: Contento, Pedrito (and Galindo family), Andres, Christian, Alejandro, Cokin, Rene, Paulito. Paola Castaño, Ana Bothia, Maria Claudia, Angie, Erika, Elvis, don Ignacio (Q.D.E.P.), don José (Q.D.E.P.), Andres Velasco, Julio Sabogal, Munevar, Chamo, Javier, Marlio, Xavier and Diego Garzón thank you very much.

Table of Contents

List of Figures

List of Tables

List of Symbols

A_b Afferent area of the basin (km^2)

AWC Available water capacity

b Channel width (m)

b_p Width of the pedestrian foot

C_d Drag coefficient of the pedestrian foot.

dy Layer elevation increment (m)

E Exposure is the quantification of the people and elements at risk from the total available in the basin (flood events) and area of a particular crop exposed to drought (in drought events).

EAD Expected Annual damage (M€/year)

ET Evapotranspiration (mm or inches)

$f_N(x)$ Probability density function

F_N Cumulative distribution function

FTR Fatality rate (%)

g Earth Gravitational constant (9.81 m/s^2)

h Hydraulic flow depth (m)

H Hazard is the intensity of the event measured by the velocity (v) in m/s and depth (h) in m for flood risk assessment, and mm or inches in drought risk assessment.

I Rainfall intensity (mm/h)

L Losses (mm or inches)

m The mass of the consider layer (kg)

n Manning coefficient

n_m Number of molecules per unit volume $n_m = \frac{N_m}{V_l}$ (n/m³)

N_m Number of molecules in the layer

N Number of victims for particular exceedance probability

N_i Number of inhabitants in the flooded area for a particular return period

ρ Water density (kg/m³)

P Layer pressure (N/m²)

PET Potential evapotranspiration (mm or inches)

PL Potential losses (mm or inches)

PR Potential recharge (mm or inches)

PRO Potential runoff (mm or inches)

$Q_i^{c|j}$ Extrapolated discharge flow due to the j correlated station

Q_i^c Discharge flow in the station to complete in the i time position

Q_i^j Discharge flow from the station, which has the j higher correlation position value in the i time position

R Total Risk, usually expressed in M€/year or number of casualties n/year.

R_c Recharge (mm or inches)

RO Runoff (mm or inches)

Ss Soil moisture in the superficial layer

Su Soil moisture in the superficial layer

S	Channel slope (m/m)
T	Temperature (C^o or F^o)
μ	Friction coefficient of the pedestrian floor
v	Flow velocity (m/s).
V	Vulnerability is the susceptibility of the infrastructures, inhabitants (flood events) or crops (drought events) to be affected by the particular hazard.
V_l	The layer volume (m^3)
V_{ped}	Submerge foot volume of the pedestrian (m^3)
W	Pedestrian weight in the foot (N)
W_{equiv}	Pedestrian submerged weight in the foot. (N)
x	Consequences either quantified in numbers of victims (n) or euros (€)

List of Abbreviations

ACA	Catalan Water Agency (Agencia Catalana del Agua)
CECAT	Catalonia Coordination Operative Center
CECOPAL	Municipal Coordination Center
DCM	Disaster Control Management
EAFD	Expected Annual Flood Damage
EHIMI	Development of Hydro Meteorological tool for Catalonia
EWS	Early Warning System
EDA	Exploratory Data Analysis
FHM	Flood hazard maps
FLOODSite	Integrated Flood Risk Analysis and Management project webpage
FRM	Flood risk maps
IDESCAT	Statistic Institute of Catalonia
IMPRINTS	IMproving Preparedness and RIsk management for flash floods and debriS flow events http://www.imprints-fp7.eu/
INNUNCAT	Flooding areas and risk analysis of Catalonia (Plan Especial de Emergencias por Inundaciones de Cataluña) http://www.gencat.cat/
MAP or PAM	Municipal action plan (Plan de Acción Municipal)
METEOCAT	Meteorologic Catalonia Service (Servei Meteorologic de Catalunya)
NOAA	National Oceanic and Atmospheric Administration's
NSM	Non-structural measures
RISKMAP	Improving Flood Risk Maps as a Means to Foster Public Participation and Raising Flood Risk Awareness: Toward Flood Resilient Communities. http://risk-map.org/

RMP	Risk Management Planning
PATRICOVA	Action plan in case of flood emergencies in Valencia – Spain.
SAHBE	Hydrometeorological Warning System for the Besós basin.
SM	Structural Measures
SUFRI	Sustainable Strategies of Urban Flood Risk Management with Non–Structural Measures to cope with the residual risk. http://www.sufri.tugraz.at/
USACE	U. S. Army Corps of Engineers
RC	Rainfed Crops

Introduction

Flood and drought are perhaps some of the most damaging hydrometeorological disasters for humans. The newest research approaches are focused on the risk assessment in order to compare possible measures to implement, and prioritize the resources in the decision making process.

In the present document the results of pluvial flood risk assessment are described. These results include structural and non-structural measures based on a developed methodology for Arenys de Munt basin, which belongs to the region of Catalonia in Spain. To include non-structural measures in risk assessment, mitigation coefficients where built in the methodology, and is further described in chapter 3. Also, steps for the optimization of their possible implementation are defined. This research shows that potential economic losses decrease with the construction of structural measures from approximately 6.6 M€ to 3 M€ (box culvert of €14Million) and, in combination with the implementation of non-structural measures, this can even decrease to 0.7 M€ if the non-structural measures are implemented (for 500 year return period event). Related potential casualties decrease from approximately 11 casualties to 8 and even as low as 2 casualties respectively if non-structural measures are implemented (for 500 year return period). This, demonstrates that non-structural measures are a way to follow in flood risk mitigation. Finally, the uncertainty in risk assessment related to hydraulics and hydrology is investigated, which brings about a new indicator: the OEAD (Optimal Expected Annual Damage).

Related to drought, few methodologies for quantitative drought risk assessment are available. In the present document a new methodology for rainfed crops is proposed. In the same, a method for hazard (through the Palmer index) and vulnerability assessment was developed. The susceptibility of a particular crop due to a drought event was linked with a classification of the

phenological stages according to two seasons: sowing and harvesting season. The case study was focused on the Llobregat basin, in which both, hydrometeorological and crop statistics data series were available. Results illustrate that the Llobregat basin has suffered at least 2 important periods of drought (2000/2001 and 2005/2006) during the length of the considered 16 year crop production record statistics. These periods of drought caused potential economic losses of approximately 40.13 M€ and 55.84 M€ in the geopolitical subdivision called "Comarcas" of the Llobregat basin. The related methodology developed in Chapter 5, demonstrates coherence in the detection of “important” drought events, and in the quantification of individual potential losses per crop type, which shows that crops, like olives (classified in category woody crop type) are more resistant to drought than vegetables (tomato, lettuce chard etc.). Finally, in addition to the presented methodology the potential losses of crop efficiency curves are proposed, as indicators for agricultural drought risk assessment.

Motivation

In the last 30 years Disaster Control Management (DCM) science has been growing strongly due to the requirement of the stakeholders to reduce and mitigate the consequences of risk coming from different natural and anthropogenic hazards like hurricanes, tornadoes, floods, earthquakes, tsunamis, volcanic eruptions, landslides, earthquakes, droughts, fires, chemical hazards and terrorism (Pearce, 2003; Quarantelli, 1988) and most recently (Jobstl et al., 2011; Luna, 2009). Droughts cause millions of euros in annual damages and eventually human losses, as a consequence of direct causes such as the losses of crop production due to severe drought events, or indirect causes, such as the increasing of mortality rates due to the lack of precipitation. Several studies have shown that droughts are one of the most costly natural risks to humanity averaging 6 to 8 billion dollars of annual damages (Stambaugh et al., 2011; Wilhite, 2000), followed by floods with 1 to 5 billion dollars (NOAA, 2014). For that reason DCM science has emerged in order to mitigate these risks. In the case of flood events the DCM (named in this topic *flood risk assessment*) is much more developed than in drought events, but less than in other cases like earthquakes or fires.

Concerning flood risk management evolution (the transposition of DCM in floods), it was possible due to the development in topics like properties and people vulnerability (Beven, 2011; Faber, 2006). Leading countries for flood risk management like the United States through the Federal Emergency Management Agency (FEMA) or England through the Department for Environment, Food and Rural Affairs and Climate Impacts Programme, delimit hazard and risk zones through hazard and risk maps. In Europe, the European Flood Directive of 2007 (European Parliament, 2007) established some deadlines for hazard and risk delimitation, and risk

management plans. In order to apply Structural and Non-Structural Measures (SM and NSM) more research is needed.

In the case of droughts, the risk assessment using quantitative risk models is less common than in flood events. Few models exist for the assessment of drought risk (Haiganoush and Westerling, 2007; Vicente-Serrano et al., 2006) and even today unified drought estimators (known as drought indices) to estimate the occurrence and intensity of a drought event are not fully developed (Tallaksen and Van Lanen, 2004). Depending on the geographical situation, different thresholds are used as indexes. For this reason, different locations are not quantitatively comparable. This lack of drought criteria unification makes the drought risk management science more complicated than the flood risk assessment. In fact an extensive review of the bibliography revealed that still nowadays different research groups investigate the development of new drought indexes in order to define and quantify the intensity and occurrence of drought events (Ganatsas et al., 2011; Vicente-Serrano et al., 2010).

Two European research projects were tackled to cover these research topics about risk management in the GITS (Sediment Transport Research Group) as well as to have enough economical resources for different research activities. The first project subject was: "*Integrated water resources management, development and confrontation of common and transnational methodologies against the drought phenomenon within the MEDOCC region*", or MEDDMAN. It was sponsored by the European Community through the FP6 Framework initiative - INTERREG. The scope of this project was to assess, monitor, and manage drought events. The second was the SUFRI project (Sustainable strategies of Urban Flood RIsk management with

non - structural measures to cope with the residual risk). The objective was the assessment and the mitigation of the risk associated with flash-flood events. In this project, a methodology was developed for the optimal implementation of non-structural measures to reduce residual risk.

The feedback between both projects lead to the development of the drought risk assessment methodology for meteorological drought using the risk science framework, which has been applied to floods since the 80’s. The aim of this task was to obtain quantitative results of risk for drought hazard in order to apply cost benefit analysis or any other quantitative technique.

Objectives

The general scope of the thesis is the DCM. In the case of floods, the target is to improve and complete what already exists in terms of non–structural measures risk mitigation. In the case of droughts, the target is to develop a methodology analogous to the one applied for floods. With this premises, this document will intend to address the following three particular challenges.

1) Develop a methodology to optimize flood risk mitigation using non-structural measures

Exhaustive SM investments are usually made by stakeholders in order to mitigate flood risk. Constructions like retention structures (arch dams, gravity dams, stormwater ponds etc.), protection structures (dikes, vertical walls, storm-surge barriers etc.) or drainage systems (combined systems, separated systems) are frequently applied (Escuder et al., 2010). It is commonly accepted that floods can never be absolutely prevented or predicted, so there will always remain a "***Residual Risk"***, even if structural measures are exhaustively applied (Faber, 2006). Thus, the NSM implementation is the subsequent step to follow. It has been demonstrated over time, that this kind of measures is cheaper and easily implemented, but the residual risk mitigation has not yet been explored. The first objective of this thesis is to develop a methodology to compare and optimize the effect of NSM on the residual risk and to attempt to minimize it.

2) Analyse the influence of uncertainty in a flood risk assessment

There are two main uncertainty sources. The first one comes from the variable measurement process and the second from the mathematical processing of the data. In nature, only a few variables can be accurately measured. Also, some of them are indirectly assessed through other

variables like radar rainfalls, which are obtained using the reflectivity of the drops of an electromagnetic wave produced from the radar (Sempere Torres et al., 2003).

The dangerous events are usually related to extreme events. Therefore, a statistical process is required to assess them. For this process, some data fittings are performed and confidence intervals emerge from these fittings in a natural form. It is recognized that the most accurate way to address this problem is to refuse a single accurate variable and quantify the uncertainty in terms of confidence intervals. Nowadays, uncertainty analyses have been promoted in methodologies like GLUE (Beven and Binley, 1992) or models like FIA (USACE U.S. army corps).

The second objective of this thesis is to quantify and propagate variable uncertainties until the final risk value is obtained and their corresponding uncertainty.

3) Develop a drought risk assessment methodology to link the potential economic losses in crops due to meteorological drought events

The previous objectives of the thesis could be considered improvements on the existing methodologies for flood events, but they could not be performed in drought risk assessment: it still lacks the basic risk science methodologies to obtain a quantitative value of risk. The objective focuses on the adaptation of quantitative techniques of other risks into the drought framework, relating *"Meteorological Drought"* with possible economic losses in crops.

Document Structure

The present thesis contains in Chapter 1 the state-of-the-art in risk management with a review of the flood and drought risk assessment theory. The tools used in risk analysis are also displayed in Chapter 1.

Chapter 2 provides a description of the cases of study: the Arenys de Munt basin in the pluvial residual risk assessment and the Llobregat basin in the drought risk assessment study, both located in Catalonia, Spain. Also a description and the data quality control have been completed in this chapter in order to minimize the errors coming from poor quality data.

Subsequently, Chapter 3 revels the methodology developed for the optimization of non-structural measures in pluvial flooding events in which the steps to follow for the inclusion of the NSM in the risk assessment are defined.

Chapter 4 analyses the influence of the uncertainty over the pluvial risk assessment results and the benefits of the NSM implementation.

Chapter 5 details the drought risk assessment model proposed to assess the potential economic losses in crops due to drought events and correlating the Palmer indexes with the losses in the crop production.

Finally, Chapter 6 presents the conclusions and envisaged future work related to the topics of this present thesis.

Chapter 1: State-of-the-art on risk management

Flood and drought risk management belongs to the DCM science. DCM is a discipline that has grown strongly over the last 30 years, as a result of the frequent events that occurred due to different natural hazards like tornados, drought or floods (IAEM, 2007; Luna, 2009). Four components are universally identified in DCM: prevention, preparedness, recovery and reaction (see Figure 1.1).

Figure 1.1 Disaster Control Management component scheme

Flood risk management applies these concepts to the flood phenomenon. For instance, the rainfall forecast and runoff, through hydraulic models, can be fitted into the prevention component. The mobilization of sandbags as flood barriers can correspond to the reaction component.

1.1 Risk definition and tools for risk assessment

Several risk definitions have been made during the last years, which derive from the application areas in which the risk assessment science has been applied (computational, medical, social science etc.). Probably, the most suitable definitions for the present thesis are those relating a probability of occurrence value with the possible consequence (West and Council, 2013). In Jonkman (2007) the risk is defined as *"a function of the probabilities and consequences of a set of undesired events"*. Definitions also vary according to the type of risk assessment which has been conducted. Particularly, in the present chapter, a brief description about the risk assessment tools and classification is summarized.

It is commonly recognized that the risk can be assessed through the intensity of a related natural hazard (H) times the susceptibility of the infrastructures or inhabitants to be affected by this phenomenon (V). It is logical to consider that the risk will increase if more infrastructures or inhabitants are present in the affected area. Here is where the terms people at risk and element at risk appear (Jonkman, 2007; Kron, 2002). This variable is represented by the exposure (E). The final equation (1.1), in a very simple way, according to several authors like FLOODSite, is:

$$R = H \cdot V \cdot E \tag{1.1}$$

In order to explain the related risk units, before hand it is required to denote that they directly depend on the type of analysed phenomenon (drought, floods etc.), it means, the consequence that one is seeking to assess. In flood analyses, the consequences analysed are usually potential human casualties and potential economic losses. More variables could be analysed in relation to flood events, for instance the environmental impacts or the increase/decrease of infectious viral agents in flood events. At this point, the convenience of the risk management

science is evident, as it tries to show (qualitative) and assess (quantitative) the benefits of implementing some measures to mitigate the risk (Coleman and Marks, 1999; Rot, 2008). The problem lies in the fact that some consequence variables are difficult to assess/fix. That is why for flood events, studies are usually developed only considering these two variables. In drought scenarios, the behaviour consequences are even less fixed, this is the reason why few risk assessment models have been developed for the drought phenomenon.

The hazard units for flooding risk assessment are the depth (y) and velocity (v) related to the discharge flow Q (m³/s) with the linked return period (years). The vulnerability units for the potential economical damage are the percentage of damage (%) expressed in euros per area (€/m² of damaged structures in the flooded area), and for potential casualties, the fatality rate (FTR) which multiplying by the number of inhabitants exposed to risk (N_i) gives the potential casualties for each return period ($FTR * N_i = N$). The exposure for potential economical damages is the equivalent area in m² of the elements at risk and for societal risk the people at risk (numbers of inhabitants present in the flooded area). In Chapter 3 the risk assessment procedure in case of flood events is better explained. The hazard unit for meteorological drought risk assessment is the rainfall deficit defined in the Palmer drought index (mm or inches) related to the return period of this particular event (years). The drought vulnerability unit is the economical losses in €/m² of crop production in the affected area. Finally, the exposure is the crop area in m². Like in the flooding assessment case, the developed drought methodology attempts to follow a coherent and unified procedure to assess the risk. In this latter context, it is worth mentioning the great effort that means having the equation (1.1) dimensionally coherence in order to delimit the drought hazard and drought vulnerability in coherent units.

Nowadays different programs/models are available for risk assessment analysis for different hazards like: chemicals, tornados, economical, earthquakes, fires, debris flows, terrorism and flood events among others. Depending on the considered (natural or anthropogenic) hazard, the risk models are more or less developed. Likewise, the principal differences between them lie in the way the risk is assessed (West and Council, 2013).

The possible tools used for risk assessment induce two kinds of models which estimate the risk in terms of numerical (comparable) values, called quantitative models, and those which bring a classification of the risk through some classes or levels called qualitative models (Coleman and Marks, 1999; Rot, 2008). These models could also be subdivided in partial or complete models (Jobstl et al., 2011). For drought events, few models are available to relate the drought hazard to their consequences. For flood events, models are a bit more advanced than for drought models, but less advanced in comparison to models developed for nuclear and aeronautical industries (Jonkman, 2007). Remarkable computational models like: HEC-FIA, FRMRC, CAPRA, EPA PMF 1.1, Ipresas or HAZUS are presented on the internet to evaluate different sources of risk in different ways (qualitative or quantitative). Qualitative risk assessment could help the people in charge of risk policy, decision making-process and measures to implement (called managers in action forces). Qualitative methods have been the most applied and have contributed to identify and prioritize which research topics are needed (Rot, 2008).

Table 1.1 Advantages and disadvantages of qualitative vs quantitative methods

Risk Analysis	Advantages	Disadvantages
Qualitative	• Allow to identify the areas of greater risk without big effort and time • Analysis is relatively easy and cheap, and requires not much information in respect to the Quantitative analysis • People who are not experts in flood risk assessment could be more easily involved • Faster to implement than the quantitative analysis	• Does not relate the events probabilities • Cost-benefit analysis is more difficult. • Difficult to justify investments through the result with different measures • Results depend directly from the risk assessment team who is developing the study (their knowledge)
Quantitative	• Allows for definition of consequences (economical damage and casualties) in quantitative way, which facilitate the costs benefits analysis • The results are comparable between different scales • The results tend to be more accurate	• Results are subjected to uncertainty, which leads to believe in a false knowledge of the possible consequences. • Results can be confusing • Analysis conducted with a quantitative scheme can be more expensive and demanding greater experience and tools • Calculation can be complex and time expensive • Results require more information than the qualitative analysis

Several factors could contribute to skew the decision in choosing a qualitative analysis versus a quantitative analysis. Evidently, a quantitative analysis is usually preferred over a qualitative analysis, but if there is no data available a quantitative risk assessment will not be possible. Similarly, many variables like data series, economical resources, employees or time could not permit a complete quantitative analysis. Nevertheless, it would not necessary mean that a quantitative analysis could not be made (Rot, 2008). The advantages and disadvantages of quantitative and qualitative analyses are recapitulated in Table 1.1.

1.1.1 Expected Annual Damage

One estimator of the impact for a particular flood event with a related intensity is called the Expected Annual Damage (Arnell, 1989; Jonkman et al., 2003). This parameter gives a value for potential losses (1.2), and is a direct measure of risk (Feyen et al., 2012). In literature,

some procedures are available to assess this value, and in the present document this will be used in Chapter 4 as per Arnell (1989).

$$E_N(x) = EAD = \int_0^{\infty} f_N(x)\, x\, dx \tag{1.2}$$

Where $f_N(x)$ is the probability density function of the potential damages x. The units for EAD are M€/year.

1.1.2 Uncertainty Analysis

Uncertainty is always present in physical problems due to the impossibility of total and complete knowledge in a particular topic. In risk assessment analysis it could be critical especially when high consequences assessment are made like in global climate change or nuclear reactor failure analysis (Paté-Cornell, 1996), due to the fact that consequences can vary considerably and public sensitivity to the outcomes is really high.

It is important to distinguish the difference between uncertainty and variability, also called "randomness". Generally a random variable requires some very restrictive definition. A random variable, or randomness, refers to the behaviour of the variable itself, in other words, the chaotic behaviour. Uncertainty refers to the "places" or variables by which this behaviour is chaotic. To clarify, imagine a width distribution of a screw in a particular screw machine/factory. The width behaviour is "randomness", and the uncertainty of that behaviour rise in different variables like the impossibility of an accurate width measurement, the impossibility of the machine in making a standard/unique width screw, the possible differences in the material density which could lead to different width screw sizes, etc.. With the above example, it makes out that uncertainty could be parameterized, defining all individual variables uncertainty.

1.2 Floods risk management

Floods cause millions of economic losses and casualties. For example, in 2007 *"There were 200 major floods worldwide, over 180 million people affected. The human cost of all the floods in 2007 was more than 8,000 deaths and over $ 23 billion worth of damage. But even against that dramatic back-drop, the floods that devastated England last year ranked as the most costly flood in the world in 2007"* (Pitt, 2008). In the last decades the main scientific efforts in this area have been fixed to improve the numerical models for the rainfall forecast and propagation (runoff). These efforts yielded significant progress thanks, in part, to the recent computational developments. However, due to various reasons, including the uncertainty (hydrological, hydraulic, statistical, etc.), a complete prediction of the flood phenomenon is still utopic. Since the beginning of this new millennium the major studies related to floods have been directed towards the management and flood risks assessment science.

1.2.1 Floods triggering factors

Floods are produced by different interactions between human and natural variables. Initially, one may think that the unusual precipitation is the only cause of floods but, although it is the main one, there are other causes provoking them (Jobstl et al., 2011; Pender and Faulkner, 2011). Some of the most important causes are described below:

- Unusual precipitation: High rainfall intensity may produce high runoff in the main streams. The discharge flow is proportional to the amount of the fallen precipitation.
- Geometric and river characteristics: A change in the river section, location or longitudinal profile could induce flooding risk in the zone. This kind of floods are

commonly identified when a river course is relocated or when a structure is constructed over the river. They are mostly produced by anthropogenic actions.

- Human settlement: Risk is directly related with the human behaviour. Nowadays, due to the densification of the cities and, generally, of the territory, the new cities development areas are closer or in the river flood plains; it means, in hazardous zones, which will induce more people and elements at risk subjected to floods.
- Maritime floods: Extreme sea events could induce floods over coastal areas. This is related to hurricanes. Furthermore, if the urban areas are located below the sea level, and the structures are not able to contain the inlet sea water, the flood consequences could be very significant.
- Snow melting: Sudden snow melting could produce high discharge flow as in the Armero natural disaster.
- Structure failure/collapse: The typical example is obtained in the dam break case, were a dam failure could produce huge discharge flow over the river.
- Climate change: This cause has been referenced with a high probability, for human reasons. Leaving aside the discussion about the anthropogenic origin, global warming has left evidences (Min et al., 2011) over the hydrological cycle that extreme events are becoming intense and frequent (intense floods, droughts, tornados etc.).

Nowadays, SM have been extensively applied and investigated and that is why the new actions are redirected to the NSM implementation. There is a lack of knowledge surrounding NSM risk mitigation. However, stakeholders are lately implementing NSM like Early Warning Systems or Insurance aids.

1.2.2 Control measures

The DCM defines 4 components to apply in order to produce risk mitigation. These components (Prevention, Preparedness, Reaction and Recovery) fix activities to all the entities who act in case of emergency events. In case of flood emergencies, these activities (or measures) to mitigate risk are subdivided in two types: Structural and Non Structural measures (SM and NSM respectively). Jobstl et al. (2011) describe the SM as the amount of measures involving tangible physical resources (constructed infrastructures), and the NSM as the ones related to activities like risk communication, awareness, entity coordination, knowledge development, public commitment and participation (Andjelkovic, 2001). The latter are one important part of the present thesis and will be discussed in Chapter 3.

1.2.2.1 Structural Measures (SM)

SM are all measures that involve construction of civil works to protect areas against floods. Structures vary depending on the particular situation, but could generally be classified according to Figure 1.2 (Jobstl et al., 2011):

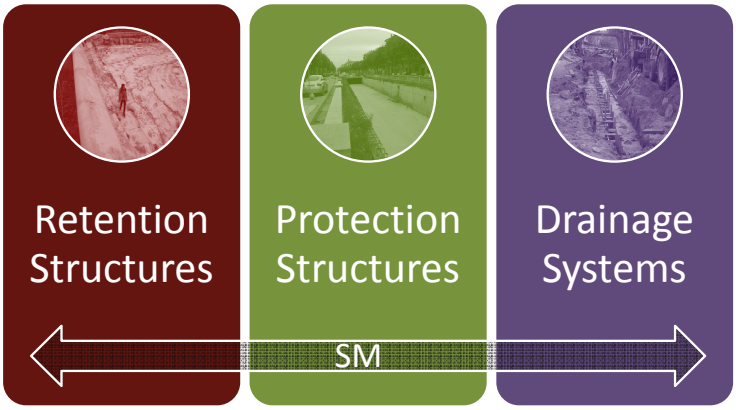

Figure 1.2 Structural Measures Classification

Retention structures are constructed to retain flood water in order to diminish downstream flooding. The most common structures are dams and ponds upstream of the areas being protected (Jobstl et al., 2011). These structures accomplish different tasks like hydropower generation, water supply, sport uses and shipping.

Figure 1.3 Retention Structures

Retention structures are mainly composed of dams. Dams mitigate flood risk because they reduce peak flows downstream during an extreme event (Jobstl et al., 2011; Thampapillai and Musgrave, 1985). However, dams are not always effective because they are designed for a specific discharge flow return period and if this event is exceeded, the dam could break or progressively lose its effectiveness.

Protection structures: With these structures the areas are directly protected from possible entry of water, preventing the flooding of urbanized areas. Structures like embankment, walls, storm-surge barriers, dune construction and dikes are designed to this purpose. Also, some structures modifications like the waterproof of the area, the flood adapting uses or the fortification of the basement of the adjacent structures could reduce risk (Thampapillai and

Musgrave, 1985). Over the river catchment some changes can be done in order to diminish the risk, like diminishing the river bed roughness, new channelling, modifying the catchment characteristics or the river width in order to decrease the water depth, change the river course, promote the infiltration process or allow more “room for the river”. In Figure 1.4, measures that are included in the protection structures classifications are displayed (Jobstl et al., 2011).

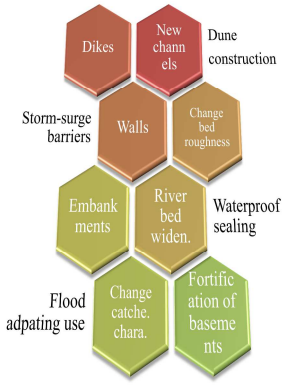

Figure 1.4 Protection Structures

Embankments, walls, storm-surge barriers, dune construction and dikes measures are vertical structures. Their main function is to avoid the overtopping and the flooding of land from the flood source (Thampapillai and Musgrave, 1985). The waterproof, flood adapting uses and fortification of the basement, is a kind of improvement to the existing structures applied to mitigate the risk. The river catchment modifications, like the change of the riverbed roughness or river width (like in channelization’s), involve actions over the river morphology in order to increase its drainage capacity, reducing flood consequences. The depth and velocity of the discharge flow are proportional to the flow resistance (Manning coefficient). Thus, changes in the bed roughness will lead to changes in the depth and velocity of the flow. The river widening increases the drainage capacity because it increases the transversal area of

the river. New channel works could divert the river from the areas attempted to protect. Finally, changes in the slopes of the hills like the construction of terraces will increase the infiltration process and delay the time of concentration of the river with the consequent risk mitigation.

Drainage systems: In urban areas, these measures are the most broadly used. They prevent the surface runoff managing the flood's water through sub-ground structures (Jobstl et al., 2011). The underground retention structures, infiltration trenches, combined and separated drainage system belong to this category (Figure 1.5).

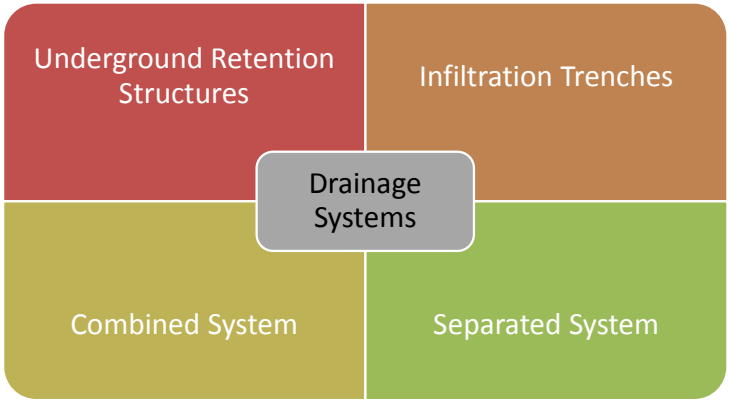

Figure 1.5 Drainage Systems Classification

Megastructures are designed to diminish the discharge flow peak of possible floods and tsunamis events. The difference between the combined and the separate drainage system lies in the management of the domestic foul water, because in the separate system the rainfall water discharge and the domestic water discharge are collected separately. Infiltration trenches, as their name suggests, aim to improve the infiltration process within the area being protected.

1.2.2.2 Non-Structural Measures (NSM)

The Non-structural Measures classification usually involves activities to improve or generate awareness or increase the public commitment and resilience in case of flood events (Andjelkovic, 2001). Generally, they are known as measures that do not associate concrete or civil works. Previously, the Structural Measures merely focused on decreasing the flood hazard of the affected areas, whereas nowadays, the NSM focuses on reducing the population's vulnerability.

The SUFRI project has subdivided the NSM into six general groups (Jobstl et al., 2011):

1. **Urban planning and policies:** in Spain, they correspond to the municipal and regional Action Plan, which are the adaptation of the Risk Management plans imposed by the (EU) Flood Directive.
2. **Flood forecasting:** mainly composed of the Early Warning System (Nowcasting, Forecasting and Ensemble models)
3. **Communication:** this activity includes the communications media (fax, internet etc.).
4. **Mobilization:** usually implemented by the rescue corps like the firefighters, police or civil protection. Usually, it is understood as the resources like medicines, food or sand bags needed to cope with the emergency.
5. **Coordination and operating practices (disaster exercises):** This activity aims to promote harmonization and training of the actors involved in the emergencies scenarios (Entities and population)
6. **Insurance and aids mechanisms:** The insurance acquisitions have a vital importance in the economic recovery. Insurances implementation, aids and resources coming from charity can reduce the expenses of the damage that are not easily quantifiable as

the cultural damage. Some authors do not consider this measure as a NSM because it does not prevent damages from the event (Jobstl et al., 2011). Instead, once the event has happened, the zones covered by insurance can get back part of the economic damage.

Urban planning and policies

Nowadays, at city's development includes a strategic urban planning and policies. This is a result of the heavy growth that took place in cities during the last century, which has induced uncontrolled evolution of the urbanized areas resulting in some buildings and infrastructures occupying potential flood areas. Thus, appropriate urban planning will diminish risk avoiding the urbanization over the hazard-prone areas, or building measures to mitigate the risk. The EU Flood Directive (2007) forces the development of Flood Risk Management plans, which could be considered as an "Urban Planning and Policies" non-structural measure. In these plans, hazard identification and risk assessment are mandatory, and this is the essence of Urban Planning; the "Planning".

Flood Forecasting

One skill of an engineer is to predict behaviours from an analysed phenomenon. This issue is usually known as "Forecasting estimation", particularly from a hydrometeorological point of view. It involves using measured data to assess the future state of the variables. In the hydrological cycle, it means knowing the precipitation and flow discharge behaviour over time.

Undoubtedly, if a flood could be accurately predicted, this would lead to a reduction of economical damages and casualties risk, because it would leave enough time to implement measures like communication and mobilization, to mitigate the risk.

Flood forecasting has been divided in two main stages. The first is related to the weather forecasting, where the main scope is to assess the future meteorological state. Once the weather is predicted, the second stage corresponds to characterize the flood event through some hydrological model (Velasco, 2009). It means transforming rainfall to discharge flow in a specific river. All along this process, the uncertainty is always linked and grows as much as all the related variables are unknown. The interval of time during which the variables are predicted is known as the "lead time". This time is crucial to manage measures, because it will leave (or not) enough time of reaction to the action forces. Nowadays, the research focuses on developing an accurate early warning system of 6 hours of lead time, but is still far away from systems of days of "lead time" which are required for some catchments.

Communication

Communication is perhaps one of the most developed characteristics of human beings. It is defined as the activity of "conveying information through the exchange of ideas, feelings, intentions etc." (Gifu et al., 2014). It is the meaningful exchange of information between two or more participants. The Communication of risk is a complex process, which has been investigated over the last years in order to mitigate the flood risk. There are different classifications in the communication process, but in general terms they can be divided into activities that generate awareness and knowledge of the flood phenomenon known as "Prevention" activities, and activities that relate to when a flood event is occurring (Jobstl et al., 2011). The action procedures during a flood event will mitigate risk. Reporting to the population the flood development in the hazard-prone areas could be classified as a "Reaction" DCM activity.

The population can be warned by different sources like:

- Media: television, internet, radio etc.
- Warning systems: speakers or sirens.
- Personal dissemination: by civil protection or social networks.
- Other communication systems: Posters, signs, telephone calls or text messages (see Figure 1.6).

Figure 1.6 At the entrance of Arenys de Munt a traffic sign has been placed to warn the people about floods

Mobilization

Mobilization measures involve direct works and activities to mitigate flood consequences, like evacuation plans, sandbag usage or wooden table's implementation. In the evacuation process different variables are involved. They generally depend on the size, time of reaction, knowledge, resources and entities involved in flood events on the basin. Some papers have shown that not all the shortest paths in an evacuation are the optimum escape routes (Kolen et al., 2008; Mak, 2008). This exemplifies the interconnection of the evacuation variables (Jha et al., 2012). A good evacuation plan needs to define evacuation procedures and all the roles

of each authority and action force in the basin. The efficiency of these plans is usually related to the communication skills and the lead time of the EWS implemented. Barrier mobilization like sandbags (Figure 1.7) or wooden table's implementation, have been identified in the Arenys de Munt case study and are explained in Chapter 3.

Figure 1.7 Valley City neighbourhood use sandbags to create a levee along the Sheyenne River (by Patsy Lynch/FEMA)

Coordination and operation practices

The main goal of coordination and operation practices is to improve the communication skills between different actors involved during flood events. It can occur between entities or between entities and action forces (like firefighters, police corps or population). A proper coordination between the actors will increase the time available for mobilization, will improve the communication between all the involved actors and consequently flood consequences will decrease (Jobstl C. *et al.*, 2011).

Insurances and aids mechanism

The *"Recovery"* component defined in the DCM is decisive in a post-flood resumption and comeback to the initial state before the flood event happened. The insurances help with this

task by redistributing the individual economic risk through different insured people. Also, national governments have responsibilities in the flood recovery, providing economic and material resources. The insurances aid allows for the sharing of responsibilities from national governments to private insurance companies. Therefore, when big disasters happen, countries are not greatly affected from an economic point of view. This is possible because nowadays some insurance companies are big enough to support large risk.

Several countries such as the United States of America or Australia have specific rules and laws for flood insurance purchase. On the FEMA web page, hazard and risk maps can be downloaded. These maps are spatially specified with areas that have higher or lower flood risk. The cost of the flood insurances is given based on these maps and the particular situation of the element at risk.

1.3 Drought risk Management

The definition of drought is quite abstract, and generally the literature shows that there is no single definition of this phenomenon. This is due to the complexity of the hydrological cycle, and the various ways to quantify it. Thus, even today this topic is still a focus of research, particularly concerning the causes of the rainfall, its behaviour on the surface (superficial flow) or underground (subsurface flow), when it returns to its gaseous state (evaporation) or when it is in solid state like in glaciers or at the poles. It is possible to conclude that the processes and the amount of water in the hydrological cycle are assessed using methods that are *"relatively"* accurate (Figure 1.8). If the hydrological processes are separately modelled, successful results are obtained. However, due to the interconnections of the same processes, small errors can be amplified through the different model processes (rainfall, evaporation, percolation etc.) of the hydrologic cycle (Maidment D., 1993), obtaining significant errors at

the end of a numerical simulation. In consequence, the accuracy of the prediction depends on the time window for which the prediction is wanted.

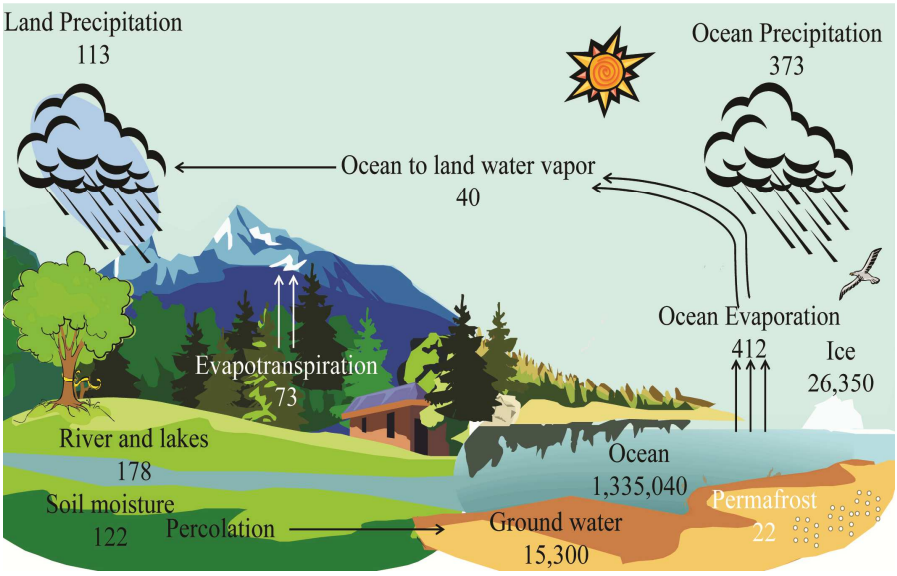

Figure 1.8 Hydrological cycle, units in 10^3 km^3/year modified from Trenberth et al. (2007)

This time window is usually known as lead time, but in drought events the condition developed in a basin to arrive at a deficitary state could be around several weeks even months or years, which means that the drought forecast is even more difficult than the wet event predictions. For this reason, current work focuses more on the assessment of drought disaster consequences than on the predictions itself promoting the idea that the drought risk assessment is the promising field within which to “fight” against drought.

1.3.1 Drought risk origins and classification

As previously mentioned, the processes related to the development of drought events are quite complex but they generally start from the lack of, or high decrease in precipitation. One classification of drought events is based on the characterization of the area or field of knowledge in which the drought affects, likely subdivided into: *"Meteorological Drought"* or deficit of water resources in the atmosphere (Palmer, 1965), *"Hydrological Drought"* or

deficit of water resources in rivers, lakes and aquifers (Hisdal and Tallaksen, 2003), *"Socio – Economic Drought"* or deficit of water resources for economic sustainability (Ballard, 1965), *"Agricultural Drought"* or resource deficit for the normal development of crops (Kerstin S., 2002) and *"Ecological Drought"* or resource deficit for the normal development of the flora and fauna (Tallaksen and Van Lanen, 2004). What they have in common is that they attempt to characterize the affected environment by the lack of water, focusing the analysis on the interaction of the environment with regard to water resources, for example, *"Socio – Economic Drought"* attempts to analyse the economic losses and the social problems caused by lack of water resources.

In conclusion, a drought is defined as a phenomenon that occurs when there is not enough water in any state (surface, subsurface etc.), which could lead to a negative impact on economic, environmental and social development, of the fauna, flora or humans themselves. Because drought starts from a lack of precipitation analysed in the *"Meteorological Drought"*, it is recognized that other types of drought begin with the latter definition. Obviously due to the processes involved in the hydrological cycle, the development of other kinds of drought, such as the *"Hydrological"*, *"Agricultural"* or *"Socio-Economic"* begins with some delay respecting to the *"Meteorological Drought"*, meaning that often, even other types of droughts will not be present when a *"Meteorological Drought"* has started (see Figure 1.9). An example can be a river, which is studied in the *"Hydrological Drought"*. The fact that in the correlated basin it is not raining (meteorological drought) does not imply that the river immediately develops a *"Hydrological Drought"*, due to the base flow of the river, which delays the development of a *"Hydrological Drought"* (Tallaksen and Van Lanen, 2004).

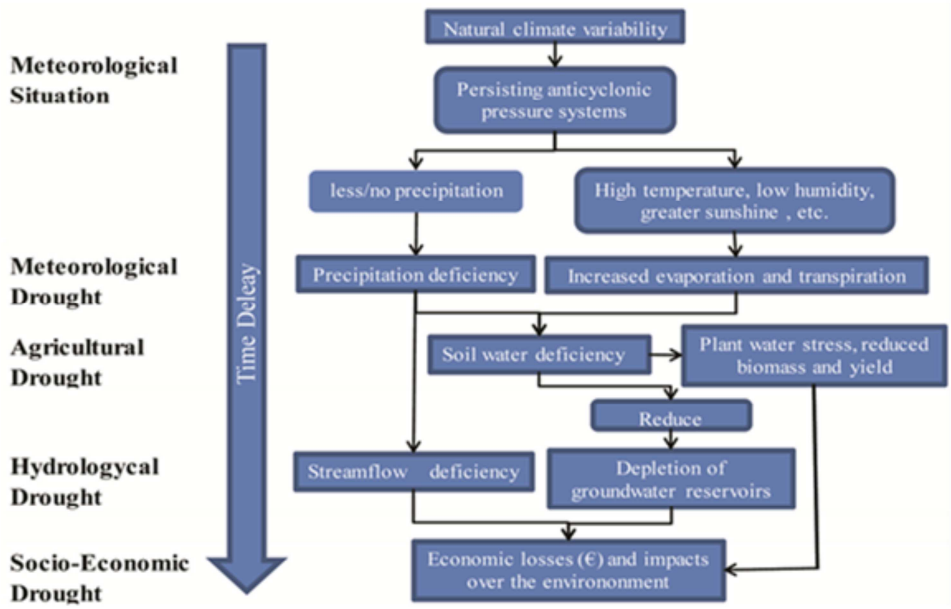

Figure 1.9 Drought types and development adapted from Stahl (2002)

1.3.2 Meteorological drought and affectation over crops and woods

Different studies on agricultural crop production in the world bring disturbing conclusions about the decrease of forest and natural areas with the corresponding increase of crop areas. Additionally, the constant increase of world population causes that the balance of natural resources known as *"self-sustainability"* of the earth to be at critical levels. In (Dixon and Trevor (2009)), it is exposed that $1.5x10^9$ ha of land are used worldwide for crops (world total available arable land is $3.1x10^9$ ha), in which $966x10^6$ ha correspond to developing countries, with an annual increase of around $5x10^6$ ha, with Latin America responsible for 35% (mainly deforestation). If we also superimpose the fact that most of these areas are in places with low rainfall which will diminish even more due to climate change (see Figure 1.10), it results in risk management tools needing to be implemented and optimized. As it will be seen in Chapter 5 a model to correlate the crops losses with the *"Meteorological Drought"* is proposed in this thesis to optimize the available resources.

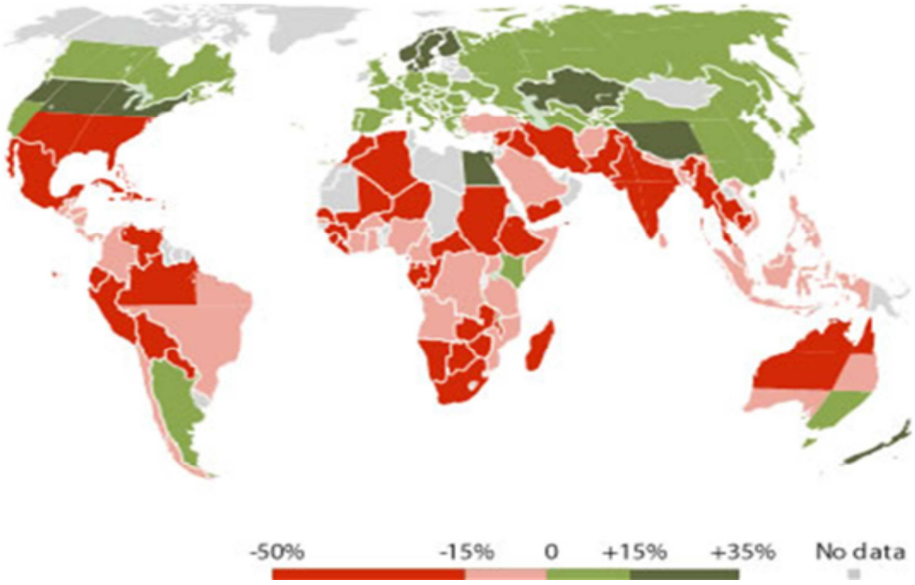

Figure 1.10 Predicted changes in global crop productivity (%) for 2080 from (Climate Communication Center, 2014)

It is important to remember that the land in terms of crops is a finite and difficult to renew resource (due to erosion, nutrient depletion, desertification and contamination). Worldwide soil losses have been assessed in terms of quantity which could be around 1 - 5 x10^7 ha/year (Dixon and Trevor, 2009). Evidences in recent years suggest that extreme events (droughts and floods) are becoming more severe. Heavier rainfall events and longer periods of drought are expected (Min et al., 2011) with their respective increase in soil degradation (Figure 1.11) and a decrease in crops productivity.

The correlation between variables such as drought (section 1.3.3), temperature changes, diseases or disease vectors, fires with respect to mortality of trees in forests or crop plants, is direct (Allen et al., 2010).

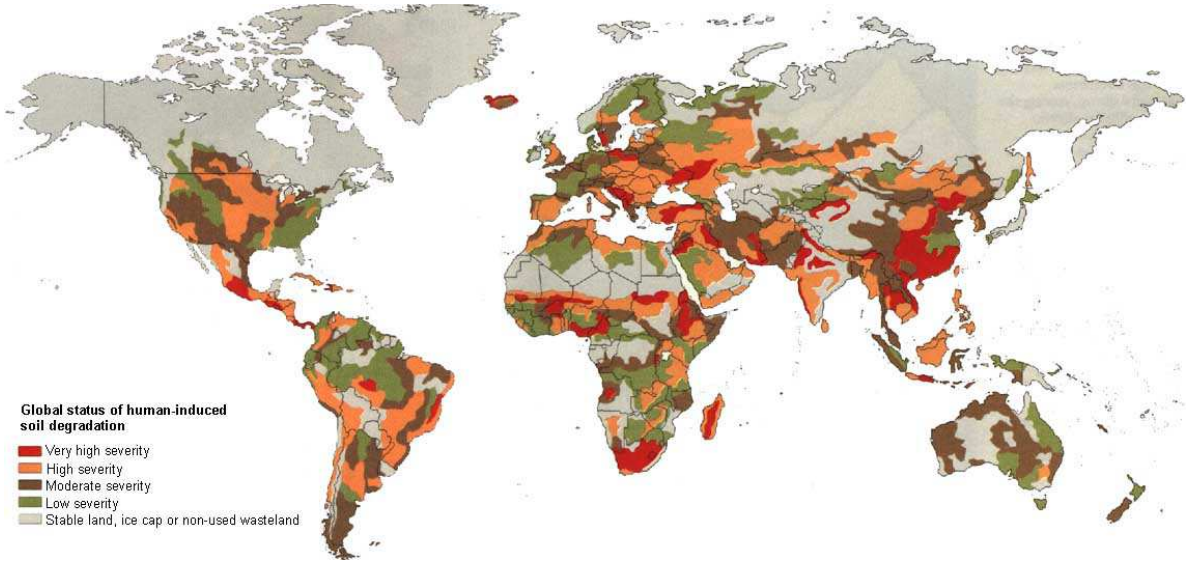

Figure 1.11 Areas of concern for soil degradation (extracted from FAO, 2007)

These variables may affect in a different way the growth and development of vegetation, because to perform the capture of carbon through the photosynthesis process, water is necessary as a conductive medium in the vegetation (Van der Molen et al., 2011). For this reason the *"Meteorological Drought"* is directly related to the growth and development of plants in crops and woods. In the following subchapters, it will be briefly described how the drought affects the phenological development of the plants. There is also a discussion on how fires could make a basin more vulnerable to drought events consequences, in order to understand how the absence/decrease of rainfall (Meteorological Drought) could affect the crop production and vegetation over the woods.

1.3.3 Phenological development affectation due to drought events

It has been extensively studied that hydrometeorological conditions and particularly drought events affect the phenological development of vegetation (Chiatante et al., 2006; Drunasky and Struve, 2005; Hsiao and Acevedo, 1974). Droughts usually affect plants' biomass, their

size and their chemical processes. Consequently, droughts retard plant growth, decrease net photosynthetic rate and increase the number of days in which the stomata are closed (Hinckley et al., 1979). But obviously this relation is different among species, stages of development, tissues and organs involved (root, stem, etc.). Another characteristic is that this behaviour is reversible until a certain point or threshold beyond which the damage is hardly reversible (Chiatante et al., 2006). Figure 1.12 illustrates the number of fruits of the cucumber plant as a function of the soil humidity in which the plant is growing.

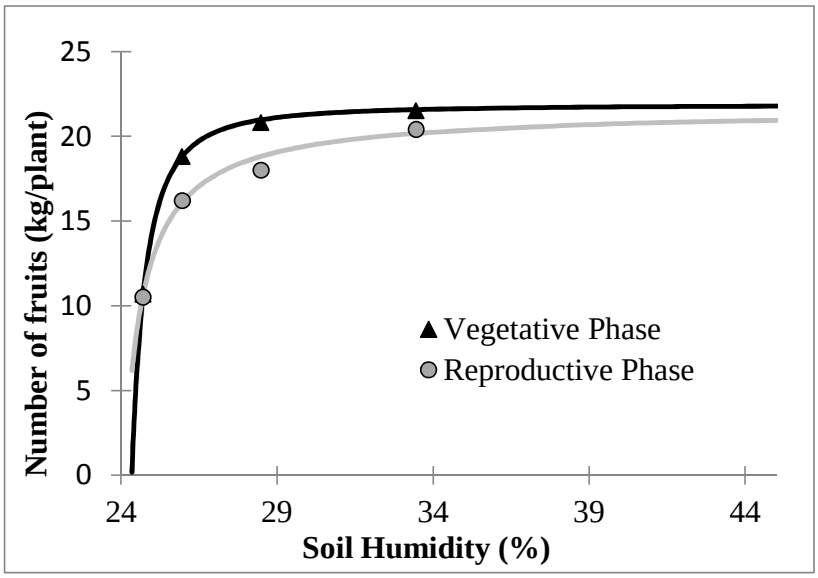

Figure 1.12 Number of fruits as a function of soil humidity for Japanese cucumber grown in greenhouse (created from data stored in Oliveira E., et al., 2011)

It can be seen that if the soil is drier, the plant produce less fruits, and that below a threshold (in Figure 1.12 equal to 24%), the plant stops to produce and can even die. In vegetation genetics, it is recognized that endemic and native species of arid climates tend to be more tolerant and resistant to drought events (Drunasky and Struve, 2005; Newton et al., 1991). This is achieved by techniques such as a lower leaf area; a better resistance to dehydration and deeper and more developed root system (see Figure 1.13).

Figure 1.13 Olive trees in dry soil (from www.laverdad.es newspaper)

Indifferently from the changes experienced by the vegetation caused by drought events, it is impossible not to refer to the interconnections between all variables: The potential of soil water content, soil type, type of plant or tree, precipitation and finally the temperature (Hsiao and Acevedo, 1974). This is because sometimes there can be a non-resistant drought plant located at a good soil type, which delays the drought damages over the mentioned plant. A provision of efficient water use often correlates with drought resistance of the plant (Hsiao and Acevedo, 1974).

1.3.4 Models and methods for drought evaluation and risk assessment related to *"Meteorological Drought"*

The processes involved in the meteorological and agricultural drought development are quite complex and highly nonlinear (see previous subchapters). However, some attempts have been made over the years at ordering and analysing the drought behaviour. With these simplified models, some authors like Stambaugh et al. (2011) relate the size of tree rings (drought consequences) with the PDHI drought index (Palmer Drought Hydrological Index), which is

assessed through the precipitation data series (Palmer, 1968). In that way, with dendrochronological techniques, the analysis of drought could be made over thousands of years and relate the vegetation development consequences (width of rings) to the meteorological behaviour.

In fire management tools, it is also common to find drought indices that correlate the meteorological conditions to the potential occurrence of fires in uninhabited zones. Some of the most relevant indices are: Keetch - Byram Drought Index (KBDI) Keetch and Byram (1968), Nesterov Index (NI). Swedish Angstrom Index (SAI), Cumulative Water Balance Index (CWBI), Drought Index (Drobyshev et al., 2011). Most of these indices are cumulative (in a time period) except the SAI, which is daily constructed (Ganatsas et al., 2011). Some authors such as (Drobyshev et al., 2012) illustrate that indices like the PDSI (Palmer, 1965), the calibrated PDSI (Wells et al., 2004) and SPI (Mckee T., 1993) can be used as a correlation tool for the occurrence of fires. This is because the potential moisture existing in the soil and in the vegetal mass (fuel) is directly correlated to the potential of a fire ignition. That is why these indices that make a balance between rainfall and atmospheric water demand are indicative tools of the soil moisture (Liedloff and Cook, 2007; Ruiz-Gonzales, 2004). Nevertheless, the analysis of the moisture present in the plant is a nonlinear problem, which can vary with the phenological development, growth cycle, temperature and different variables of the plant (Castro et al., 2003), which simplifies the fire prediction applying meteorological indices seem to be a suitable and operatively way of work.

In Iglesias et al. (2009), guidelines are defined in order to develop drought management plans, and evaluate their impacts (consequences) over the environment. These guidelines were the product of the research project MEDROPLAN and are summarized (Moneo, 2008).

However, in these documents, the complexity to have an implicit qualitative drought risk assessment model becomes clear (types of models in subchapter 1.1). This is because all the components for a good risk management planning are defined, but the transposition for a quantitative assessment is not proposed. To do this, the vulnerability and the hazard need to be assessed through a numerically comparable model, and as it has been mentioned, the drought definition could vary from place to place, with which a qualitative model is not the best tool to make this comparison. Nevertheless, it is remarkable that qualitative models are currently the only available tools for drought risk assessment.

The mentioned drought indices could be indicators of the hazard intensity. Sometimes they are discretized according to different drought levels (see 1.3.5) but the vulnerability assessment can be problematic, because the same drought does not always produce the same impacts over the environment either in the same place. To solve this, the recent tools developed to quantify the *"Meteorological Drought"* attempt to be comparable in spatial and temporal scales and include a previous model calibration in order to adapt the local impacts to the model. In the present thesis the Self-calibrated Palmer Drought Severity Index (SC-PDSI) is used to relate the potential economic losses in crops with the meteorological conditions. In relation to the original PDSI it can be said that it had some spatial and temporal limitations, this is the reason why in 1993 McKee proposed the Standardized Precipitation Index (SPI), which theoretically attenuate these limitations. In the next subsection the original PDSI is explained. It can be observed that the PDSI index depends on some constants that vary from place to place. These constants were the spatial limitation of the index, because in the original paper of PDSI (Palmer, 1965), the author proposed some constants that were obtained from the data series of Kansas, Iowa and North Dakota. Evidently, they are not representative of other countries in the world. The SC – PDSI improve the weakness of the

original PDSI as the PDSI constants are directly calculated from the input data, which is used to assess the index. In terms of the time scales limitation of the PDSI, this index was originally planned to be assessed at a monthly scale, reason why a comparison between different time scales has not been possible. Contrary to the PDSI index the SPI index makes temporal comparisons possible because, in order to build it, a statistical fitness is made and different time scales of statistical fitness could be done in order to have different time scales. A positive point of view concerning the PDSI is that the drought events are developed due to prolonged episodes of no rainfall and that is why an analysis of daily or weekly time scales do not have much sense.

Finally, the data input for the SPI index are the precipitation data series. In the PDSI case, there are the rainfall and temperature data series, the available water capacity (AWC) and latitude of the analysed station to make a correction of the potential evapotranspiration at that location. Only one variable input of the SPI makes more operational this index, but obviously it simplifies the processes involved in the drought phenomenon. The drought behaviour according to sections 1.3.2 and 1.3.3 depends on different variables. Therefore, including them in the analysis in their largest quantity could make the model more reliable. In this sense the PDSI and particularly the SC – PDSI have an advantage in respect to the SPI. The last idea was reflected in Vicente-Serrano S. et al. (2010b), which proposed a new index called SPEI and also suggested a prediction of crop production using this index in the Ebro Valley.

1.3.5 PDSI (Palmer Drought Severity Index):

The Palmer Index was developed as a tool for describing the “Meteorological drought”. The PDSI attempts to balance water demand of the atmosphere against the fallen precipitation in

the area (Palmer, 1965). This means that places where it rains very little and having low temperatures, would not be affected as other places with the same amount of precipitation and higher temperatures (typical of arid climates). To make an adequate balance, the PDSI employs the AWC (Available Water Capacity) that is an agronomist's parameter used to weigh the amount of water in the subsoil as a potential water reservoir (N.R.C.S., 1998). An example can be found in a comparison between a typical rice crop planted in a fertile organic soil and in a cactus yield located over basaltic subsoil. Under the same conditions of precipitation and temperature, the zone with the rice crops will develop delayed severe drought conditions than the cactus crop zone. Summarizing, the AWC quantify the propriety of the pair soil/land uses to retain water, because the amount of water present in the soil and land uses (type of crop) can affect meteorological drought development (Heddinghaus and Sabol, 1991).

As explained before, a great advantage of the Palmer index is that it uses the precipitation, temperature, phenology (type of crop) and soil characteristics (implicit in the AWC parameter), where the SPI index only compares precipitations. Conceptually it is clear that meteorological drought does not only depend on rainfall. The PDSI makes a hydrologic water balance using the variables found in Table 1.2.

Table 1.2 PDSI water balance variables

Acronym	Variable	Acronym	Variable
PET	Potential Evapotranspiration	Ss	Superficial soil moisture (soil divided in 2 layers)
PR	Potential Recharge	Su	Deepest soil moisture (soil divided in 2 layers)
PRO	Potential Runoff	PL	Potential Losses
RO	Runoff	ET	Evapotranspiration
L	Losses	R_c	Recharge
AWC	Available Water Capacity		

The original PDSI index equation is shown in equation (1.3):

$$X_i = 0.897 X_{i-1} + Z_i / 3 \tag{1.3}$$

Where X_i is the Palmer index in the i time step, X_{i-1} is the PDSI index in the $i-1$ previous time step and Z_i is the moisture anomaly index in the i time step. From equation (1.3), it can be distinguished that the PDSI index depends on itself in order to update with different time steps. Therefore it is possible to conclude that the PDSI has *"memory"*: wet seasons affect dry seasons and vice versa. In a sense, the previous idea is justified because if a basin is suffering from a dry season and it suddenly starts to rain, it does not necessary mean that it will immediately recover from the drier period. These models are usually known as Autoregressive Stochastic Models (AR). The PDSI is a particular case of these models. It is an autoregressive model of order 1. Appendix C shows that applying the integral scale theory to the PDSI AR (1), the number of significant previous time steps that affect the current value (X_i) are $9.2\,\Delta t$. This means that to develop a drought or wet season the previous 10 months in the PDSI index assessment are decisive (if monthly scale is analysed). Table 1.3 shows how the different PDSI values are classified.

Table 1.3 Palmer drought classification

PDSI Value	Type of Drought	PDSI Value	Type of Drought
4.0 < PDSI	extremely wet	-4.0 >PDSI	extreme drought
3.0 <PDSI< 3.99	very wet	-3.0 <PDSI< -3.99	severe drought
2.0 <PDSI< 2.99	moderately wet	-2.0 <PDSI< -2.99	moderate drought
1.0 <PDSI< 1.99	slightly wet	-1.0 <PDSI< -1.99	mild drought
0.5 <PDSI< 0.99	incipient wet spell	-0.5 <PDSI< -0.99	incipient dry spell
0.49 <PDSI< -0.49	near normal	0.49 <PDSI< -0.49	near normal

Appendix D explains how the different variables of Table 1.2 are involved in the hydrologic balance to assess the moisture anomaly index Z_i in the PDSI. In the PDSI original bulletin, Palmer warned about the spatial limitation of his index, this is the reason why he proposed a spatial correction factor called *Climatic Characteristic Factor* K. However, later studies proved that index behaviour is biased, as the climatic characteristics are far away from the original zone of study (Hu and Willson, 2000). However the self-calibrated PDSI proposed in 2004 attempts to improve this weakness (Wells et al., 2004)

.

1.3.5.1 Self – Calibrated PDSI (Wells N., Goddard S., Hayes M., 2004):

The SC-PDSI proposed by (Wells et al. (2004)) is more operative with respect to the original PDSI. This algorithm aims to improve the spatial limitation replacing the empirically duration factors (0.897 and 1/3) and the climatic characteristics K based from the historic data of the analysed location. Also the SC-PDSI helps to smoothen the index behaviour, i.e. when sudden droughts periods occur in a time series, which is experimenting a wet season, the SC-PDSI filters this event in order not to affect the wet periods, and vice versa. The SC-PDSI expression can be seen in (1.4).

$$X_i = pX_{i-1} + qZ_i / 3 \tag{1.4}$$

Where p and q are empirical coefficients derived from the input data of the currents analysed location (Wells et al., 2004).

1.3.6 Drought monitoring:

The above mentioned indexes have been implemented in different agencies around the world in order to follow and monitor drought development and behaviour. These agencies warn the

population and evaluate the drought threat through hazard maps which could be a representation (qualitatively or quantitatively) of the corresponding potential damage of the current drought. Relevant pages like the U.S.A drought monitor web page (see Figure 1.14) or the European Drought Observatory, make hazard maps plotting the SC-PDSI in different locations and making spatial interpolation with GIS statistical tools like ordinary Kriging to obtain values in areas without hydrometeorological information., or the SPEI Global Drought Monitor among others, are available to observe the drought development in different places around the world.

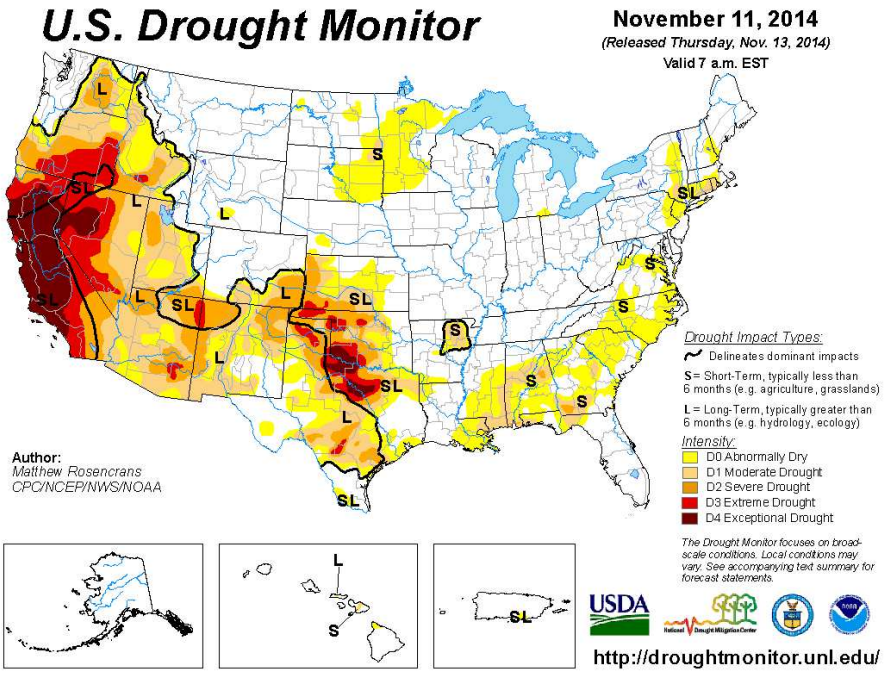

Figure 1.14 U.S.A. Drought monitor based on SC-PDSI (picture extracted from http://droughtmonitor.unl.edu/)

Chapter 2: Case Studies and data analysis

In the present chapter, the experimental basins for the residual risk assessment in the case of pluvial flooding and for the case of the drought risk assessment model are presented. The first corresponds to the Arenys de Munt basin, which is used in Chapter 3 and Chapter4. The second corresponds to the Llobregat basin and is used in Chapter 5. Both basins are located in the high - central part of Catalonia, in eastern Spain. Finally, a description of the available data and the quality control are detailed in order to improve the results.

2.1 Arenys de Munt basin

The Arenys stream is located in the Catalonia region in the geopolitical subdivision of Maresme (Figure 2.1), which is the area between the towns of Badalona and Blanes enclosed by the Besós and Tordera rivers. The Arenys basin is known for its historical flood events caused by intense convective storms (Forn i Salvà, 2002).

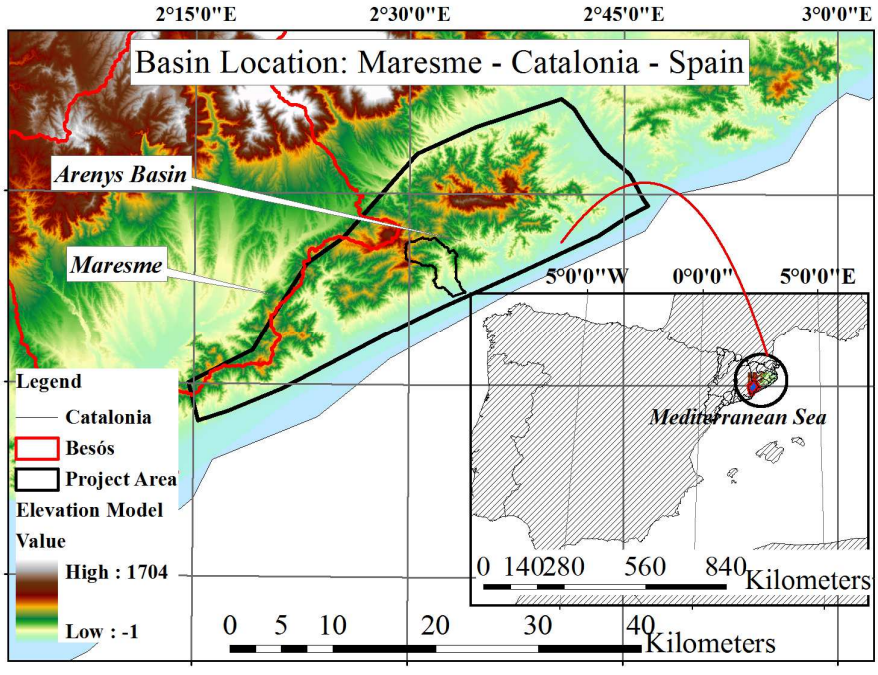

Figure 2.1 Arenys basin location in the Spanish peninsula

The aforementioned region is located on the Catalan coast and is surrounded by mountains and the sea, which makes it a singular region, compared to other basins of the Mediterranean region and affects the weather of the local area. The main mountains are El Montnegre (763 m.), El Corredor (648 m.), El Montalt (598 m.), Céllecs (534 m) and Sant Mateu (498 m.) (CEDEX, 2007). This basin is composed by the towns of Arenys de Mar (downstream) and Arenys de Munt (upstream). The Arenys basin has a total area of 16 km² with an average slope of 25%.

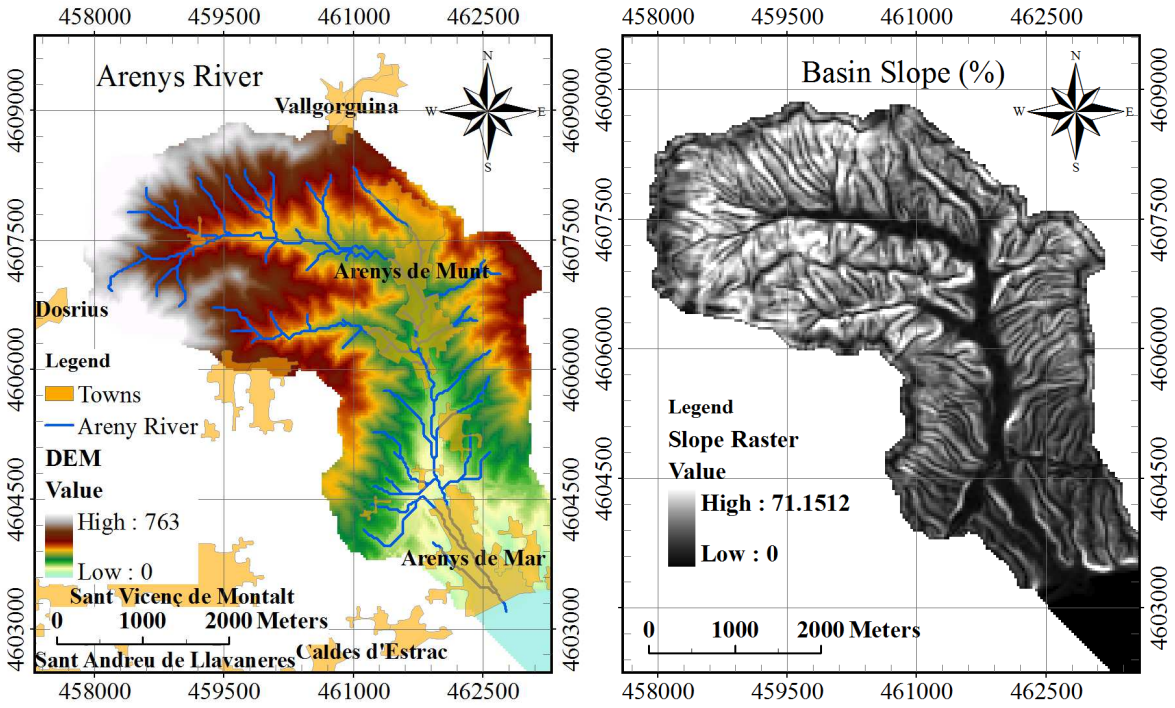

Figure 2.2 Arenys de Munt DEM and towns (left) and basin slope (right) with the UTM projection

2.1.1 Geology and land uses

The Maresme is a geologically diverse area, located not far from Barcelona. The geological formations in combination with the erosion processes (soil losses, laminar erosion, river erosion etc.) bring to the main river stream a large amount of sand which is locally known as “Saulo”. In

fact, the name of the river (Arenys) is a Catalan word that means sand (ICC, 2002). The heavy rainfalls, in addition to the sand availability, make for a high rate of solid discharge in the Arenys River. The typical material diameter is 0.5 – 1.0 mm (see Figure 2.3).

Figure 2.3 Arenys de Munt bed material

Concerning land use, there is a large forest, beaches, resorts, greenhouse production and vineyards areas (CREAF, 2009). The majority of the inhabitants live in the Arenys basin and surroundings and during the day they go to work in Barcelona (IDESCAT). In this region the greenhouses crops are extensively applied, so it has a considerable weight on the total agricultural production of the Barcelona metropolitan area. Greenhouses tend to locate in two types of places: in the flat part of the streams, relatively near to the coast and in the hill slopes, in the upper parts of the basin (Forn i Salvà, 2002). The harvesting on steeped slopes causes numerous problems, due to the fact that it removes the vegetation layer that intercepts the rainwater, and consequently increases the flood risk. The geology and land uses maps are displayed in Figure 2.4.

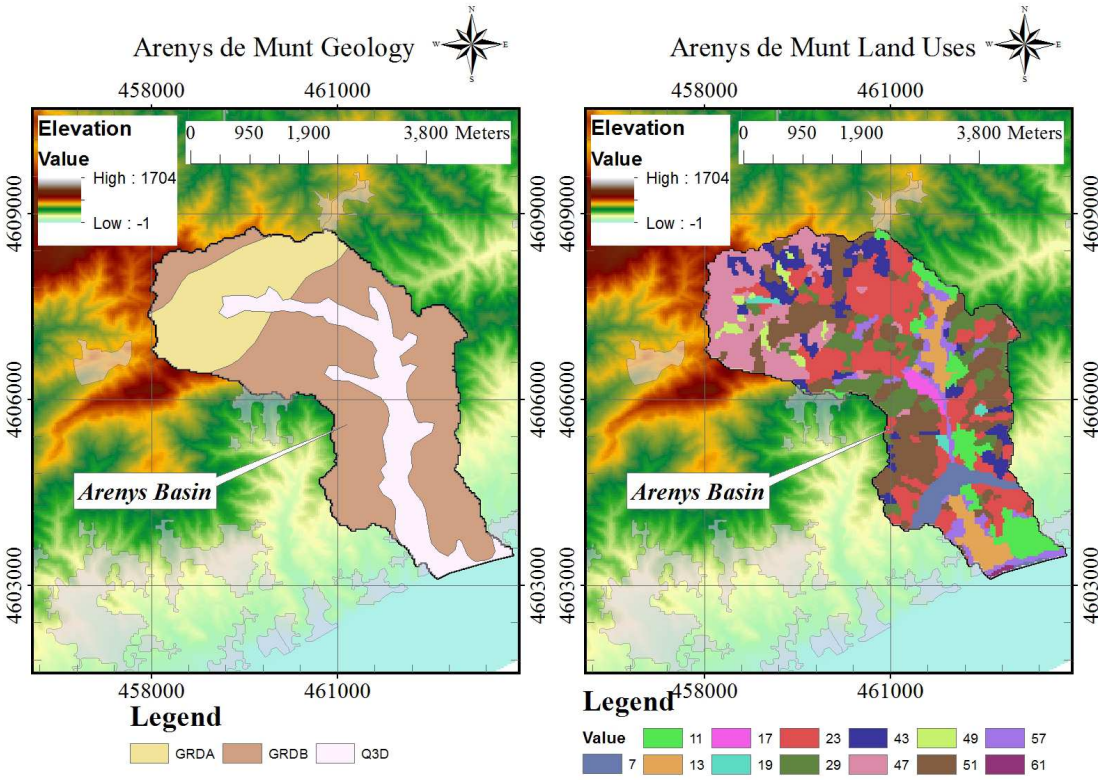

Figure 2.4 Arenys de Munt Geology (left) and Land Uses (right), labels on Table 2.1 Table 2.2

Residential buildings and other impermeable surfaces in steep slopes may also cause a significant increase in soil loss like the greenhouses. The railway line in the Maresme region is another reason for the loss of vegetation cover. The vestiges of natural vegetation along or near the Maresme coast are small and scarce. Instead, a predominance of pine (*Pinus Pinea*) with many others species (Forman, 2004) has been noticed.

Table 2.1 Label of Arenys Geological Formations in Figure 2.4 (ICC, 2002)

Digital Code	Description	Digital Code	Description
GRDA	Granodiorites biotíties	Q3D	Gravels, sands and clays
GRDB	Granodiorites hornblendic-biotític		

Table 2.2 Label of Arenys Soil Uses in Figure 2.4 (CREAF, 2009)

Digital Code	Description	Digital Code	Description	Digital Code	Description	Digital Code	Description
7	Road Infrastructure	17	Industrial and commercial zones	29	Nut plantations	49	Deciduous Forest
11	Urbanizations	19	Dry Arable Crops	43	Shrubs and lawns	51	Forest aciculifolios
13	Urban cores	23	Irrigated Herbaceous Crops	47	Sclerophyllous forests	57	Soil with little or no vegetation
61	Areas of sand and beach						

2.2 Llobregat Basin

The Llobregat River is the main water course which flows next to the city of Barcelona, capital of the autonomous region of Catalonia (Figure 2.5). The Llobregat River is born in the town of Castellar de n'Hug (1295 m.a.s.l.). It is surrounded in the southwest by the Foix River catchment, in the west by the South Subsystem catchments (Gaia, Francolí and Riudecanyes rivers), in the north and northwest by the Inter-communitary catchments (those which are contributive to the Ebro River), in the southeast by the Besós-Maresme catchments and finally in the east by the Ter River (Berga, 1995). The Llobregat River basin has an area of approximately 5000 km² and is characterized by its Mediterranean torrential regimes, which include low precipitation during most of the year, especially in June-August and December to February, but with intense rainfall episodes that usually occur in the months of October-November or April-May. This is one of the distinctiveness by which the Llobregat River basin is potentially prone to floods or drought events. On the other hand, the average annual rainfall in the Llobregat basin is not very high (about 700 mm / year) and temperatures can reach around 40 Celsius degrees (c^{o}) during summer. This causes the average flows over the main channel to not exceed 20 m³ / s near the

mouth of the river in the Mediterranean Sea, except for the peaks due to floods (October-April) in which it is very usual to see the averaged flow multiplied by a factor of ten (200 m^3/s).

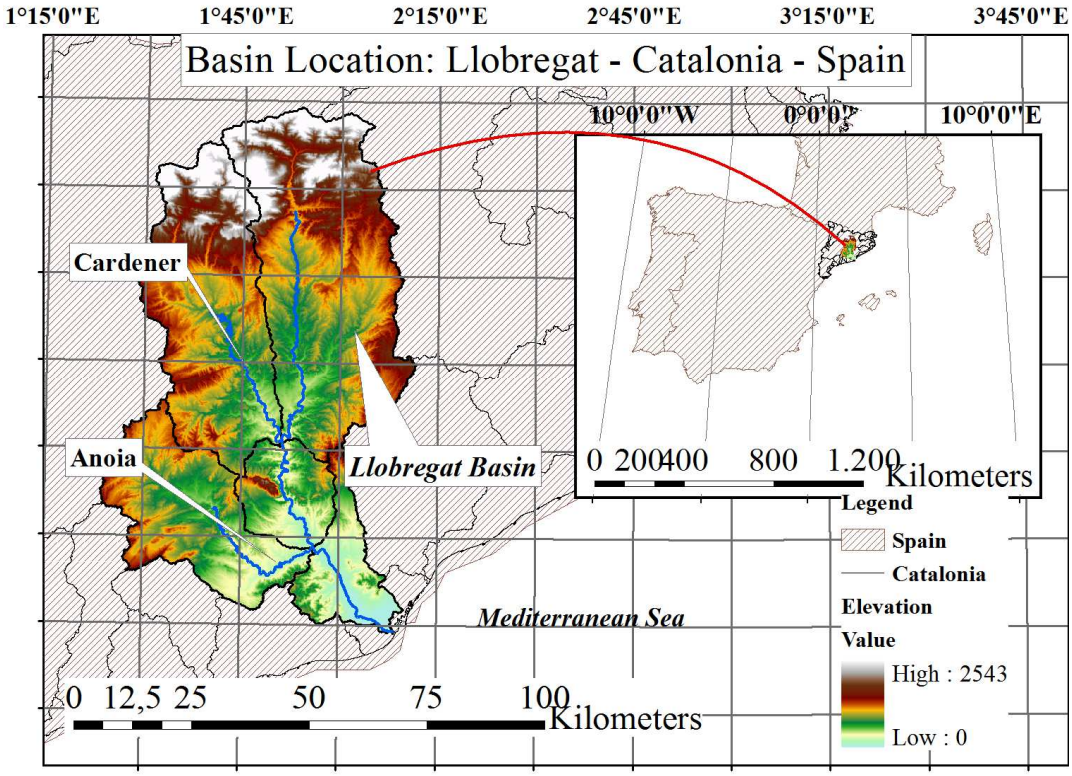

Figure 2.5 Llobregat basin location (DEM 30x30m).

Major tributaries of the Llobregat River are (Figure 2.5) the Anoia (middle basin) and Cardener (upper basin). Other small tributaries are the streams: Saldes, Bastareny, Peguera, Merdançol, Merle, Gavarresa and Calders. About the population, it is estimated that approximately 4.5 million people are living in the basin (2 million in Barcelona) and the main economic activity is the industrial work, which is one of the most important water demands on the river. The highest elevation in the basin is the Puig de la Canal Baridana Mountain at 2648 m.

2.2.1 Geology and land uses

The geology of the Llobregat River has been exhaustively referenced and nowadays it is widely known. Different studies like (Catalan (1997); Custodio et al. (1976); Gallart (1991); Manzano (1986); MOP (1996); Sole Sabarris (1963)), in which the paleontological, hydrogeological and the sedimentological aspects are defined, help on understanding the soil behaviour in the basin. The geology of the Llobregat basin is quite diverse and wide, from a lithostratigraphic point of view (Figure 2.6 left).

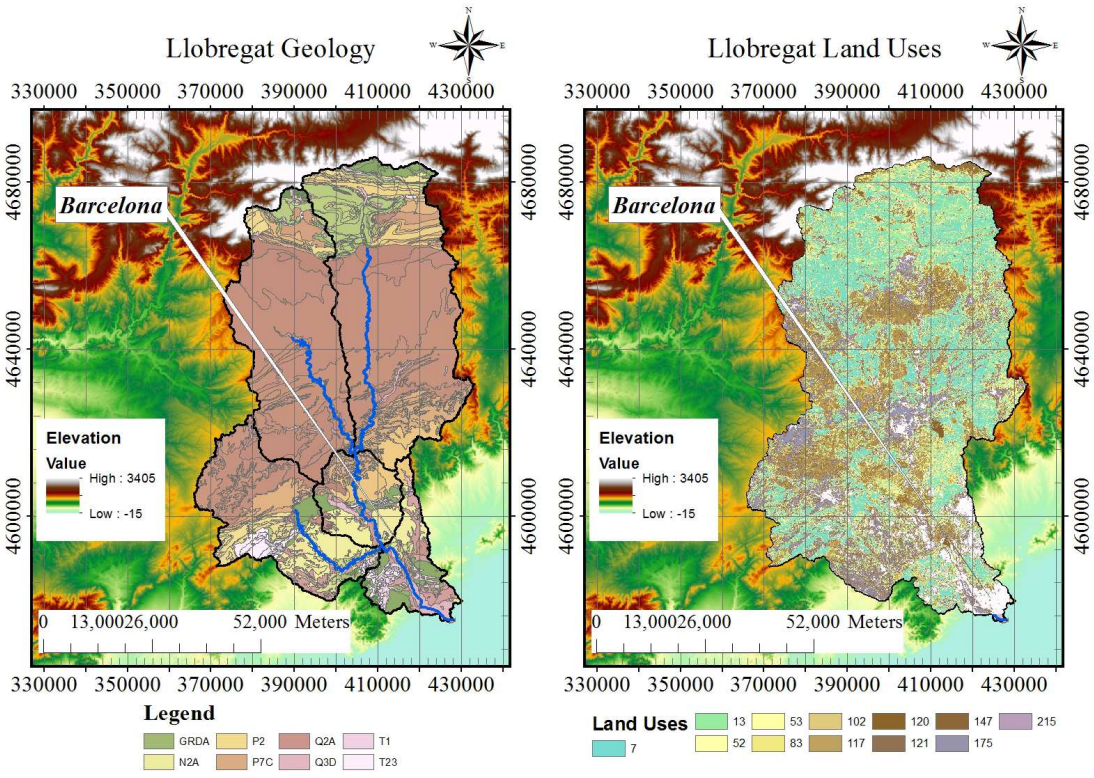

Figure 2.6 Llobregat Geology (left) and Land Uses (right), labels on Appendices A

The river source is located in a spring on a calcareous permeable massif, with an elevation of 1295 m. In its first few kilometres, the river flows through steep mountains receiving inlets from high mountain rivers such as the Arija, the Bastareny and Saldes. Additionally, these rivers

provide huge amounts of solid discharge due to the heavy soil losses caused partially by the natural erosion processes and also by changes in the land use (Figure 2.6 right). In this area, the population density is much lower than the middle and lower Llobregat River basin. Other important elements in the Llobregat River basin are the 4 major reservoirs for water retention: The La Baells, Sant Ponç, Llosa del Cavall and Sant Martí de Tous dams (Figure 2.7). Once the Llobregat River flows through the middle basin, it breaks through the Paleozoic and Triassic formations. Agricultural farms are located mainly in the middle and lower basin. These farms profit from the alluvial river behaviour, in which new fertile areas are created with the lateral displacement of the river bed course. The lower Llobregat basin is distinguished by its final delta area (also very referenced), which has been the object of extensive aquifer exploitation.

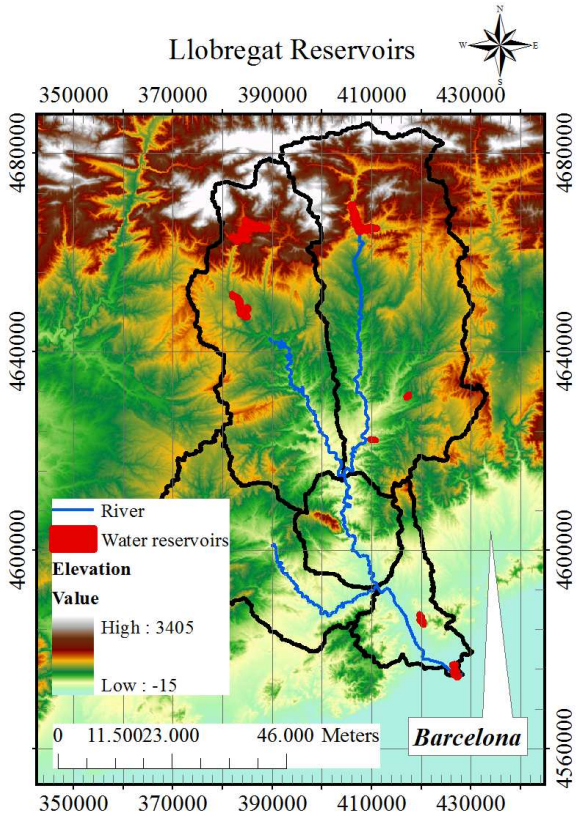

Figure 2.7 Main Llobregat water reservoirs

2.3 Data description

Generally, in a drought or flood event analysis, it is suitable to have extensive hydrometeorological series with the best possible quality. Due to that, an analysis on the quality, consistency and length of the data is developed. Data are obtained from different public organisms, which mean different formats of time intervals and locations: the rainfall from METEOCAT (the EMA network) and ACA (the SAIH network), flow discharge from ACA and temperature data from ACA and INM.

Table 2.3 Available information from different Spanish entities (numbers of data series)

Entity	Precipitation	Temperature	Discharge Flow
INM/METEOCAT	78	43	23
ACA	34	34	22

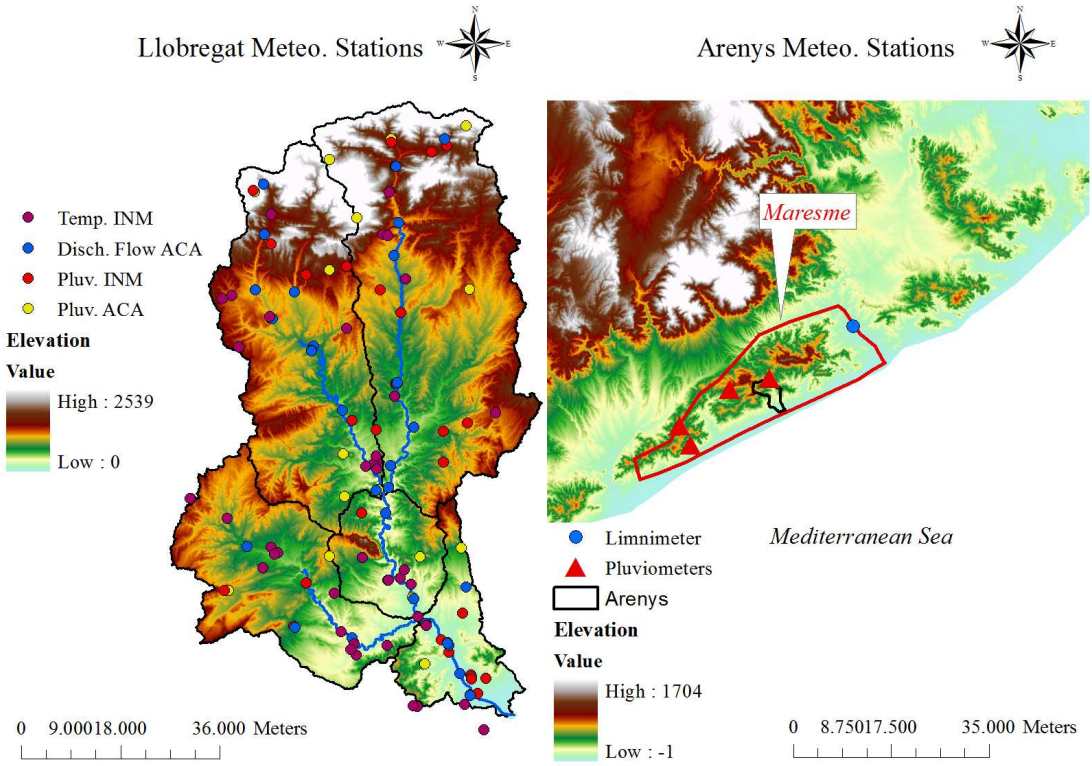

Figure 2.8 Hydrometeorological stations

Table 2.3 shows available information. Concerning the geographical localization, different data series can represent the same localization i.e. for temperature, 43 historical data series are available from INM, which represent 27 geographic locations (Figure 2.8).

2.4 Data management: The quality control through the EDA

Methods used herein for flood and drought risk assessment are quite sensitive to the quality of the data, which imposes a stringent and rigorous quality control, making sure that no exogenous errors are induced (Fleig, 2004). On the other hand (and contradictory), applying a very restrictive quality control could lead to the removal of too much information from the hydrometeorological data series, whereby few information to analyse will be disposed. Therefore, the quality control needs to find a balance between the quality and the quantity of the results. Generally, the hydrometeorological data errors come from different sources like instrumental errors (defectuous devices, growth of weeds on the pluviometers, etc.) and human factors such as a poor interpretation of the record data series by a technician. Depending on the analysed variable, the errors can be difficult to detect. An example of this is obtained from the discharge flow and precipitation series, since the first variable is less dispersed than the second. For short time intervals (i.e. day to day intervals) is unlikely to have dramatic oscillations in discharge flow as could be feasible from the precipitation variable. The quality control begins with the analysis of the measurement process and data collection. During the development of this thesis, we have been in contact with the hydrometeorological responsible people several times.

Finally, the EDA analysis is defined as a set of tools which as a result could bring graphs (histograms, scatter or box diagrams, etc.) to explore, present and understand the data

(Zambrano, 2010). The EDA analysis helps in the detection of atypical values. Once the data collection and measurement process is understood, other quality criteria included in the EDA methodology are performed, by means of scatter plots, as explained in the next subsections.

2.4.1 Constant discharge periods

Some extended periods with a constant discharge over a time interval could be possible errors and are frequently observed (Figure 2.9). This can be caused for example by malfunctioning of the measuring instruments. This behaviour is presented in dry and wet seasons. During wet season, it is more easily identified (a constant higher value always is doubtable). During a dry period with low flows, a constant discharge value could be observed because the variation in the discharge flows values is so small and probably the resolution of the instrument is not enough to recognize the small oscillations (i.e.: 0.015 to 0.019 m³/s could be registered as 0.02 m³/s).

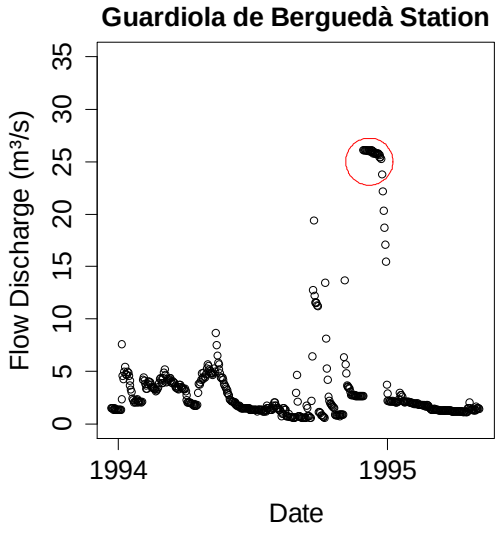

Figure 2.9 Flow discharge data series of Guardiola de Berguedà station, in which it is illustrated higher constantly flows during the year 1994 in red circle. This station it is controlled by the Berga channel.

2.4.2 Sudden picks or data fall down

At some points in the data time series, individual values could be recorded which are the product of sudden drop downs or picks that seem incompatible with the rest of the data (Figure 2.10). This means that they do not follow the trend in the data. These errors are very difficult to determine due to the random nature of some variables. For that reason, it is often very difficult to assess whether the existing data is the result of the chaotic process of the variable, or an error in the data. For historical series, the removal process of the sudden peaks and unusual values was performed by visual inspection through the EDA analysis.

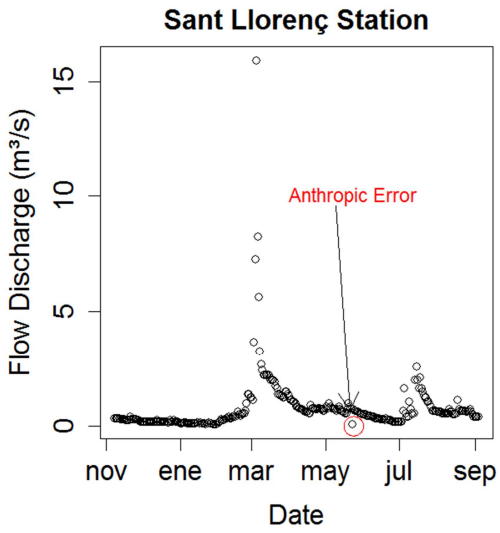

Figure 2.10 Flow Discharge data series in Sant Llorenç Station (year 1947), in which the data collection were manually collected by a limnimeter.

2.4.3 Selection of the hydrologic year

One of the main characteristics of the hydrological stochastic variables is the implicit deterministic component in each of them. This component is clear when it establishes the

seasonality of the series, which are determined by the annual seasons. Thus, in summer it is usually "expected" to have values of low discharge flow and rainfall, and high temperatures. With this idea, the determination of the hydrological year is essential for an appropriate drought and flood analysis (Tallaksen and Van Lanen, 2004). The hydrological year chosen begins in September 1st and ends in August 31st of each year (Díaz et al., 2008). Depending on the drought or flood method analysis, the choice of the start date and end of a year can lead to a large variation in the results. One hydrological drought method affected by this concept is the MAM (Mean Annual Minimum), in which the minimum annual average of the series reflects the dry periods for each year (Tallaksen and Van Lanen, 2004).

2.4.4 Zero data rainfall and discharge flow

Often, zero discharge flow or rainfall periods have a strong influence on the drought and flood characterization. Specifically, the influenced parameters are: the volume deficit, the drought intensity and duration, the PDSI and the flood return periods. These can be often attributed to the sensitivity in the measuring instruments (Figure 2.11), as mentioned previously in subsection 2.4.1. However, they are very difficult to detect, since the constant discharge errors or sudden picks errors cannot be easily distinguished where these values are the product of chaotic random nature or are errors in the data series. These errors were corrected with visual inspection by the EDA.

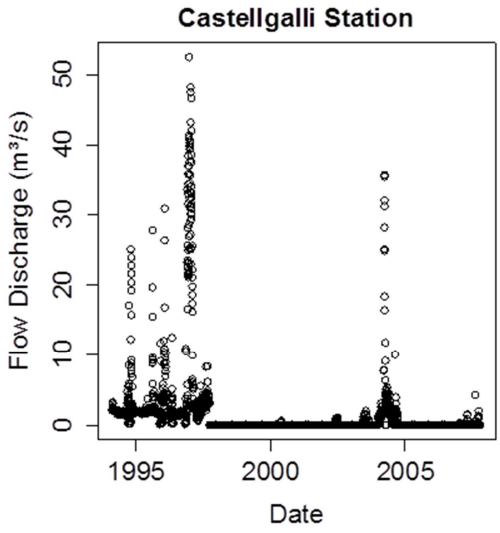

Figure 2.11 Flow discharge in Castellgalli, where the missing values were provided as zero discharge values (0 m³/s).

2.4.5 Drought events from incomplete data series

It is common to find drought events which start just before a hole in the data time series (Figure 2.12).

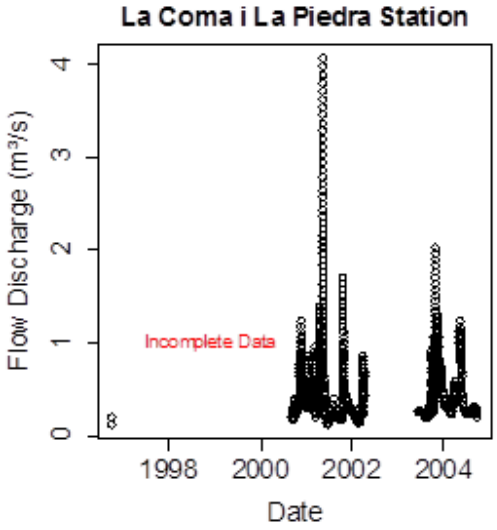

Figure 2.12 Discharge flow in the La coma I La Piedra station (m³/s)

Thus, the duration of this drought event cannot be easily assessed. For this reason, it is important to filter the errors in the drought indices coming from holes and determine the exact ends of the drought events. There are various methods to filter these kinds of errors additionally of EDA analysis. One example is the discharge flow data series, in which incomplete drought events are detected based on the threshold level method. This technique assigns a final drought event date when a lack of data lasts more than 15 consecutive days (Tallaksen and Van Lanen, 2004). Table 2.4 and Table 2.5 display the threshold level method in which an event just started before a gap appeared in the data series; this is the reason why the drought duration of this event was 1436 consecutive days.

Table 2.4 Threshold level method without filtering drought events of incomplete data series

Threshold Level Method (Q85= 0.14 m³/s)								
N	Initial Date	Final Date	Deficit Volume	Real Duration	Average Deficit Volume	Minimum Flow	Date Average Flow	Average Flow
	(D/M/Y)	(D/M/Y)	(m³)	(Days)	(m³/Day)	(m³/s)	(D/M/Y)	(m³/s)
1	10/09/1985	13/11/1985	292032	64	4563	0.06	17/10/1985	0.09
.	.....	.....	.....	.....	.....	.....	.....	.....
20	18/04/1996	22/04/1996	36288	4	9072	0.01	18/04/1996	0.04
21	**30/09/1996**	**05/09/2000**	**2481408**	**1436**	**1728**	**0.12**	**30/09/1996**	**0.12**
22	18/06/2001	24/06/2001	9504	6	1584	0.12	19/06/2001	0.12

Table 2.5 Threshold level method with drought events filtered

Threshold Level Method (Q85= 0.14 m³/s)								
N	Initial Date	Final Date	Deficit Volume	Real Duration	Average Deficit Volume	Minimum Flow	Date Average Flow	Average Flow
	(D/M/Y)	(D/M/Y)	(m³)	(Days)	(m³/Day)	(m³/s)	(D/M/Y)	(m³/s)
1	10/09/1985	13/11/1985	292032	64	4563	0.06	17/10/1985	0.09
.	.....	.....	.....	.....	.....	.....	.....	.....
20	18/04/1996	22/04/1996	36288	4	9072	0.01	18/04/1996	0.04
21	**30/09/1996**	**14/10/2000**	**25920**	**15**	**1728**	**0.12**	**30/09/1996**	**0.12**
22	18/06/2001	24/06/2001	9504	6	1584	0.12	19/06/2001	0.12

The precipitation and temperature data series can also show drought events disturbed from incomplete data series. The SC-PDSI is computed through a model provided by the National

Drought Mitigation Center at the University of Nebraska (www.unl.drought.edu), in which, if the input data (precipitation or temperature data series) has some gaps or periods without values, the algorithm can work (see subsection 1.3.5.1), but if they are very long the models brings inconsistent results.

2.4.6 Missing Values

Missing values influence the drought and flood data analysis either due to the reduction of the data time series length (Figure 2.13), or because the distribution of the recorded data has changed from the real distribution of the original values (Marsha T., Anderson J., 2002). Appendix B shows the methodology applied to fulfil the missing values of temperature and discharge data series. Contrary, precipitation data series were not modified, although some methodologies like the double mass curves are available, in order to avoid the errors coming from these procedures in the final results, because they are not accurate enough to take them into account. This subchapter is closely related with the previous one.

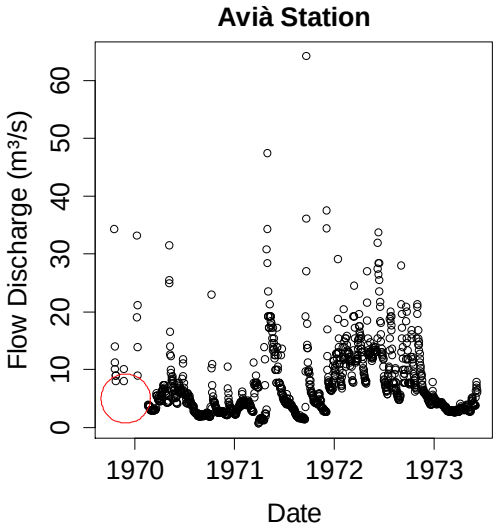

Figure 2.13 Missing values at the beginning of 1970 year (red circle) in the Avià Station

The difference lies in the fact that previous subchapter identified the errors over the assessed indices and the present paragraph focuses on the hole of the original data proposing methodologies to complete it.

Chapter 3: Methodology for optimization of non-structural measures in pluvial flooding residual risk mitigation; The Arenys de Munt basin

3.1 Abstract

Risk management is an essential component for good governance by stakeholders in events of emergency flooding. This paper shows the implementation of Non-Structural Measures (NSMs) in the Arenys de Munt basin to mitigate flood risk. A complete methodology was performed in order to apply these measures in the so – called risk management plan known in Spain as Municipal Action Plans (MAPs). The NSMs implementation was optimized with respect to the basin resources, referred to in future as restrictions. The case study is focused on pluvial flooding, obtaining societal and economic risk with and without NSMs implementation to establish the advantages (risk mitigation) of the NSMs performance.

The materialization of the NSMs was performed by means of worksheets for action forces included in the so-called municipal action plan, focused on NSMs and based on different emergency scenarios.

KEY WORDS: Non–structural measures, residual risk, emergency planning, risk reduction.

3.2 Introduction

This chapter conveys the results of the SUFRI project developed between 2009 and 2011, which achieved its objective of improving the management of flooding events, especially with respect

to NSMs. The SUFRI project belongs to ERA NET Crue Network (European Flood Research). Recently flood risk management has received major public interest and sustainable transnational strategies have been developed to focus on early warning systems, vulnerability and residual risk. Six universities from four European countries have been involved with five experimental catchments. The Arenys Creek belongs to the internal basins of the Catalonia region in the geographical subdivision of Maresme (Figure 3.1) more specifically in the area between the towns of Badalona and Blanes. The Arenys basin has been historically subject to events of severe flooding due to its hydrometeorological regime and basin characteristics (Forn i Salvà, 2002). In this basin, several important lessons have been learned from the behavioural experience and flood risk communication.

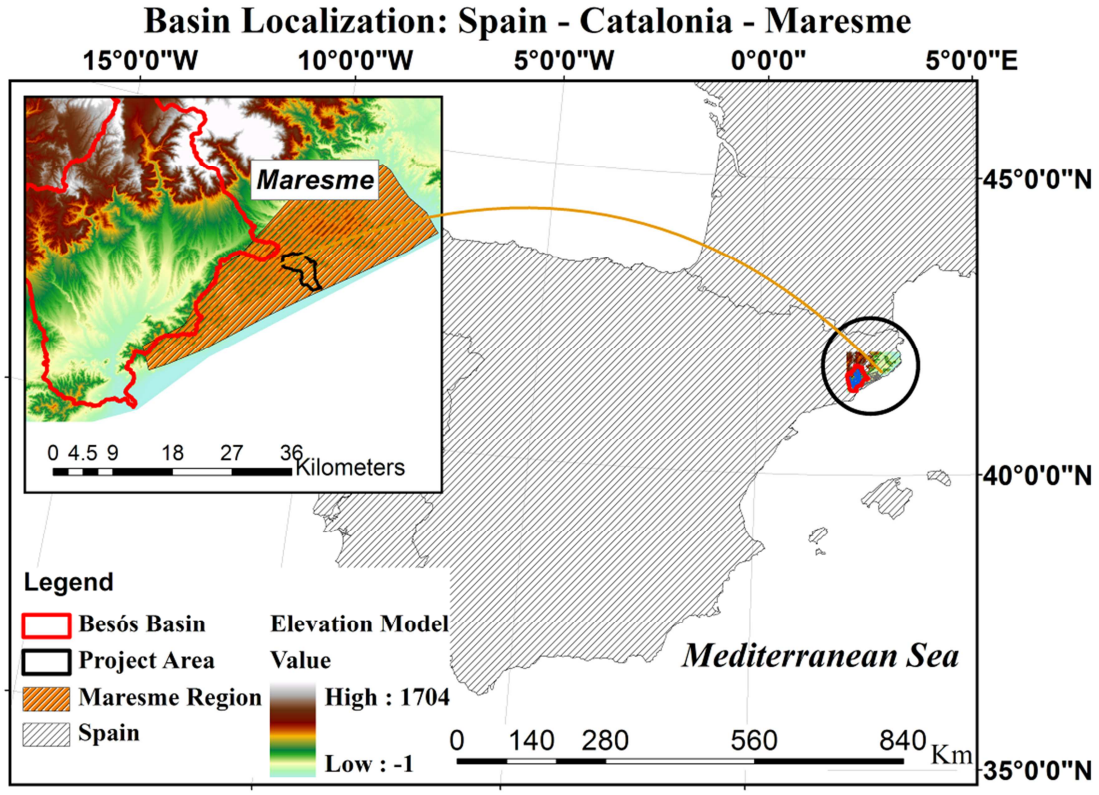

Figure 3.1 Arenys de Munt location

An analysis of the residual flood risk assessment in the Arenys basin due to pluvial flooding events was conducted; several NSMs were included in the action plan developed for the agencies acting in the affected areas. Under Spanish law, these plans should be implemented by municipalities in case of any natural hazard (INUNCAT, 2010). The NSMs can be cheaper and faster to implement for flooding scenarios than structural measures, as a consequence flood research topics are focused on this type of action (CRUE, 2009; Wheater et al., 2007).

The pluvial flooding phenomenon was selected because the fluvial part of the Arenys de Munt flood risk has been mitigated due to the implementation of structural measures (Barriendos and Pomés, 1993; Forn i Salvà, 2002). Specifically, the recent construction of a check dam in the upper part of the basin in order to retain the surface runoff and an encroachment of the Arenys Creek in the towns of Arenys de Munt and Arenys de Mar to mitigate the risk. Following the definition of the SUFRI project, the residual risk is quantitatively the part of the risk that remains after structural measures are applied. Nowadays, floods can never be absolutely prevented or predicted, so there will always remain a "***Residual Risk"***, even if structural measures are exhaustively applied (Faber, 2006). Due to this mitigation requirement, the study and research of NSMs in urban flood risk management has raised its importance over recent years. It includes considerations such as preparedness and communication which can change unequivocally according to the geographical and political situation of each region. Hence the international normalization becomes a complex task (Andjolkovic, 2001; Jha A., Bloch R. and Lamond J., 2011).

Establishing the residual risk after the structural measures implementation and quantifying the NSMs risk reduction (mitigation) is not a trivial task. A methodology for risk management planning (RMP) focusing on NSMs was developed in the SUFRI project. These RMP are not new, in fact the European Flood Directive of 2007 (EU-FD 2007) has established three different phases: i) preliminary risk assessment (Dec. 2011), ii) construction of hazard and risk maps (Dec. 2013), and finally, iii) flood risk management plans, known in Spain as MAPs (Dec. 2015). The SUFRI methodology for NSMs application agrees with the EU flood directive because it includes these steps. This methodology defines the practices and procedures to quantify the risk mitigation due to NSMs implementation, devoted to perform the MAPs. For the Arenys de Munt case study risk mitigation coefficients were developed by applying expert judgment (Sayers et al., 2011). As these coefficients are not extensively justified, they have been left as a research topic for future studies.

In the present work, the methodology announced before is applied, in this way the work has been subdivided in different sections. Firstly an introduction of the available NSMs is described on section number 3.3. Section 3.4 describes the SUFRI methodology. Each step will be described in the following sections.

3.3 NSMs and risk management planning for flood emergencies

To improve the flood emergency management by means of the MAPs, the proposed methodology follows a series of steps subdivided in two classes: those related to the analysis of the organization (type I) and those related to the NSMs implementation (type II). In the former, the requirement is to detect and identify the national structure and stakeholders' responsibilities;

the chain of communication between the involved organizations and finally the advantages and disadvantages of the current distribution of assigned responsibilities. In the latter, a set of NSMs implementations coupled with risk assessment and risk mapping converge to form the MAPs (Risk Management Plan). The set of NSMs can include insurance mechanisms, urban planning, communication, evacuation plans, etc. The kind of NSMs analysed and the specific measures applied in Catalonia are shown in Figure 3.2.

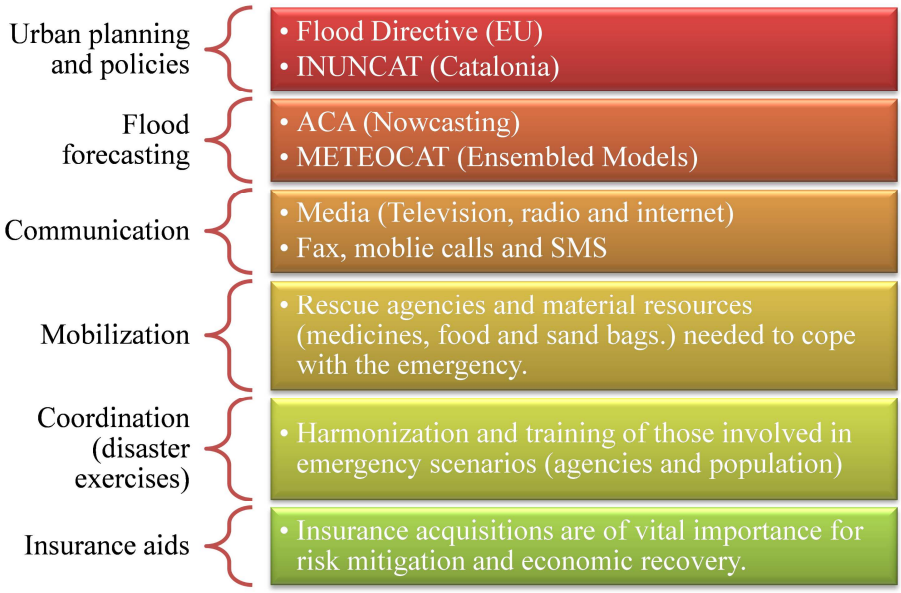

Figure 3.2 Description of NSMs for flood emergency events

3.4 The SUFRI methodology of risk management planning focused in NSMs

The methodology has been classified into two types. The first type includes an integral analysis of the agencies involved in flooding events (type I) and the second includes an analysis of the basin situation (type II). The above mentioned types are described below:

- **Step 1. Analysis of the emergency entities organizations structure (type I):** It is important to recognize and analyse all the institutions and the actors involved in flood emergency events, attempting to identify the weak points in each organization and take advantage of all the organizational strengths. The analysis of these structures could generate ideas from which NSMs can be implemented and which measures are harder to perform (for institutional or organizational reasons). This analysis could also show deficiencies / disadvantages in the organizations as they stand, which can subsequently be focused on to rectify the defects.
- **Step 2. Identification of flooding residual risk (type II):** is to identify and define the type of risk considered, and set the hypotheses to assess the risk. The present case was focused on the pluvial residual risk. All the steps involved could be analysed for different sources of flooding (river, urban, hurricane, etc.).
- **Step 3. Risk assessment (type II):** is the part of the study where the amount of risk (either societal or economic) is assessed numerically. (Escuder et al., 2011; Faber, 2006; Sayers et al., 2011; Wheater et al., 2007).
- **Step 4. Evaluation of NSMs (type II):** Within the list of the NSMs, those that could be implemented in the basin should be chosen. Not all NSMs will always be implemented because they depend on national/regional conditions and the available resources.
- **Step 5. Assignment of those who are to perform NSMs (type II):** is to establish who has to act in case of an emergency (which of the individuals, agencies and population). It is important to emphasize at this point, that to achieve the previous objectives it is necessary to develop meetings and agreements with the different actors and agencies involved in flood emergencies.

- **Step 6. Establishment of restrictions concerning the implementation of NSMs (type II):** This is the result of the basin authorities' limitation in which the resources are finite and sometimes quite inadequate. Occasionally the NSMs implementation requires investment of resources and the agencies involved need to optimize their own resources (monetary, human or time).
- **Step 7. Construction of the NSMs vs mitigation matrix (type II):** Due to the resource restrictions, different combinations of NSMs performance must be constructed. This means building different NSMs implementation in order to cover different possible combinations to get the best risk mitigation. This is where the optimization is performed, because different NSMs application can lead to different values of societal or economic risk mitigation.
- **Step 8. Worksheet for the action force (type II):** It contains a set of roles that comes from the NSMs combination, which can be adjusted for each entity in order to maximize the potential economic and societal risk mitigation. It is important to note that the NSMs choice option that maximizes the economic risk mitigation is not always the same one that maximizes the societal risk mitigation.

3.5 Analysis of the structures of the emergency organization

As previously mentioned, the analysis of the organization could bring ideas of which NSMs can be implemented and which measures are harder to perform for institutional or organizational reasons (DEFRA, 2010). The proposed NSMs implementation for the agencies involved in the Arenys de Munt is listed in Figure 3.3 with their corresponding responsibilities Figure 3.4.

Figure 3.3 Catalonia entities and command chain in flood emergencies.

Figure 3.4 Responsibilities for the Arenys de Munt basin entities who act in case of flood events

3.6 Risk identification

The type of flood risk considered in the Arenys de Munt case study corresponds to the pluvial risk, thus some streets have been selected to drive the SUFRI methodology analysis over the town. The risk assessment has been made according to Kron W., 2002:

$$R = H \cdot V \cdot E \tag{3.1}$$

Where H is the hazard (m and m/s) (assessed in section 3.6.3), V the vulnerability (economic losses/year) (assessed in subsection 3.6.4) and E the exposure (number of persons or m^2 of build structures). In the SUFRI project the exposure is implicitly managed in the vulnerability assessment. The hypotheses for both variables (Hazard and Vulnerability) are explained in the present section.

3.6.1 Hazardous identification zones

Once the pluvial flood risk has been identified as the main natural phenomenon, it is essential to define the components (hazard and vulnerability) and impose the assessment hypothesis to estimate the residual risk in the basin (DEFRA, 2010). The exposure is implicitly managed in the vulnerability assessment. The hazard in the pluvial flooding is quantified in terms of depth and velocity and the vulnerability through the curves of depth - percentage of damage (for economic losses) and potential casualties (societal losses) (DEFRA, 2010; Tapsell, 2011). Due to the small size of Arenys de Munt and to quantify the pluvial flooding as a residual risk in the basin, the risk assessment has been developed along the main streets of the town. A total of 10 streets were selected in accordance with their drainage area and their slope (Figure 3.5), identifying the most hazardous streets.

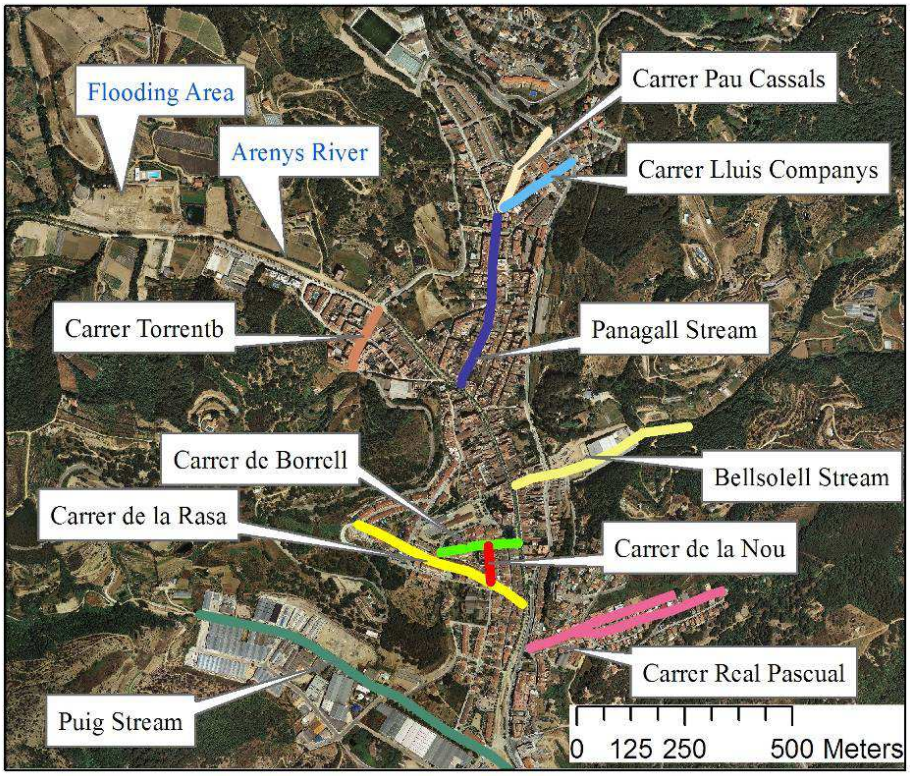

Figure 3.5 Satellite photo of Arenys de Munt identifying hazardous streets, and the main tributaries

3.6.2 Arenys de Munt - selected streets

To drive the analysis in the Arenys de Munt basin, a 15x15 m digital elevation model resolution was obtained, which was used to extract the slopes and widths of the streets, for the purpose of this paper it was considered accurate enough. Taking into account the aforementioned criteria the hazardous velocities and depths, are shown in Table 3.1 . As commented by Faber, 2006 slope and drainage area affects the risk considerably. Applying the aforementioned criteria the chosen streets should have the highest velocities v or hydraulic depths y (Table 3.1),

Table 3.1 Geometric characteristic of the Arenys de Munt streets

Street	Area (km²)	Width (m)	Stream Slope (%)	Elevation Diff. (m)	Maximum Stream Longitude (m)	Proportion Urbanized (%)
Panagall	0.238	4.0	14.6	284	1939	50
Puig	0.1114	8.0	12.2	423	3460	15
Bellsolell	0.0172	3.0	12.6	197	1557	10
Calle Real de Pascual	0.0180	3.0	12.2	184	1506	15
Carretera de Torrentbo	0.0151	7.0	18.7	111	593	40
Carrer de la Rasa	0.0519	3.0	14.7	133	902	60
Carrer can Borrell	0.0059	2.7	3.6	4	110.0	100
Carrer de la nou	0.0031	2.0	1.1	1	87	100
Carrer Pau Casals	0.0134	3.3	7.8	16	203	100
C./ Lluis Companys	0.0138	3.8	8.5	15	175.0	100

3.6.3 Hazard assessment

To quantify the hazard it was assumed that all the roofs of the houses and other buildings are not connected to the main drainage system, as is the case in the reality. So, the precipitation in the town will run directly through the streets. Moreover, it is necessary to impose some conceptual hypotheses to develop the calculations. These are:

1. In case of heavy rainfall the potential of the flow to drag vegetation and debris is very high. Consequently, the worst case scenario considers that all buildings and street gutters are filled up.
2. In the hydrologic rational method the runoff coefficient is one. This means that evaporation, transpiration and infiltration are not significant in the calculation of these events.

3. The flow regime developed along the streams and streets is considered in uniform steady state. This means that the friction slope is equal to the street slope and the friction losses could be estimated with the Manning's formula.

Applying these hypotheses it is possible to obtain the following expressions for hydraulic depth and velocity (Chow, 2000):

$$h = \left(\frac{n A_b I}{S^{1/2} b} \right)^{3/5} \tag{3.2}$$

$$v = \frac{1}{n} \left(\frac{n A_b I}{S^{1/2} b} \right)^{2/5} S^{1/2} \tag{3.3}$$

Where: v is the flow velocity (m/s), I is the rainfall intensity (mm/h), A_b is the contributing area (km^2), n is the Manning coefficient (s/m$^{1/3}$), h is the hydraulic depth (m), b is the width of the channel (m) and S is the channel slope. A total of seven return periods were considered according to those managed in the flood warnings issue by METEOCAT (2, 10, 20, 50, 100, 200, 500 years) and are conveyed in Figure 3.6, where the return period is expressed in terms of exceedance probability.

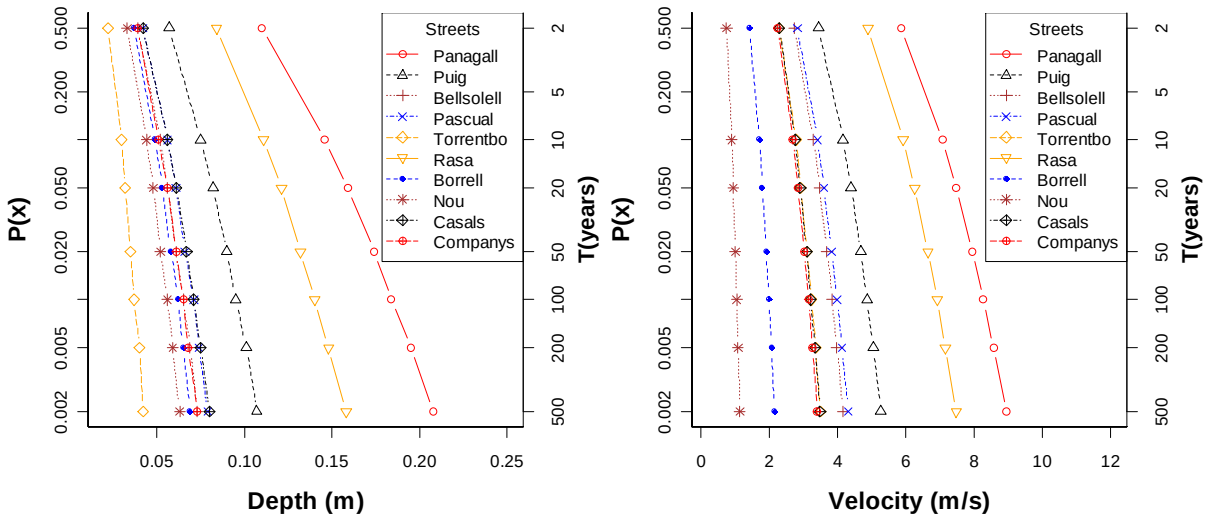

Figure 3.6 Depths and velocities for different return periods in the Arenys de Munt town

3.6.4 Vulnerability assessment

The susceptibility of the pedestrian to be affected by the surface runoff phenomenon can be caused by two factors: the pedestrians can slip and the overturning moment caused by the flow drag forces on the foot of the pedestrians (Nania, 1999). Obviously, there are other variables that can affect a pedestrian's stability while crossing a flooded street (age, experience, vision, strength, etc.) but in order to address the problem it was decided to manage only these two variables.

Stability criteria

The stability criteria of a person crossing a flooded urban street according to the drag force of the flow can be approximated by (Nania, 1999):

$$v^2 h \le \frac{2\mu(W - V_{ped}\gamma)}{2C_d b_p \rho} \le \frac{2\mu W_{equiv}}{2C_d b_p \rho} \tag{3.4}$$

Similarly if we consider the overturning moment the following equation can be obtained (Nania, 1999):

$$v^2 h^2 \le \frac{W_{equiv} b_p / 4}{2C_d b_p \rho} \tag{3.5}$$

Where μ is the friction coefficient, (W , W_{equiv} in Newton's) are the pedestrian weight and the equivalent weight in the foot respectively (subtracting the buoyancy force of the submerge foot volume V_{ped} in (m^3)), the C_d is the drag coefficient, b_p (m) is the width of the pedestrian foot and ρ (kg/m^3) the water density. The results are summarized in the Table 3.2. Relationships (3.4) and (3.5) are consider security factors as they are calculated as stabilizing forces over destabilizing forces. This security factor should be greater than 2.0 to be stable otherwise it could be unstable. As an example, if we consider a friction coefficient equal to 0.3 (Concrete - Rubber), density =1000 kg/m³, a drag coefficient 0.8, an equivalent weight of = 650 N and a foot width for the pedestrian equal to 0.2 m the above relationships gives:

$$v^2 h \le 1.0\left(m^3/s^2\right) \tag{3.6}$$

$$v^2 h^2 \le 0.2\left(m^4/s^2\right) \tag{3.7}$$

Table 3.2 Stability criteria for different return periods

T(years) Stream / Street	2		10		20		50		100		200		500	
	v².h	v.h	v².h	v.h	v².h	v.h	v².h	v.h	v².h	v.h	v².h	v.h	v².h	v.h
Panagall	3.77	0.64	7.34	1.04	8.87	1.19	11	1.38	12.6	1.53	14.3	1.67	16.7	1.86
Puig	0.67	0.2	1.31	0.31	1.58	0.36	1.95	0.42	2.25	0.46	2.55	0.51	2.97	0.56
Bellsolell	0.29	0.11	0.56	0.17	0.68	0.19	0.84	0.23	0.96	0.25	1.09	0.27	1.27	0.31
Pascual	0.33	0.12	0.65	0.19	0.79	0.22	0.97	0.25	1.12	0.28	1.27	0.31	1.48	0.34
Torrentbo	0.12	0.05	0.23	0.08	0.27	0.09	0.34	0.11	0.39	0.12	0.44	0.13	0.52	0.15
Rasa	2	0.41	3.9	0.66	4.71	0.75	5.82	0.88	6.7	0.97	7.6	1.06	8.85	1.18
Borrell	0.07	0.05	0.14	0.08	0.17	0.1	0.21	0.11	0.24	0.12	0.28	0.13	0.32	0.15
Nou	0.02	0.02	0.04	0.04	0.04	0.05	0.05	0.05	0.06	0.06	0.07	0.06	0.08	0.07
Casals	0.22	0.1	0.43	0.16	0.52	0.18	0.64	0.21	0.73	0.23	0.83	0.25	0.97	0.28
Companys	0.19	0.09	0.37	0.14	0.45	0.16	0.55	0.18	0.64	0.2	0.72	0.22	0.84	0.25

Flood Severity chosen levels

Different reasons of susceptibility could cause loss of human life in flood conditions. In pluvial flooding events loss of life has been assumed proportional to the hazard intensity (velocity and depth) and the vulnerability parameters (exposed above). In the SUFRI project five flood severity levels were discretized (Escuder et al., 2011) in accordance to the different vulnerabilities combination criteria (see Table 3.3).

Table 3.3 Flood severity for different vulnerability criteria

Flood Severity (S)		Depth h(m)	Velocity v(m/s)	Overturning parameter v.h(m²/s)	Sliding parameter v².h(m)
S0	Negligible severity	<0.45	<1.50	<0.50	<1.23
S1	Low severity	<0.8	<1.60	<1.00	<1.23
S2	Medium severity	<1.00	<1.88	<1.00	<1.23
S3	High severity	>1.00	>1.88	>1.00	>1.23
S4	Extreme severity	>1.00	>1.88	>3.00	>1.23

Fatality rates (FR)

For the Arenys de Munt study two different situations were compared, a complete established Early Warning System (EWS) and a poor warning operative system (without EWS). The last situation is referenced to as the “worst case” and the fatality rate values are extracted from Table 3.4.

Table 3.4 Fatality rates for both categories in terms of flood severity without EWS (Escuder et al., 2011)

Flood severity	S0	S1	S2	S3	S4
FR without EWS	0.0003	0.0018	0.0033	0.0090	0.0384
FR with EWS	0.0002	0.0015	0.0027	0.0075	0.032

The risk assessment methodology focusing on urban areas includes the early warning system (Escuder et al., 2011), other NSMs such as evacuation, mobilization or planning measures were

not taken into account. In this paper these NSMs are included in the mitigation coefficients developed specifically for the NSMs. The flood severity categories for Arenys case study (Table 3.5) were delimited combining the fatality rates of Table 3.4 with the vulnerability criteria of Table 3.3 in accordance with the hydraulic variables (depth and velocity) for each street and return period.

Table 3.5 Flood severity levels by pluvial flooding

Stream Way	T=2	T=10	T=20	T=50	T=100	T=200	T=500
Panagall	S3	S3	S3	S3	S3	S3	S3
Puig	S3	S3	S3	S3	S3	S3	S3
Bellsolell	S3	S3	S3	S3	S3	S3	S3
Pascual	S3	S3	S3	S3	S3	S3	S3
Torrentbo	S3	S3	S3	S3	S3	S3	S3
Rasa	S3	S3	S3	S3	S3	S3	S3
Borrell	S0	S2	S2	S3	S3	S3	S3
Nou	S0	S0	S0	S0	S0	S0	S0
Casals	S3	S3	S3	S3	S3	S3	S3
Companys	S3	S3	S3	S3	S3	S3	S3

Economic potential losses assessment (€)

To define the potential economic losses the vulnerability curves within the INUNCAT plan for the Catalonia region were employed (INUNCAT, 2010) and they are similar to the curves developed by the USACE (USACE, 2006). The damage is a function of the hydraulic depth as shown in Table 3.6.

Table 3.6 Damage Curve defined from the INUNCAT plan of Catalonia. See SUFRI project

Water depth (m)	0	0.2	0.4	0.6	0.8	1	1.2	1.4	1.6	1.8	2	4.9
Damage (%)	0	1	2.5	5	14	40	60	67	71	75	77	77

To evaluate quantitatively the reduction in economic losses due to the development and commissioning of an EWS, the Crue Era - Net project (EWASE, 2008) was used as a reference.

In the EWASE project, a damage reduction study of the industrial and private property was elaborated (see Figure 3.7 and Figure 3.8). The experimental basin of the EWASE project corresponds to the Besòs stream which borders the Arenys de Munt basin (see Figure 3.1). Consequently the same industrial and private damages could be expected or at least of the same order.

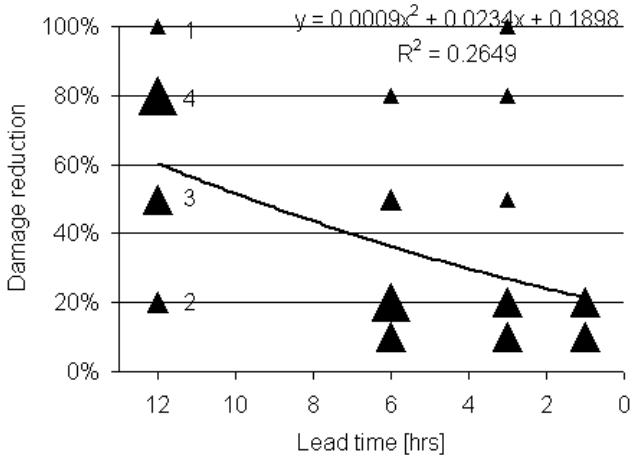

Figure 3.7 Damage reduction as a function of EWS lead time in the industry sectors (EWASE, 2008)

Taking into account that the METEOCAT (Catalan Meteorological Agency) has been working on the reliability of an Early Warning System 6 hours of Lead Time accuracy, the reduction for the private sector and industrial sector are: 0.22% and 0.33% respectively.

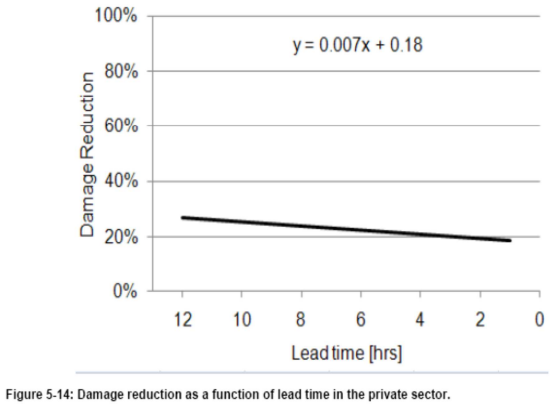

Figure 5-14: Damage reduction as a function of lead time in the private sector.

Figure 3.8 Damage reduction as a function of EWS lead time in the private sector (EWASE, 2008)

Finally the simplest way to include all the damage costs related to the flood events (direct and indirect costs) is to evaluate directly the cost of the flooded surface of a building (INUNCAT, 2010). Obviously, this form of economic risk assessment dramatically affects the results, especially if the cost does not vary with respect to the flood depth or hazard intensity. The flood damage costs are beyond the research topic of this paper. Again closely related information is available in the INUNCAT plan of the Catalonia region. The fixed value for the experimental basin is 894.6 €/m² for residential zones and 717.2 €/m² for industrial and commercial zones.

3.7 Risk assessment

The total risk in the basin is the result of the total contributions of individual street risks. This hypothesis is based on the fact that the catchment area is small enough to assume that the events are simultaneous in all Arenys de Munt streets. In fact only one rainfall gauging station was available (Forn i Salvà, 2002), therefore; all the hydrology is developed for this particular geographical spatial point. It is also reasonable to suppose that the risk analysis depends on the season. It is obvious that the probability of economic and human losses events is directly related to the probability of a rainstorm event (Escuder et al., 2011; Nishat et al., 2011). In order to evaluate the annual probability of occurrence of an event, a year is divided into winter and summer seasons and day and night time periods (WT). From the rainfall series the probability of occurrence in a specific time window can be evaluated. To do so, the day and night are considered as the periods between 08:00h to 20:00h and 20:00h to 08:00h, respectively. Summer is defined as the time window from 1st July to 1st September and winter the rest of the year. The evaluated probability for Arenys de Munt city is shown in Table 3.7.

Table 3.7 Probability that one event occurs in winter-summer and day-night window time

Winter 0.46		Summer 0.54	
Day	0.75	Day	0.5
Night	0.25	Night	0.5

Different land uses could bring different values of risk (Escuder et al., 2011). For the test basin two types of land uses were considered: residential (CU_1) and commercial (CU_2) as shown in Table 3.8.

Table 3.8 Number of people exposed to pluvial flooding risk in Arenys de Munt in the window time periods

People located at the study area	Summer/day	Summer/Night	Winter/day	Winter/night
	(WT_1)	(WT_2)	(WT_3)	(WT_4)
$CU_{1(Res.)}$	883	111.3	590	81.9
$CU_{2(Com./Ind.)}$	267	0	267	0
TOTAL	1150	111.3	857	81.9

To quantify the risk, the results of the individual streets risk contributions to the risk assessment in the Arenys de Munts in terms of consequences are displayed through the FN - curves (Jonkman et al., 2003):

$$1 - F_N(x) = P(N > x) = \int_x^{\infty} f_N(x)\,dx \tag{3.8}$$

In which FN - curve is the probability of exceedance in terms of the potential loss of life or the economical damage (consequences) and the $f_N(x)$ is the probability density function of the consequences per year. With these curves it is easy to find the expected value (of the number of fatalities or economical losses per year) also named for the economical losses as the Expected Annual Damage.

$$E_N(x) = EAD = \int_0^{\infty} f_N(x)\, x\, dx \tag{3.9}$$

This value is an predictor of the total flood risk value (Dawson et al., 2005) and has units of casualties/year or M€/year (Jonkman et al., 2003). Evidently due to the time windows defined above (2 season and 2 day intervals), the probability density function needs to be conditioned by the time window probability flood event r. Therefore (3.8) and (3.9) expressions would lead to:

$$F_N(x) = \int_0^{\infty} f_N(x)\, f_N(x|r)\, dx \tag{3.10}$$

$$E_N(x) = \int_0^{\infty} f_N(x)\, f_N(x|r)\, x\, dx \tag{3.11}$$

Where $F_N(x)$ is the exceeding probability to have social or economical risk conditioned by consequences in the time window probability of flood events. To build the FN – Curves use the total exposures in the city of Arenys the Munt summarized in Table 3.8. On the one hand, the contribution of social risk for each street has to take into account the fatality rates shown in Table 3.4 in which each value depends on the flood severity levels (Table 3.5). On the other hand, for the case of economic risk losses, the values in Table 3.6 were used.

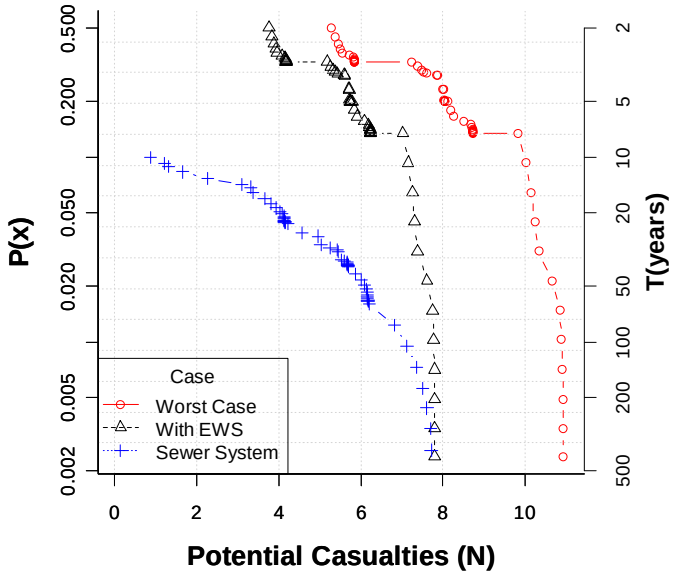

Figure 3.9 Societal Risk due to pluvial flooding

Three different cases for social risk are presented in the Figure 3.9. The first case, called the "worst case" considers the urban drainage main system collapsed for low return periods and without NSMs (circles in red). An intermediate case considers the urban drainage system collapsed but implementing an EWS (triangles in black). The last case considers the implemented EWS and the urban drainage system working properly for 10 year return period design (crosses in blue).

It is important to note that due to the urban drainage system collapse hypothesis there are life loss values for very low return periods for the first and second cases as shown in Figure 3.9 (red and black marks). This is the maximum potential life loss value for the town of Arenys the Munt. Including the drainage into the calculation model, it is clear that the "societal risk" values

decreases significantly (AUDACIOUS, 2008), but does not signify to reduce to zero the loss of life due to the discretization in the flow severity range. The introduction of the EWS reduces around 28% of the societal risk related to the "worst case", but in the case that combining the EWS and the drainage system, the reduction is more significant.

Economic risk for the three aforementioned cases is shown in Figure 3.10. It is clear that the potential economic losses are reduced by the implementation of an EWS coupled with a properly working urban drainage system.

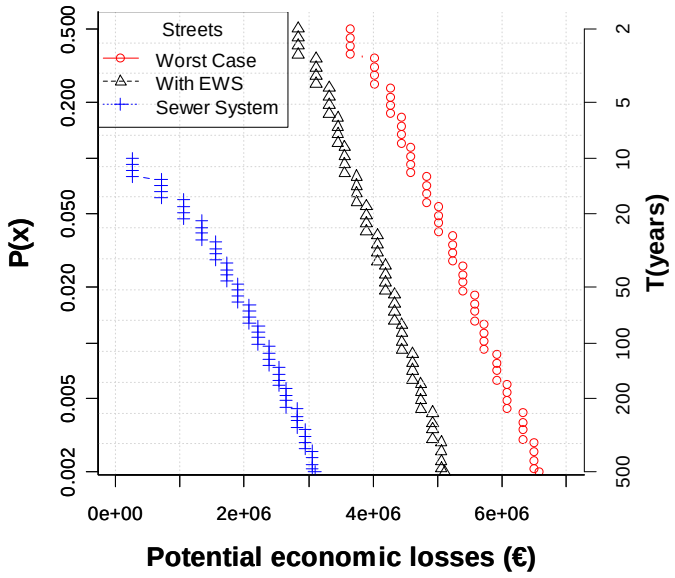

Figure 3.10 Economic Risk due to pluvial flooding (all cases)

It is very important to note that the economic risk reduction by EWS implementation is more significant than in societal risk, this is because a few hours of lead time could represent

significant economic loss reduction. This reduction could even be up to 90 % of the initial "worst case" value in the coupled case (Figure 3.10).

3.7.1 Risk mapping (delimitation of unsafe zones)

The risk delimitation through risk maps is one of the most important and essential topics in flood risk management planning (DEFRA, 2010). Table 3.9 reveals the delimitation of the streets that do not satisfy the vulnerabilities criteria.

Table 3.9 Affected streets under the uncertainty analysis

	Return Period						
Street	T=2	T=10	T=20	T=50	T=100	T=200	T=500
Panagall							
Puig							
Bellsolell							
Calle Real de Pascual							
Carretera de Torrentbo							
Carrer de la Rasa							
Carrer can Borrell							
Carrer de la nou							
Carrer Pau Casals							
Carrer Lluis Companys							

To build this table an uncertainty analysis is carried out considering the criteria of pedestrian stability (Nania, 1999). In this analysis the hydrology (and consequently the discharge flow) is obtained for the upper and lower rainfall confidence interval. Red is assigned to those streets in the risk analysis for which the vulnerability criteria fail for the upper and lower rainfall intervals. These streets are named as a *"Dangerous zone"*. The yellow colour is assigned to those streets in the risk analysis for which the vulnerability criteria fail with the upper **or** lower rainfall intervals and is named as a *"Risky zone"*. Finally, if in both cases (with upper and lower rainfall

intervals), no events are detected, the colour green is assigned and it is classified as a "*Safe zone*" (Wheater et al., 2007).

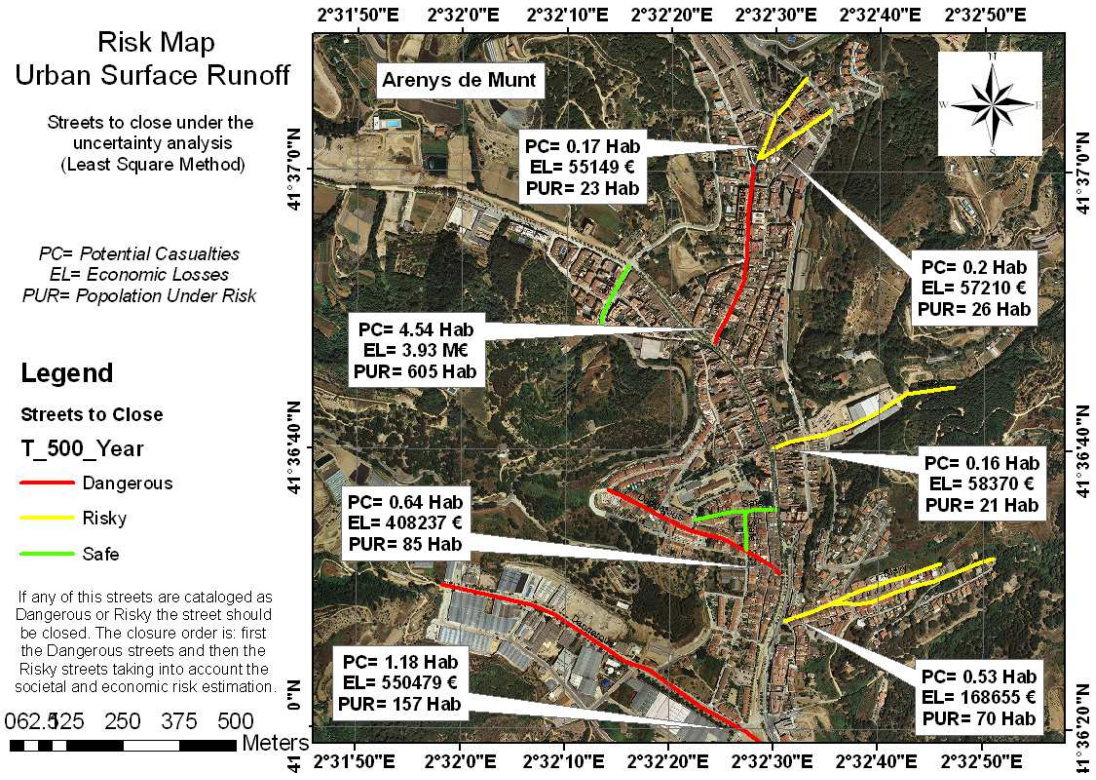

Figure 3.11 In the Map the Dangerous and Risky zone streets are shown. In case of flood emergency the dangerous streets should be closed first than the risky

In this way, the risk delimitation is not made in terms of a return period it is delimited by detecting which events are classified as hazardous in the uncertainty analysis (See Table 3.9). In the Crue Era-Net project RISKMAP (Fuchs et al., 2009), some risk mapping recommendations were set out. For the SUFRI project these mapping recommendations have been adapted for local requirements as shown in Figure 3.11.

3.8 Evaluation and feasibility of existing NSMs

From the organizational analysis discussed in section 3.3 and following different meetings with the agencies involved in flood emergencies the next NSMs for the Arenys basin have been identified (Figure 3.12).

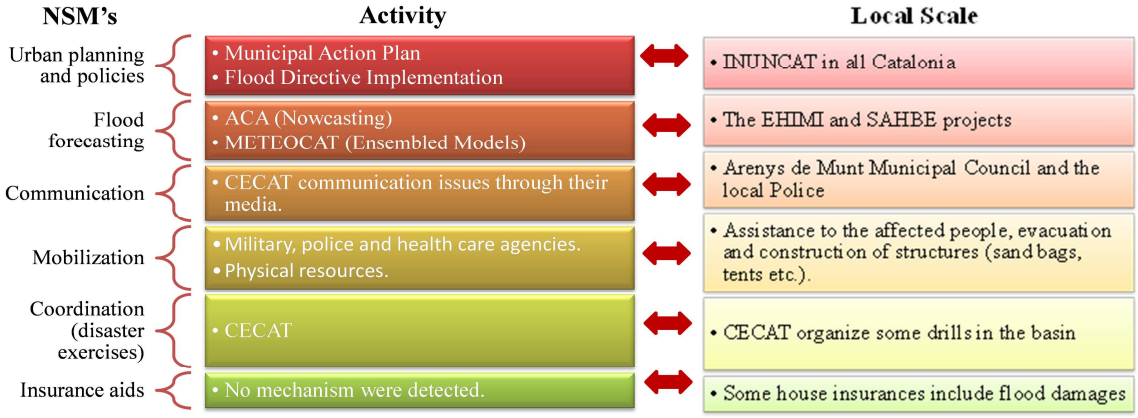

Figure 3.12 List of NSMs analysed for the Arenys de Munt basin

3.8.1 Implemented NSMs

The SUFRI project has tackled the issue of population and the ways to communicate risk in the basin. Basically communication occurs at two levels: between agencies and from agencies to the population. Warnings are issued by CECAT (Catalonia coordination operative centre), which is the entity in charge of different emergencies in Catalonia, and CECOPAL (Municipal Coordination Center) that is a command committee within the CECAT that includes the Ministry of the Interior and the Mayor of Arenys de Munt. The CECAT takes the decision whether to forward them to different levels and onto the agencies (First NSMs established). Once the municipality receives a warning, the police are informed and they are in charge of communicating the warning to the population. The second well established NSMs is the

mobilization of physical resources. Specifically, Arenys de Munt has significant experience in the implementation of the wooden boards called *"Post"*. This can be considered as a physical resource. These boards are designed to block the buildings doors and protect them against water, in some cases they are combined with sand bags. These measures are directly managed by householders and frequently used, 1-3 times per year. The rapid reactions of Arenys de Munt inhabitants to flood warnings make it possible to move cars from the streets (Figure 3.13) in just a few minutes (Piperno and Sierra, 2007). For the forgotten vehicles, the firemen are tasked with fixing them to trees in order to prevent them from being washed away by the water. All these elements give an idea of the population preparedness and education about floods.

Figure 3.13 Risk communication and evacuation of the Arenys stream, (10 – 15 min.)

Finally, the last NSM found is the Arenys de Munt land plan, which was updated in 2003. In this plan different zones were delimited as special protection areas which cannot be industrialized or urbanized (Llistosella and Pàmies, 2003).

3.8.2 NSMs developed currently

Nowadays, work on NSMs implementation continues, including different measures such as the delimitation of hazard zones, risk assessment and the risk management planning due to the European Flood Directive (Dueñas, 2010). In Catalonia the INUNCAT plan forces the municipalities, identified as "under risk", to develop a Municipal Action Plan (MAP) as shown in Figure 3.14. The MAP includes hazard delimitation, risk assessment and a risk management plan. Evidently due to the current economic crisis the implementation of the MAP process has been delayed in many municipalities despite the directives being very clear on the deadline

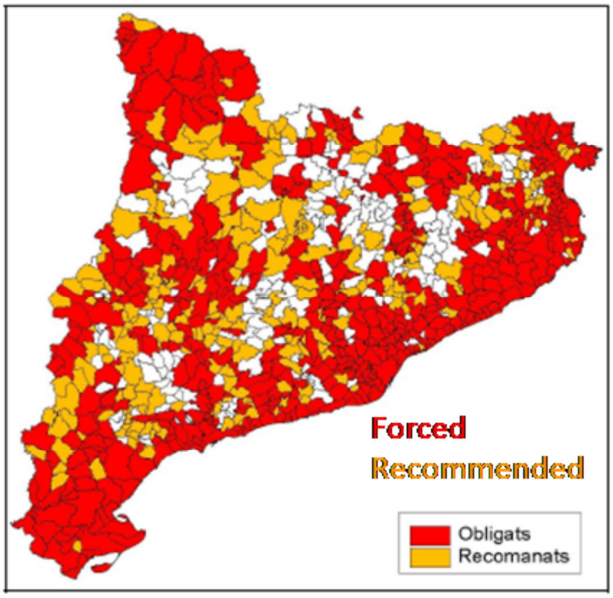

Figure 3.14 Municipalities Forced to develop a Municipal Action Plan, the red colour indicates mandatory and the orange means recommended (INUNCAT, 2009)

The EHIMI (Hydro meteorological development tool for Catalonia) project and the Early Warning Systems (EWS) for Catalonia are still under improvement. Different projects such as the IMPRINTS or the COST 731 (2010) have been developed to build up an accurate EWS making it feasible to have at least a 6-hour lead time. Finally CECAT develops risk exercises and carries out training in flood emergencies. Most of this training is the responsibility of the CECAT staff. In Arenys de Munt there is no evidence of risk exercises or training by CECAT.

3.8.3 NSMs to be implemented

Insurance aid is a kind of NSM that could help with recovery from a flood event. It is important to emphasize that usually it is not considered a mitigation measure (just a recovery measure) because it does not diminish the possible flood damage (in terms of casualties and economic losses). In fact it only helps with the economic recovery. In the Maresme region and specifically in Catalonia, no specific flood insurances were detected.

3.9 Assignment of those responsible for performing NSMs

A total of seven NSMs have been analysed (see Table 3.10). For each NSM it is established which agency must act in flood emergencies (the Actors). Actor recognition and allocation implies in itself the assignment of responsibilities, and this obviously implies the integration of various agencies to fill any gaps (actions to perform) that might exist in the management of flooding events. Table 3.10 shows the responsibilities-actor distribution. In this table it can be seen that the population appears as an *actor* for flood emergencies as it is specifically responsible for the installation of the *"Post"*.

Table 3.10 NSM-Actors assignation for Arenys de Munt Basin

N.	NSMs	Regionally	Locally	Observation:
I	Land Uses Planning	Checked by the Government of Catalonia, without being officially involved	The Arenys de Munt municipality: Specifically the Director of Urban Planning	Only the Arenys de Munt Municipal Council has this responsibility. The land planning will be checked every 5 years.
II	Flood Directive Implementation	Government of Catalonia, ACA, METEOCAT, CECAT (Interior Minister	Arenys de Munt Municipal Council	Until now an official decree was enacted on July 2010. Different deadlines were established for FHM, FRM and FRMP also called MAP.
III	Flood Forecasting (through EWS)	ACA and CECAT	Local meteorologist.	With only 6 lead time hours of forecast potential damages and casualties could be mitigated.
IV	Communication	CECAT	Arenys Municipal Council and Police	The weak point of the risk communication has been excessive use of warnings. A check by a local expert can lead to an improvement in the system
V	Mobilization	Government of Catalonia	Population, Police and Fire Dept.	The evacuation, streets closure and physical resources mobilization (*Post*) will be implemented during the flood scenarios.
VI	Disaster Exercises	CECAT	Municipal Council, Police and Fire Dept.	The Municipal Council acts only if a disaster control exercise is made in Arenys de Munt
VII	Insurance and Aid	Government of Catalonia	Arenys de Munt Municipal Council	The Government has to legislate new insurance rules and the Arenys de Munt Municipal Council to promote insurance acquisition.
*Also in the Maresme Area Council have experts in the Hydro Meteorological Dept.				

3.10 Establishment of restrictions regarding the implementation of NSM

From the previous subsection, 7 actors (or agencies) were assigned to the NSMs. In most of them, more than one actor is involved, so interference or "restrictions" could exist between them because actor resources are finite. With the aim of making the application as simple as possible (focused in NSMs optimization) the following restrictions and protocols for each actor involved were established (Table 3.11 and Table 3.12). The Arenys de Munt restrictions are focused on the physical limitations that the NSMs might have in the basin.

Table 3.11 Acting protocol for each agency (actor) identified in the Arenys de Munt basin

Entity	Involved in:	Obligation
CECAT	II, III, IV, VI	Due to its own responsibilities, CECAT will have to monitor and improve warnings in order not to worsen the communication of risk (NSM) in Arenys de Munt. Moreover CECAT needs to implement more flood emergency drills.
Catalonia Government	I, II, V, VII	The Government of Catalonia through its management departments must control land use planning and the implementation of the European Flood Directive and improve the flood insurance system.
ACA	I and III	The ACA efforts need to be focused on the improvement of the forecasting systems (cooperating with METEOCAT and CECAT)
Arenys de Munt Municipal Council	I, II, IV, VI, VII	This contributes a significant part of the NSM, so, the ACA needs to coordinate tasks between all those involved to help as much people as possible.
Police	IV, V, VI	The police in addition the responsibility of oversight the police must communicate risk and close streets.
Fire Dept.	V, VI	Firefighters will attend all flood emergencies and will carry out any evacuation.
Population	V	The population has to insert the "*post*" (wooden boards) and be alert to new information

Table 3.12 Arenys de Munt NSMs restrictions

Communication	Up to 4 person
Mobilization	Up to 6 person
EWS	Up to 10 000 €/year
MAP (include Land Planning)	Up to115000 € every 5 years

For our experimental basin an annual budget of 500.000 € was granted to be distributed annually according to the different activities. Note: The land use plan will be included in the MAP study to avoid paying twice for studies that are closely correlated.

3.11 Construction of the NSMs vs. mitigation matrix

Once the NSMs restrictions are known, multiple combinations should be performed taking into account these restrictions (mathematical constrains), these NSMs combinations should mitigate risk in different ways. An optimization procedure has to be performed in order to obtain the optimum one. To evaluate the NSM's mitigation, as well as to optimize their possible

application, the coefficients of risk mitigation (of economic and societal risk) have been worked out in Arenys de Munt. All the mitigation coefficients were constructed (Table 3.13 to Table 3.16) based on “Expert Judgment” and adapted to the features of Arenys the Munt. The tables reflect the percentage reduction for potential loss of life (column “Lives”) and for economic damage (column “€”).

The development of these coefficients was beyond the scope of the SUFRI project. Expert judgment for flood risk management has been considered for support in investment and decision making processes (Sayers et al., 2011). This is basically due to the large uncertainties associated with these topics. Little information about mitigation coefficients is available in the NSMs literature. In fact, only in the EWS measures risk reduction coefficients were found, specifically in the aforementioned EWASE project. To obtain these coefficients in this project a survey was conducted. The survey was focused on asking what percentage of risk would be mitigated if there had been a warning of a certain lead time. In order to establish the expert’s judgment coefficients different meetings were held out with the agencies involved in flood emergencies as well as the results obtained from 3026 household’s surveys in Arenys de Munt. Obviously the development of coefficient mitigation is a decision left to the stakeholders and will be a future research topic for NSMs implementation. There are two ways to apply the risk mitigation coefficients: the first one is to reduce vulnerability (fatalities rates Table 3.4) categorized according to the NSMs that have been considered. The second one involves considering a coefficient as a percentage of risk reduction (present scheme). The coefficients for percentage of risk reduction of communication, mobilization, MAP and EWS NSMs are shown Table 3.13 to Table 3.16.

Table 3.13 The Communication NSMs reduction/mitigation percentage in Arenys de Munt (%)

Number of Person needed	%Lives	%€
1	15	15
2	19	18
3	22	21
4	23	24

Table 3.14 Table Mobilization NSMs reduction/mitigation percentage in Arenys de Munt (%)

Number of Person needed	%Lives	%€
2	15	18
3	19	22
4	23	26
5	27	30
6	31	34

Table 3.15 MAP NSMs reduction/mitigation percentage in Arenys de Munt (%)

5 years investment (€)	%Lives	%€
100.000	22	30
105.000	22.5	31
110.000	23	32
115.000	23.5	33

Table 3.16 EWS NSMs reduction/mitigation percentage in Arenys de Munt (%)

5 years investment (€)	%Lives	%€
5.000	14.28	20
10.000	28.57	22.25

The reduction coefficients of Mobilization and Communication (NSMs) are in terms of numbers of persons working for the specific measures, conversely, the MAP and EWS are in terms of the annual investment of these NSMs. For coordination and operative practices (disaster exercises) and insurance no coefficients of risk mitigation were established in the present analysis. Consequently, they will not vary the NSMs optimization. The risk mitigation percentage in the potential casualties and losses is the division of the risk obtained when specific NSMs combinations are applied (under a specific return period) with respect to the risk assessed without measures. This could also be questionable, because when different NSMs are

implemented, the mitigation coefficients' behaviour is not necessarily the same as if only one NSM is implemented. A matrix for NSMs implementation is shown in Table 3.17.

Table 3.17 NSMs combination for Arenys de Munt, (Comb=3 in SUFRI final report)

NSM	Fire fighters	Police Officers	EWS (Expert & Maintenance)	Press Officers	Other	Global Cost	Annual Cost
Municipal Action Plan	0	0	0	0	1.15	115000	23000
Early Warning System	0	0	1	0	0	10000	10000
Communication Improvement	0	2	0	1	0	110000	110000
Mobilization	6	0	0	0	0	240000	240000
Coordination and Disaster Exercises	0	0	0	0	1	40000	40000
Disasters Insurance & Aid	0	0	0	0	1	77000	77000
Total							500000
Optimal (by two variables) Potential fatality mitigation = 69.69%							
Optimal (by two variables) Potential economic loss mitigation = 71.8%							

For the Arenys de Munt case study, an optimization considering both variables at the same time was made (potential casualties and economic losses). This is because the optimal solution for the potential casualties that brings the maximum mitigation is not always the same as the solution for the potential economic losses. Some restrictions are implicit in Table 3.13 to Table 3.16, also the mitigation related is displayed. For example, as a restriction is the need to employ an entire number of persons. The previous combination shows a risk reduction of around 70 %.

The final societal and economic risk is shown in Figure 3.15. In this figure it is clear how the structural and NSMs mitigate the risk. Potential casualties are reduced by about 80% from 11 to 2 lives lost, and a 90% reduction of potential economic losses from 6.6M€ to 0.7 M€.

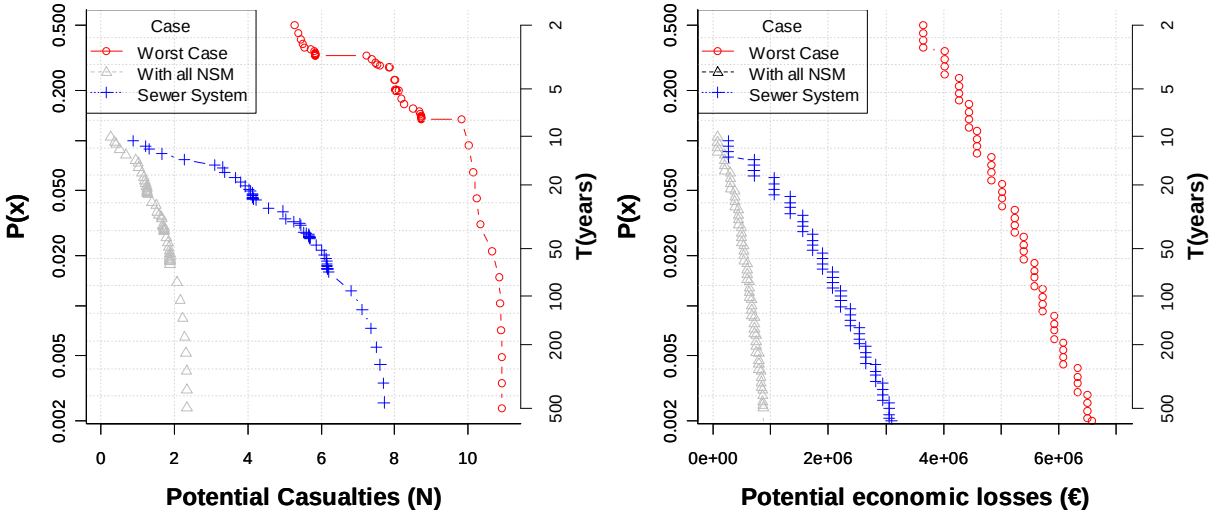

Figure 3.15 Societal and economic risk by different NSMs implementation conditions

3.12 Action Force Worksheet

Finally a very simple and easy to understand worksheet for the action forces and population are laid out in Table 3.18, according to the 5 warning levels used by the CECAT agency:

Table 3.18 Worksheet for the action forces and population for flood emergencies

Entity	Pre-Advice	Pre-Alert	Alert	Emergency Type 1	Emergency Type 1
CECAT	Warning advertisement	Warning advertisement	- Warning advertisement - CECOPAL conformation	- Warning advertisement - CECOPAL conformation. - Ask for Regional assistance	- Warning advertisement - CECOPAL conformation. - Ask for National aids.
Government of Catalonia	-	-	- Follow the established protocols	- Follow the established protocols - Aid management	- Watch the established protocols - Aids Management -Monitor the emergency and physical resources
ACA	Warning advertisement	Warning advertisement	- Warning advertisement	- Warning advertisement	- Warning advertisement

Arenys de Munt Municipal Council	Follow advice	Mayor and Police warn of implications	- Manage the warning to the population. -Specific Orders to the police	- Provide all the available resources. -Inform the disaster consequences to CECAT and Government of Catalonia	- Provide all the available resources. -Inform the consequences of disaster to CECAT and Government of Catalonia.
Police	-	-	- Follow the situation - Warn the population	- Warn the population. – Close streets (to pedestrians)	- Warn the population. – Close streets – Evacuation help
Fire Dept.	-	-	- Follow the situation -Attend emergencies	-Attend emergencies -Start evacuation	- Evacuate affected people -Help the injured
Population	-	-	-	- *"Post"* Implementation	- Install *tajaderas* (gate wedges) - Install sand bags

3.13 Summary

Flood risk management focusing on NSMs is a promising field for the mitigation of the consequences of disasters. Large structural investments have been made in recent years by agencies and government, with which the residual risk mitigation by NSMs may be interesting to follow over the coming years. A total of seven NSMs were considered for their possible implementation or improvement in Arenys de Munt. Some of them, such as risk communication and land use planning have been implemented within the Arenys de Munt basin. Others like the early warning system and disaster exercises (drills) are in full implementation by diverse agencies such as CECAT, ACA or METOCAT.

To develop and materialize NSMs in Arenys de Munt, multiple meetings have been held with the different agencies in charge of risk management. As a shared experience we can conclude that it is a very difficult and complex task for agreement to be achieved at these gatherings. The reason

is that in order to apply the NSMs, responsibilities have to be assigned. As a result of this, the municipal action plan (MAP) for flood risk (pluvial flooding in Arenys de Munt) is a multidisciplinary task to attempt to reach common agreement between the agencies involved. In the case of Arenys de Munt, CECAT, METEOCAT, ACA, the Maresme Area Council and the Arenys de Munt Municipal Council were all involved.

Some conclusions regarding the NSMs implementation in the Arenys de Munt basin are laid out below:

1. In the risk assessment (societal and economic) different hypotheses had to be used. On the one hand, the people at risk had to be estimated (two types of land uses), on the other hand, an analysis was carried out considering an event in which urban drainage system and gutters collapsed (cited as the worst case), another case where an early warning system was applied. Finally, the reduction that the implementation of several NSMs could bring was applied (see section 3.11).
2. In Arenys de Munt, if 500,000 € per year was made available for flood risk management it would be an amount considered excessive and "fictitious" because many of the resources that are specified already exist, such as the police force and fire dept. This means that the real cost of the NSM implementation would be less. If we subtract the corresponding money from the resources available, the final cost for flood risk management in the Arenys de Munt basin is equal to the sum of the MAP (Municipal Action Plan) and the EWS, meaning around 33,000 €. The inhabitants of the town (around of 8500 people), would give a total of 3.89 € per capita. Another consideration observed relating to these types of measures or investments is the economical Expected

Annual Flood Damage (EAFD). This value can be obtained from the F-€ curve set out in Figure 3.10 (HEC, 1989), summarizing the multiplication between economic losses (each event) by its probability density. The probability associated with the events of Figure 3.10 is the cumulative probability, making it necessary to find this value. The EAFD is equivalent to 119,383 €/year, thus we can conclude that the NSMs investment in the Basin is below the amount that can be lost annually.

3. As for the NSMs application/optimization risk reduction coefficients were approximated (for societal and economic risk). It is recommended that these reduction coefficients are researched extensively, because they can lead to a greater knowledge and subsequently better risk management. Obviously these coefficients can only serve the Arenys de Munt basin.
4. One of the future ways to research NSMs is to track and follow the NSMs implemented, as could be done in some basins with fully developed NSMs and after a real event, suffered economic losses and human casualties. These basins can be useful when other events occur in order to be able to calibrate NSMs' mitigation coefficients. Additionally the NSMs have relatively high uncertainty because this kind of measures is not applied equally from one place to another, thus, the mitigation can vary significantly. However, as the measures described are executed and at the same time are subjected to flooding events, the mitigation coefficients could be corrected or modified.
5. A worksheet for the action forces (agencies) and the population is presented. In this worksheet the role to be developed by each agency in case of flood emergency is clearly laid out. This worksheet is also time discretized according to the warning types issued by CECAT.

Chapter 4: Uncertainty in Pluvial Residual Risk Assessment due to Flash Floods

4.1 Abstract

Risk management is an essential component for good governance of stakeholders in flood emergency events. The uncertainty related to the hydrologic and hydraulic variables affects the risk assessment due to the lack of knowledge of the real values of these parameters, leading to a significant variation in the result of the risk assessment. The present chapter shows this effect on the residual risk assessment, computed after mitigation by applying some Structural and Non-Structural Measures to the Arenys de Munt basin. Uncertainty analysis was developed to demonstrate the variability of the risk results after propagating the uncertainty from the hydrological and hydraulic variables. Finally, an analysis of the Expected Annual Damage was made to obtain a quantitative indicator when structural measures are designed in terms of their optimal return period. A new complementary value is defined, the Optimal Expected Annual Damage, to improve the data availability in the decision making process.

KEY WORDS: Uncertainty, Non–structural measures, residual risk assessment, emergency planning, risk reduction.

4.2 Introduction

The work presented here consists of an analysis of uncertainty propagation along with the residual risk assessment. The SUFRI residual risk analysis methodology is employed. The scope

of the SUFRI EU project (Jobstl et al., 2011) was the improvement of flash flood risk management in case of flooding events, focusing on non-structural measures (NSM). This project belongs to the ERA NET Crue Network (European Flood Research). Recently there has been a growth in public interest to develop sustainable transnational strategies for the protection and management of flood risk. Most of these strategies are focused on NSM implementation, early warning systems, vulnerability analysis and residual risk assessment. A total of six universities from four European countries with five experimental catchments were involved in this project. By performing accurate simulations of the residual risk, it was evident that the uncertainty in the parameters could not be neglected.

The experimental basin corresponds to the Arenys the Munt basin, which is located in the Catalonia region in the named geopolitical subdivision of Maresme (Figure 4.1), more specifically, in the area between the towns of Badalona and Blanes enclosed by the Besós and Tordera rivers. The aforementioned region is located on the Catalan coast, and is surrounded by a mountain range and the sea, affecting the weather of the local area. The Arenys basin is known for its historical river flooding caused by intense convective storms (Forn i Salvà, 2002). Also the impossibility of an accurate rainfall estimation under this kind of phenomena means that all the processes involved with the rainfall variable are very unpredictable. Therefore, inherently to the risk assessment, there are correlated errors due to the impossibility of good accuracy in this estimation.

The study of the behaviour and consequences of these errors is known as uncertainty analysis. Evidently, more variables like the rainfall-discharge transformation, the hydraulic characteristics

(Manning coefficient, geometric properties, the propagation model, etc.) and the vulnerability variables could affect the risk assessment, and therefore, affect the uncertainty analysis.

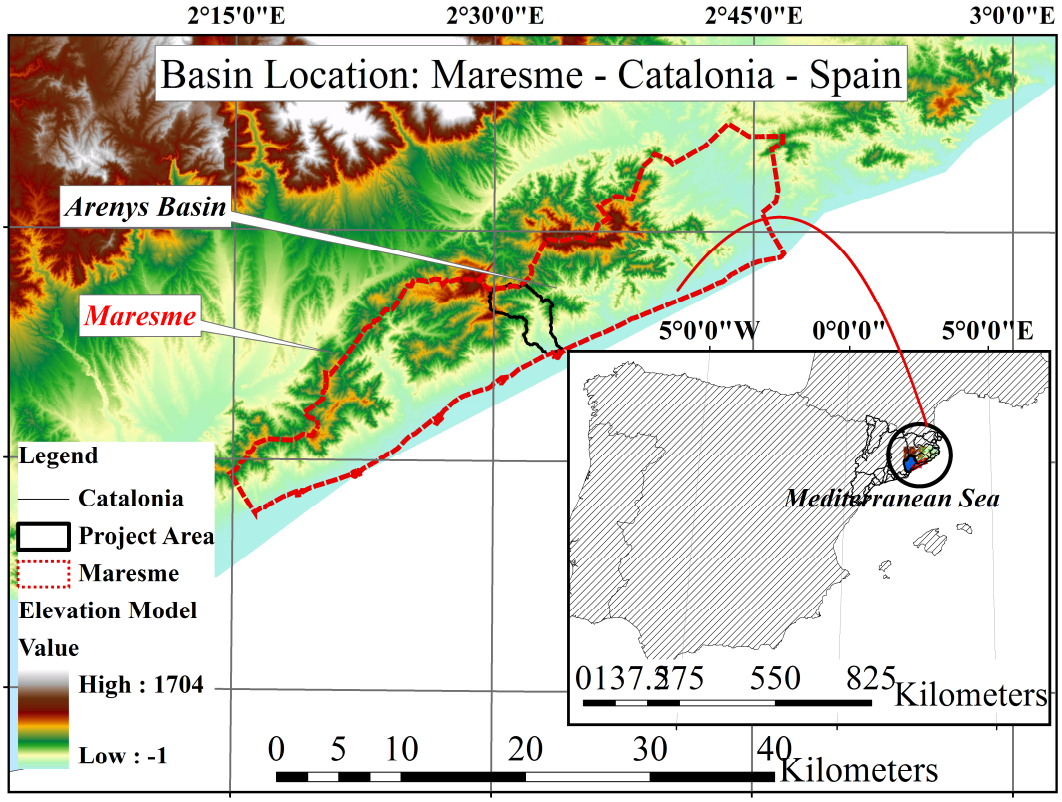

Figure 4.1 Arenys de Munt basin localization

The international community has begun to identify the benefits of the NSM implementation in flooding mitigation (CRUE, 2009; Jobstl et al., 2011; Wheater et al., 2007) due to the limited success of the current infrastructure. In many places a large amount of resources have been invested to diminish the flood risk, many of these investments correspond to structural measures (SM). The Arenys de Munt basin is included in this long list, because recently a flood diversion area was built. The main stream of the Arenys de Munt Creek has been channelized along two kilometres through a rigid encroachment by a Box Culvert. The total amount of investment exceeded 14 M€, with a cost per capita superior to 1750 €/person. Additionally the construction

of a Structural Measures almost always leads to environmental impacts. The NSM implementation can be cheaper and faster because it includes measures such as risk communication improvement, early warning system and an evacuation plan, among others things that rely more on the experience and behaviour of the entities involved in flooding scenarios.

The Arenys de Munt basin has been chosen as a test basin due to the population`s experience with flood events and the hydrologic data availability. Several lessons have been learned from the behaviour of the actors (population and entities) and their flood risk communication (Figure 4.2).

Figure 4.2 Left: risk communication managed by the police in which warning issue and evacuation is made in 10 min. Right: barriers mobilization of the main Arenys stream

The analysis of the flooding residual risk assessment in the Arenys basin due to pluvial flooding events was conducted following the definition of the SUFRI methodology , where the residual risk is defined as the part (quantitatively) of the risk that remains after structural measures are applied. Nowadays, floods can never be absolutely prevented or predicted, therefore, there will always remain a "***Residual Risk"***, even if structural measures are exhaustively applied (Faber,

2006; Escuder et al.. 2012). Hence, the uncertainty analysis becomes important because it is relevant to identify and define the error in our estimation as opposed to trying to improve the risk assessment methods themselves (Beven, 2011).

After the application of structural measures, the residual risk assessment shown herein includes seven NSM. All of these are included in the so-called Municipal Action Plan (PAM) that corresponds to the EU Flood Directive as the city council Risk Management Plan. The benefits of the NSM's implementation are discussed in Escuder-Bueno et al. (2012) and Jobstl et al. (2011). A complete methodology for the NSM's implementation and evaluation is found in Jobstl et al. (2011) and in the present document it focus on the uncertainty related to the risk assessment of the residual risk. Finally, to analyse the residual risk assessment uncertainty some hypotheses were imposed in the hydrology and, consequently, in the hydraulic estimation (known as Flood Hazard assessment) and also in the vulnerability assessment to evaluate the hydrological bias.

4.3 The SUFRI methodology of risk management planning focused in NSMs

The SUFRI Methodology includes eight steps to assess the residual risk focusing on the NSM optimization. The optimization step is executed due to the fact that different combinations of NSM implementation could bring different mitigation itself (Joebst C. et al., 2011). The mentioned steps are described below:

1. Analysis of the structures of emergency entities organization: this is the identification of all the actors involved in flood emergency events, trying to identify the organizational

weakness of the present scheme. This analysis could bring ideas of which NSMs can be implemented and which measures are harder to perform for institutional or organizational reasons.

2. Identification of residual risk of flooding: in this part the type of risk considered is identified and defined. The calculation hypotheses are imposed to assess the risk. The uncertainty analysis starts at this point where the hydrologic variables and the hydraulic uncertainty propagation could leads to a different hazard assessment and consequently, different risk values.
3. Risk assessment: in this part the amount of risk (either societal or economic) is assessed numerically. Three cases are considered in the present chapter to visualize the influence of the uncertainty on structural and NSM.
4. Evaluation of NSMs: From the entire available NSM's those seven that could be applied are chosen.
5. Assignment of those who are to perform NSMs: this is the establishment of who has to act in case of emergency. This means that all the NSM's to be implemented will materialize with the respective actor/or entity.
6. Establishment of restrictions regarding the implementation of NSMs: The available resources for risk management are limited. At this stage this limitation, in terms of budget or employees, is established.
7. Construction of the NSMs vs mitigation matrix: At this step the optimization is made. Due to the basin limitation resource, different NSMs combinations could be made (resulting in different risk mitigation). Every combination should overcome the constraints imposed by the restrictions defined in step 6.

8. Worksheet for the action force: The option that maximizes the societal and economic risk mitigation is chosen from the different NSMs combinations.

A more detailed explanation of the SUFRI methodology could be found on, Joebst et al. (2011) and Escuder et al. (2012).

4.4 Uncertainty propagation from the hydrology in the risk assessment

The first step in the flooding risk assessment is to establish the quantity of water that the river/or streams in the zone of study could have during a storm in order to assess the hazard (Pender and Faulkner, 2011). This study is focused on the pluvial residual risk that includes the analysis on the urbanized areas. Consequently the main hydrologic analysis outcome should be the rainfall. Starting from this point, the uncertainty is being propagated due to the application of hydrological methods. Leaving aside the uncertainty of the hydrological methods, the rainfall variable itself adds uncertainty to the risk assessment due to the impossibility of a complete and accurate measurement (spatially speaking) because the variable measurement is limited to one point in space (pluviometers) or coarser information for little basins (radar system). Another source of uncertainty is related to the shorter length of the time series (Quintero et al.; Velasco, 2009). It is commonly observed that rainfall extrapolation analysis up to 1000 year return period is made with a 20 year long data series.

In statistics of extreme events a probability distribution is adopted and fitted to the available data. If the data is not representing the extreme events due to limitations in the spatial resolution or the time series length wide confidence intervals emerge increasing uncertainty (spatially and timely),

if higher return periods or large areas want to be assessed. Both, the selection of a particular probability distribution and, as is demonstrated in this work, the parameters estimator method used to fit the data (moment method or least square method) play a crucial role in the whole process of the uncertainty propagation. Following the SUFRI methodology described above, in the third step, the flood hazard has to be quantified through the depth and velocity. Those are related to the discharge flow of rivers or streets, the last in the pluvial flooding case. Consequently, the uncertainty in the hydrology analysis causes uncertainty in the discharge flow estimation and hence leads to variation in the hazard evaluation.

Herein the uncertainty coming from precipitation (hydrologic uncertainty), statistical fitting method, and hydraulic parameters (Manning coefficient) has been analysed. In this chapter the Gumbel extremes distribution is considered, using two parameter distribution estimator methods: Moments Method (MM) and Least Square Method (LSM). The total amount of risk assessment cases studied includes 1080 cases: analysing nine confidence intervals, two parameter estimator methods, ten streets, two Manning coefficients (n=0.015 and n=0.030) and 3 risk configuration cases: present, Structural Measures (SM), Structural with Non-Structural Measures (SM+NSM).

4.4.1 Precipitation confidence intervals

As previously mentioned, the hydrological uncertainty has been analysed through different confidence intervals and statistical methods. In Figure 4.3 left, differences between the MM and LSM are observed which induces different results according to the statistical method implemented. In Figure 4.3 right, 4 confidence intervals for the moment method example are shown. Starting from these confidence intervals and parameter statistical methods, different

discharge flow will be generated when the rainfall-discharge transformation is made, giving a wide range of discharge flow possibilities for a specified return period (instead of a unique value).

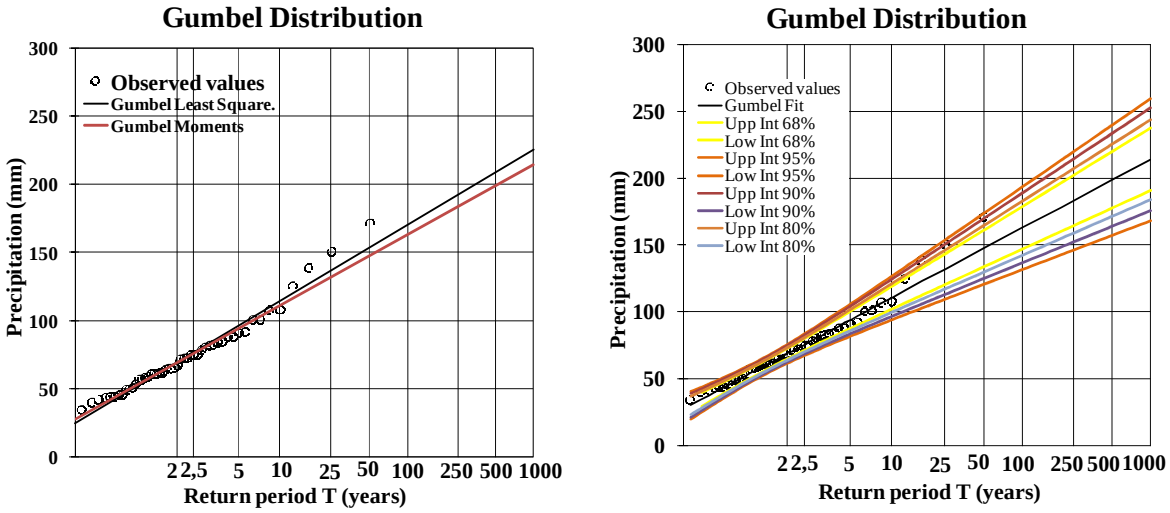

Figure 4.3 Left: Cumulative probability associated to a Linearized Return Period Variable for each statistical method. Right: confidence intervals for MM in Arenys de Munt basin

4.5 Test Case Definition

Once the pluvial flooding risk has been identified as the main phenomenon, it is mandatory to define the components, hazard and vulnerability, and impose the calculation hypothesis to estimate the residual risk in the basin (DEFRA, 2010). The exposure is implicitly managed in the vulnerability assessment (Pender and Faulkner, 2011). Due to the small size of Arenys de Munt village and to quantify the pluvial flooding as a residual risk in the basin, the risk assessment was developed along the principal streets of the town. A total of 10 streets in accordance with their drainage area and their slope were selected (Figure 4.4). This is due to the fact that the flow discharge is proportional to the drainage area and the velocity is proportional to the streets slope.

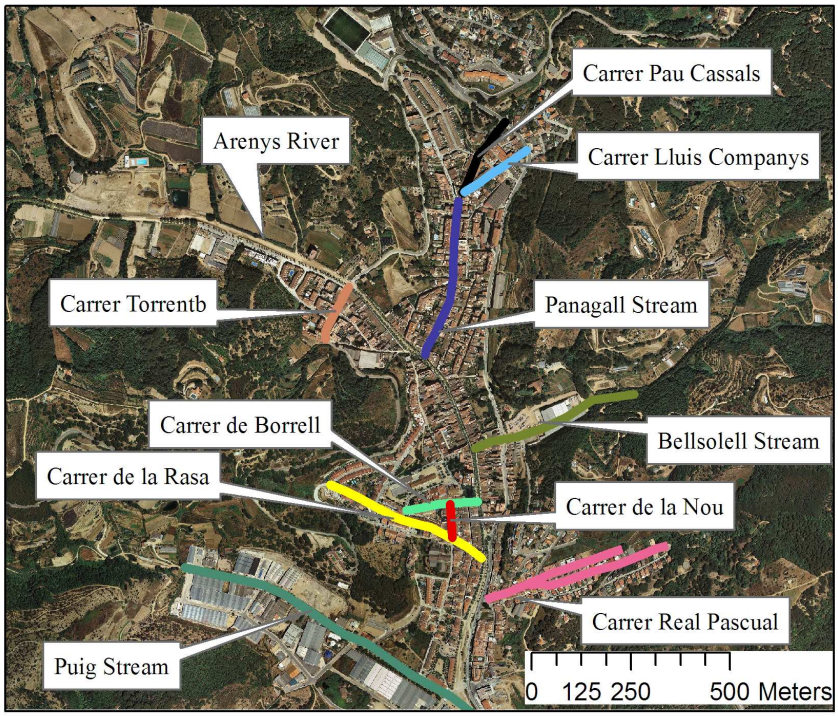

Figure 4.4 Arenys de Munt selected streets and principal tributaries

4.5.1 Arenys de Munt selected streets

Applying the aforementioned criteria the main characteristics of the selected streets are shown in Table 4.1. In this table it can be seen the higher values of the streets slopes which are directly related with the velocities on the streets, as well as the streets drainage area which also affects the hydraulics depths.

Table 4.1 Geometric characteristic of the Arenys de Mar/Munt streets

Street	Area (km²)	Width (m)	Stream Slope (%)	Elevation Diff. (m)	Maximum Stream Longitude (m)	Urbanization Percentage (%)
Panagall	0.2382	4.0	14.6	284	1939	50
Puig	0.1114	8.0	12.2	423	3460	15
Bellsolell	0.0172	3.0	12.6	197	1557	10
Calle Real de Pascual	0.018	3.0	12.2	184	1506	15
Carretera de Torrentbo	0.0151	7.0	18.7	111	593	40
Carrer de la Rasa	0.0519	3.0	14.7	133	903	60
Carrer can Borrell	0.0059	2.7	3.6	4	110	100
Carrer de la nou	0.0031	2.0	1.1	1	87.	100
Carrer Pau Casals	0.0134	3.3	7.9	16	203	100
C./ Lluis Companys	0.0138	3.8	8.6	15	175	100

As commented by (Faber, 2006) slope and drainage area affects the risk considerably. According to the FLOODsite project the risk is estimated as:

$$R = H \cdot V \cdot E \tag{4.1}$$

In which H is the hazard, V the vulnerability and E the exposure. In the SUFRI project the exposure is implicitly managed in the vulnerability assessment.

4.6 Hazard

To quantify the hazard some hypotheses are made in the hydraulic model:

1. It was assumed that all the roofs of the building and houses are not connected to the drainage system, thus, all the rainfall will run directly through the streets.
2. It is assumed that in case of heavy rainfalls the house and street gutters are filled. This will be referenced as the “worst Scenario”.
3. It is supposed that the rational method is valid to evaluate the rainfall/runoff process. This leads to neglect the evaporation, transpiration and infiltration processes in the hazard assessment.
4. Uniform steady flow regime is assumed, whereupon the losses could be assess through the Manning formula.

The following expressions for the hydraulic depth and velocity (Chow, 2000) are obtained:

$$h = \left(\frac{nA_b I}{S^{1/2} b} \right)^{3/5} \tag{4.2}$$

$$v = \frac{1}{n}\left(\frac{nA_b I}{S^{1/2} b}\right)^{2/5} S^{1/2} \tag{4.3}$$

Where: v is the flow velocity, I is the rainfall intensity (mm/h), A_b is the contributive area, n is the Manning coefficient, h is the hydraulic depth, b is the width of the channel and S is the channel Slope. The confidence intervals have been computed for all the streets using both statistical parameter estimation methods. The hydraulic uncertainty was considered using the influence of the roughness friction factor that affects significantly the risk assessment. In our study, two extremes values of 0.015 and 0.030 were used for the Manning coefficient n, that appears on both (4.2) and (4.3) hydraulic equations. In Figure 4.5 (left) the hydraulic depth for several return periods in the analysed streets are displayed. In Figure 4.5 (right) are shown an example for the Panagall street depths confidence intervals with rainfall fitted by the MM and a manning coefficient equal to $n = 0.015$.

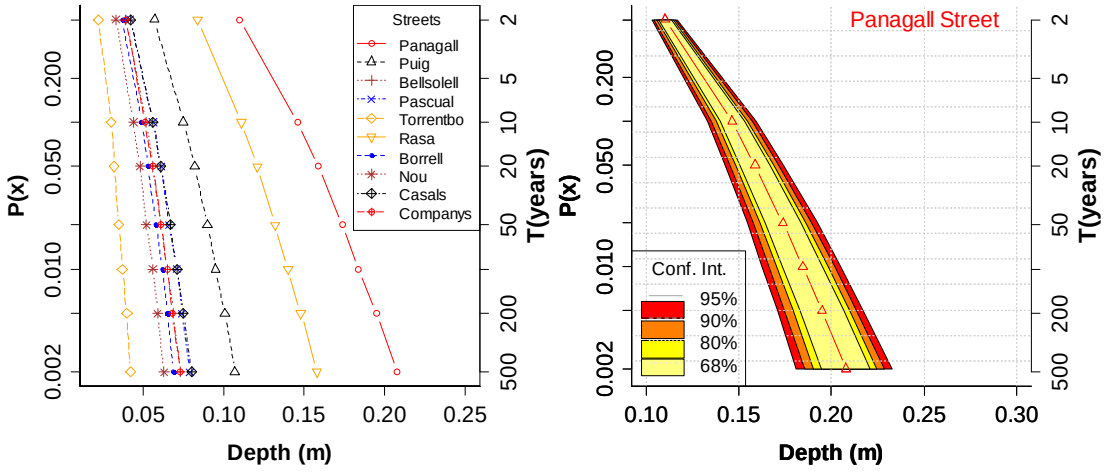

Figure 4.5 Depths and confidence intervals of Arenys de Munt streets (Moments Method and n=0.015)

Several confidence intervals could be plotted according to different Arenys the Munt streets. Also the parameters estimator method (MM or LSM) and the selected manning coefficient could generate several graphics. The vertical axis in the figures is the return period expressed as cumulative probability. It is clear that the hydraulic depth can vary significantly according to the chosen parameter.

In Figure 4.6 (left) the Arenys de Munt streets' velocities and the Panagall street example (right) are displayed (both in case of MM and a manning of 0.015). It can be seen that the velocities exhibit more dispersion than the depths for each return period, consequently more risk assessment uncertainty could be expected due to this variable.

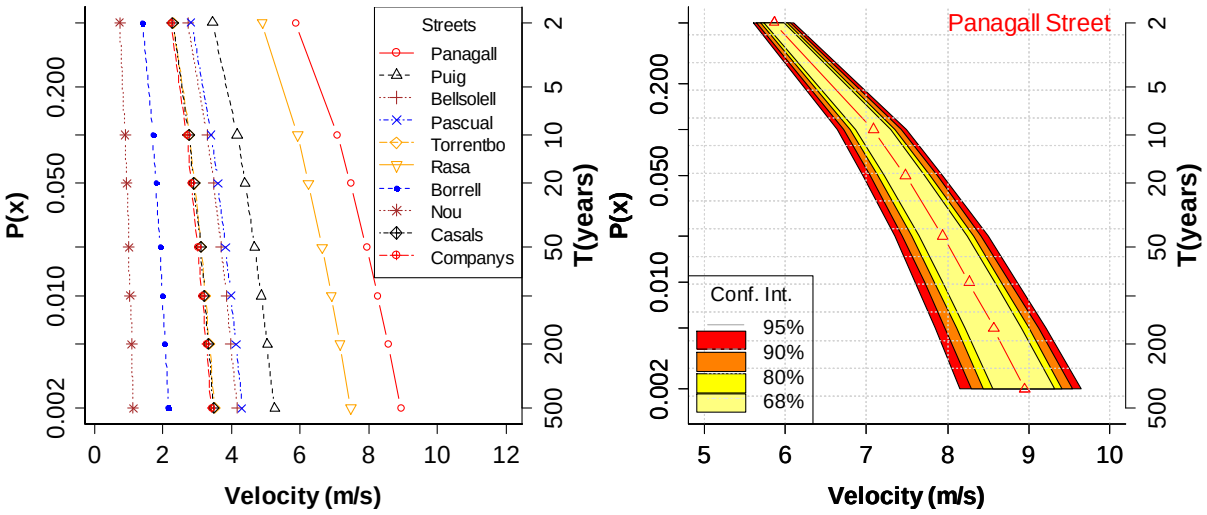

Figure 4.6 Velocity and confidence intervals of Arenys de Munt streets (Moments Method and n=0.015)

The great magnitude of the velocities evaluated over the streets is justified due to the slopes that occur throughout the town.

4.7 Vulnerability assessment

The vulnerability assessment includes a damage analysis of the structures and the possible loss of life. Vulnerability should link hazard variables to damage. Relying on the analysis performed in the previous section the hazard variables involved should be depth and flow velocity.

4.7.1 Casualties vulnerability assessment

First the hazard effect on people is described. Different variables can affect a pedestrian crossing a flooded street. In the SUFRI project two factors were considered: the pedestrian slides down and the overturning moment produced by the flow discharge forces over the pedestrian's foot (Nania, 1999). Other variables like the experience, strength or age of the pedestrian could affect the vulnerability under pluvial flooding but are discarded in this analysis due to the lack of data. These two factors combined with the flow depths and velocities are used to construct the Table 4.2.

Slide down and overturning moment criteria evaluation:

The susceptibility of a pedestrian to slide down due to the inertial flow force can be found through a security factor analysis, where the resistance against the instability forces are compared. This analysis is extensively explained in (Nania, 1999):

$$v^2 h \leq \frac{2\mu(W - V_{ped}\gamma)}{2C_d b_p \rho} \leq \frac{2\mu W_{equiv}}{2C_d b_p \rho} \tag{4.4}$$

Similarly, considering the overturning moment and applying the same security factor as before it obtains:

$$v^2 h^2 \leq \frac{W_{equiv} b_p / 4}{2 C_d b_p \rho} \tag{4.5}$$

Where μ is the friction coefficient between the street surface and the shoe sole, W and W_{equiv} are the weight and the equivalent weight of the pedestrian (subtracting the weight of water displaced by the submerged foot volume V_{ped}), C_d is the drag coefficient, b_p is the width of the pedestrian area opposed to the flow and ρ is the water density. Both parameters are in terms of the hazard parameters: flow velocity (v) and flow depth (h). The results obtained for different streets for the *"worst case"* test are summarized in Table 4.2 (only for M.M. and Manning coefficient, n=0.015 combination). Different vulnerability parameter values lead to different severity values and will be explained in the severity section. This security factor should be greater than 2.0 otherwise it could be unstable (Nania, 1999). If the following parameters are considered: a friction factor coefficient equal to 0.3 (Concrete / Rubber), water density of 1000 (kg/m³), a drag coefficient of 0.8, an equivalent pedestrian weight of 650 N and a foot pedestrian width of 0.2 m, the vulnerability criteria limits are:

$$v^2 h \leq 1.0 \left(m^3 / s^2 \right) \tag{4.6}$$

$$v^2 h^2 \leq 0.2 \left(m^4 / s^2 \right) \tag{4.7}$$

Table 4.2 Stability vulnerability criteria limits for different return period (Moments Method and n=0.015)

Stream Way	T=2 years		T=10 years		T=20 years		T=50 years		T=100 years		T=200 years		T=500 years	
	v².h	v.h	v².h	v.h	v².h	v.h	v².h	v.h	v².h	v.h	v².h	v.h	v².h	v.h
Panagall	3.77	0.64	7.34	1.04	8.87	1.19	11	1.38	12.6	1.53	14.3	1.67	16.7	1.86
Puig	0.67	0.2	1.31	0.31	1.58	0.36	1.95	0.42	2.25	0.46	2.55	0.51	2.97	0.56
Bellsolell	0.29	0.11	0.56	0.17	0.68	0.19	0.84	0.23	0.96	0.25	1.09	0.27	1.27	0.31
Pascual	0.33	0.12	0.65	0.19	0.79	0.22	0.97	0.25	1.12	0.28	1.27	0.31	1.48	0.34
Torrentbo	0.12	0.05	0.23	0.08	0.27	0.09	0.34	0.11	0.39	0.12	0.44	0.13	0.52	0.15
Rasa	2	0.41	3.9	0.66	4.71	0.75	5.82	0.88	6.7	0.97	7.6	1.06	8.85	1.18
Borrell	0.07	0.05	0.14	0.08	0.17	0.1	0.21	0.11	0.24	0.12	0.28	0.13	0.32	0.15
Nou	0.02	0.02	0.04	0.04	0.04	0.05	0.05	0.05	0.06	0.06	0.07	0.06	0.08	0.07
Casals	0.22	0.1	0.43	0.16	0.52	0.18	0.64	0.21	0.73	0.23	0.83	0.25	0.97	0.28
Companys	0.19	0.09	0.37	0.14	0.45	0.16	0.55	0.18	0.64	0.2	0.72	0.22	0.84	0.25

In Figure 4.7 the vulnerability criteria's ($v^2.h$ and $v.h$) results for the MM and the Manning coefficient equal to 0.015 are presented for Panagall Street. From these, it can be seen that the vulnerability parameter $v^2.h$ is more dispersive than the $v.h$ parameter. This is because in the first parameter, the velocity has a square exponent, and as seen previously, the velocity is more dispersive than the depth.

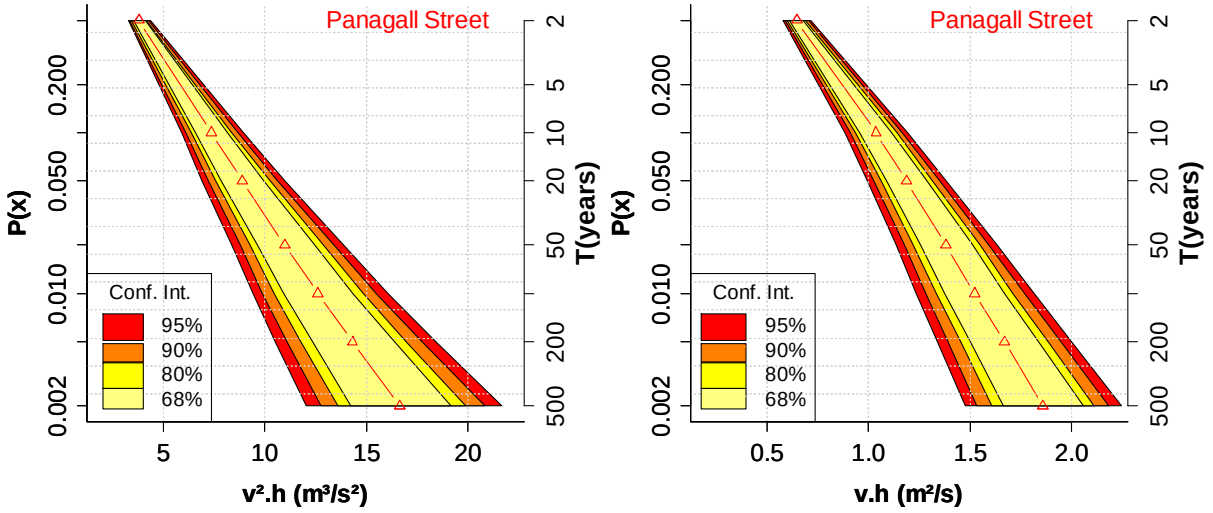

Figure 4.7 v².h and v.h vulnerability parameters in Panagall street (Moments Method and n=0.015)

To assess the risk the results are computed for the different confidence intervals, statistical methods (LSM and MM) and hydraulic roughness coefficients following the uncertainty analysis.

Severity:

As explained above different human susceptibility reasons could cause loss of life under flooding conditions events. Nowadays, in risk management sciences, the so called Flood Severities (S0, S1, …) are discretized according to flood conditions that subsequently result in fatality rates.. In the SUFRI project five flood severity levels were discretized (Joebst et al., 2011; Escuder et al., 2012) in accordance to the different possible vulnerability criteria combinations (see Table 4.3).

Table 4.3 Flood severity for different vulnerabilities criteria

Flood Severity (S)		Depth h(m)	Velocity v(m/s)	Overturning parameter v.h(m^2/s)	Sliding parameter $v^2.h(m^3/s^2)$
S0	Negligible severity	<0.45	<1.50	<0.50	<1.23
S1	Low severity	<0.8	<1.60	<1.00	<1.23
S2	Medium severity	<1.00	<1.88	<1.00	<1.23
S3	High severity	>1.00	>1.88	>1.00	>1.23
S4	Extreme severity	>1.00	>1.88	>3.00	>1.23

Fatality rates (FR):

The fatality rates should be computed for all the considered cases, named “risk configurations”. This means that the NSM risk mitigation in terms of fatality rates should be converted in a quantitative manner. The EWS mitigation effects have been previously established (Escuder et al., 2012). NSM such as the evacuation, mobilization or risk management planning measures were integrated in the mitigation coefficients developed for the NSM in the SUFRI project. The values adopted in this study are adapted to the particularities of Arenys de Munt and defined

under expert judgment. In the Arenys de Munt case study, different risk configurations with and without structural and non-structural measures have been considered. In the present chapter three cases are shown: a first case without any measures (structural and non-structural) called "*worst case*", the case in which an early warning system (EWS) is operative and the case of a sewer system completely established including the EWS. The fatality rate values are extracted from Table 4.4.

Table 4.4 Fatality rates for Arenys de Munt in terms of flood severity and the EWS (Escuder et al., 2011)

Flood severity	S0	S1	S2	S3	S4
FRp without EWS	0.0003	0.0018	0.0033	0.0090	0.0384
FRp with EWS	0.0002	0.0015	0.0027	0.0075	0.032

In Table 4.5 the severity levels for different streets are presented, the scenario considered is the "*worst case*", LSM, Manning equal to 0.015 and the confidence interval is 50%. The flood severity for all the streets and cases considered at Arenys case study was delimited combining the vulnerability criteria of the severity section and the results of the hazard assessment. In Figure 4.8, Figure 4.9 and Figure 4.10 an example for the Panagall Street with a Manning of n=0.015 and the MM method is displayed.

Table 4.5 Flood severity levels by pluvial flooding LSM and n=0.015

Stream Way	T=2	T=10	T=20	T=50	T=100	T=200	T=500
Panagall	S3	S3	S3	S3	S3	S3	S3
Puig	S3	S3	S3	S3	S3	S3	S3
Bellsolell	S3	S3	S3	S3	S3	S3	S3
Pascual	S3	S3	S3	S3	S3	S3	S3
Torrentbo	S3	S3	S3	S3	S3	S3	S3
Rasa	S3	S3	S3	S3	S3	S3	S3
Borrell	S0	S2	S2	S3	S3	S3	S3
Nou	S0	S0	S0	S0	S0	S0	S0
Casals	S3	S3	S3	S3	S3	S3	S3
Companys	S3	S3	S3	S3	S3	S3	S3

Almost all the streets have a severity of S3 as shown in Table 4.5. Also for the different confidence intervals the severity levels remain unchanged. This is one of the major reasons why in the societal risk assessment (exposed in section 4.8.1) the potential casualties' values do not change considerably. This characteristic is a consequence of the higher velocities existing in the streets making it so that all the streets analysed for different statistical methods, confidence intervals and manning coefficients are catalogued under the same flood severity (usually S3)

4.7.2 Economic potential losses (€)

To assess the potential economic losses, the vulnerability of the structures (damage in building etc.) is usually estimated through the damage-depth curves. Evidently these curves depend strongly on different parameters like the type of structure and material used for construction in the particular zone. The local official institution A.C.A. (regional water agency) has developed damage curves for the Catalonia region in the so-called report INUNCAT (2010), particularly for Arenys de Munt the data are shown in Table 4.6.

Table 4.6 Damage Curve for the SUFRI project (from the INUNCAT report)

Water depth (m)	0	0.2	0.4	0.6	0.8	1	1.2	1.4	1.6	1.8	2	4.9
Damage (%)	0	1	2.5	5	14	40	60	67	71	75	77	77

Similar to the fatality rates, the economic loss reduction due to an EWS implementation was quantitatively assessed. In order to do this, the results of the project called EWASE (2008) were used.

To assess the economic potential losses it is necessary to summarize all damage costs (direct, indirect and opportunity costs etc.) in a monetary unit per area (€/m^2). A more complete analysis could be done discretizing each type of damage cost for a particular zone.

4.8 Risk assessment results

In the case study the total risk is the result of all individual streets risk contributions. This hypothesis is based on the fact that the catchment area is small enough to assume that the events are simultaneous in all the Arenys de Munt streets. To assess the risk in equation (1) it is necessary to evaluate the Exposure E., taking into account that the societal exposure in the basin changes accordingly to the season of the year.

There could be more or less people in the basin due to holidays, day of the week, hour of the day, or at night. Another reason to discretize the risk assessment time window is found in the fact that the extreme events are more expectable in some periods of the year (October – November and March – April in Arenys de Munt) than in others (Pender and Faulkner, 2011). In the Arenys de Munt basin 4 time window intervals were used. They are the product of 2 seasonal time window intervals and 2 day/night time window intervals. From the rainfall series the probability of occurrence in a specific time window can be evaluated. To perform this, the day and night are considered as the periods between 08:00h to 20:00h and 20:00h to 08:00h, respectively. Summer is defined as the time window from 1st July to 1st September and winter is the rest of the year. The evaluated probability for Arenys de Munt city is shown in Table 4.7.

Table 4.7 The Probability that one event is present in a particular moment of the day (day-night) and a certain season

Winter=0.46		Summer=0.54	
Day	0.75	day	0.5
Night	0.25	night	0.5

Additionally, a spatial discretization was made according to the type of land use (Industrial/Commercial. and residential). This discretization is made in order to include the possible changes of the potential economic risk assessment. To determine the people at risk, a database from the National Statistics Institute of Spain (INE) was used. In Table 4.8 the people exposed to the risk in the selected streets of Arenys de Munt is displayed. Hazard assessment is made for all the individual streets therefore the population in each individual street is established according to their area.

Table 4.8 People exposed to pluvial flood risk in Arenys de Munt, discretized in time

People located at the study area	Summer/day (TC_1)	Summer/Night (TC_2)	Winter/day (TC_3)	Winter/night (TC_4)
$CU_{1(Res.)}$	883	111.3	590	81.9
$CU_{2(Com./Ind.)}$	267	0	267	0
TOTAL	1150	111.3	857	81.9

4.8.1 Potential Casualties

The potential risk of loss of life (named as potential casualties N/year) and potential damage (€/year) are represented by the F-N and F-D curves (Jonkman et al., 2003; Escuder et al., 2012). They express the cumulative probability of exceedance and the consequences of the particular event (Jonkman et al., 2003).

$$1 - F_N = P(N > x) = \int_x^{\infty} f_N(x) \tag{4.8}$$

Where $f_N(x)$ is the probability density function of the number of fatalities per year, and $P(N>x)$ is the probability to have some number of victims N higher than x. The quantification of the risk through these kinds of curves is often used in the dam risk assessment, and has the visual benefit of being able to compare the advantage/disadvantage of the structural or non-structural measure implementation. As mentioned above, the cases with a manning equal to n=0.015, n=0.030, the LSM and MM methods and the 9 confidence intervals were compared using structural and non-structural measures. The F-N curves for the "*worst case*" including the confidence intervals are presented in Figure 4.8, with the LSM and the MM, shown on the left and the right respectively. In orange and grey scale different levels of uncertainty for the cases of n=0.15 and n=0.03 are also represented.

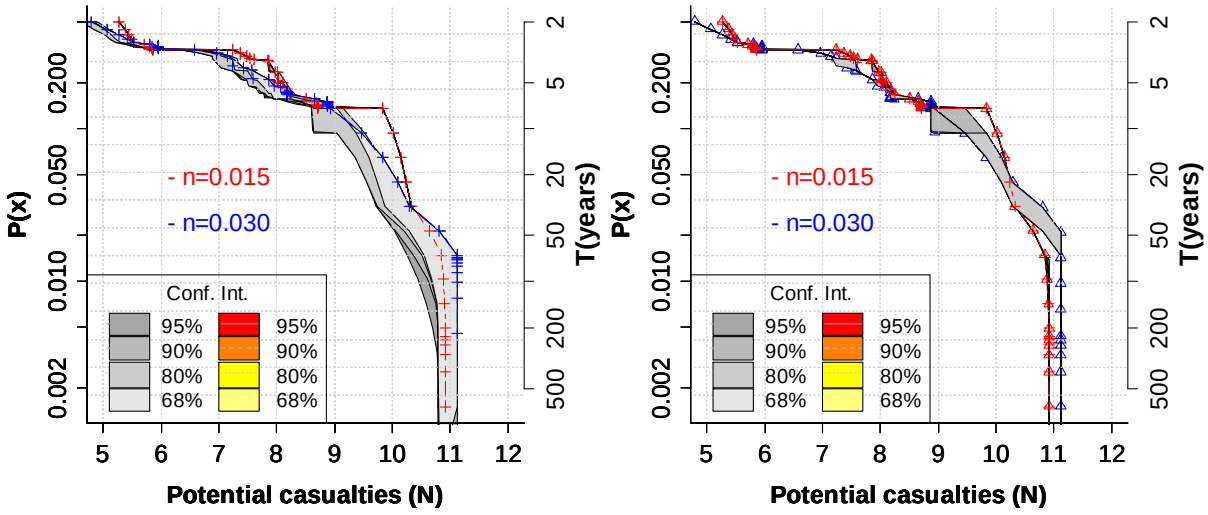

Figure 4.8 Potential casualties in the Arenys Basin in the "worst case", LSM (left) and MM (right)

Figure 4.9 represents the results for the EWS case, and Figure 4.10 presents the results of the F-N curves after the application of all NSM.

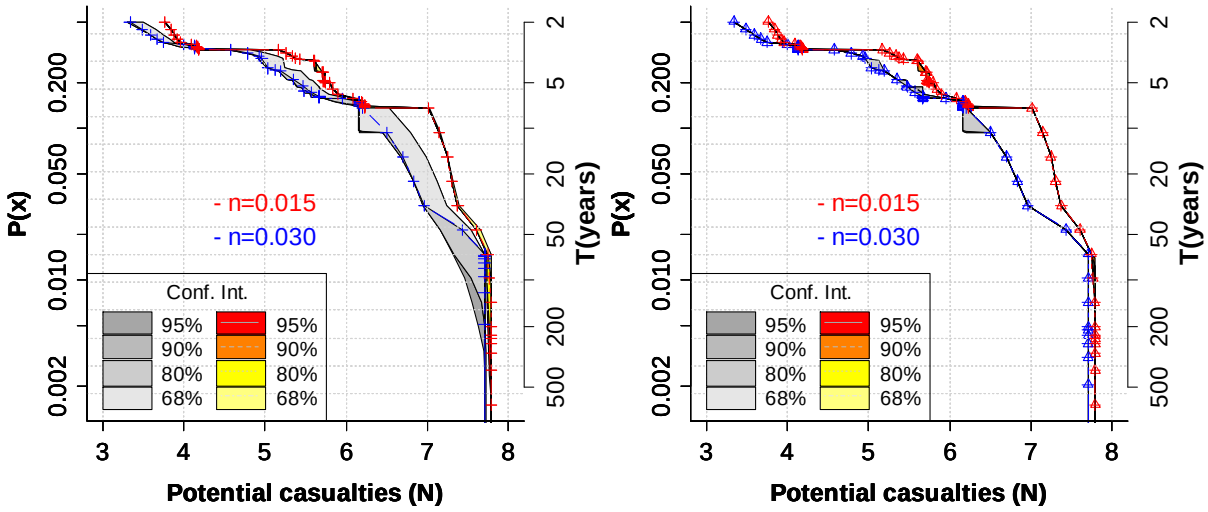

Figure 4.9 Potential casualties in the Arenys basin under EWS, LSM (left) and MM (right)

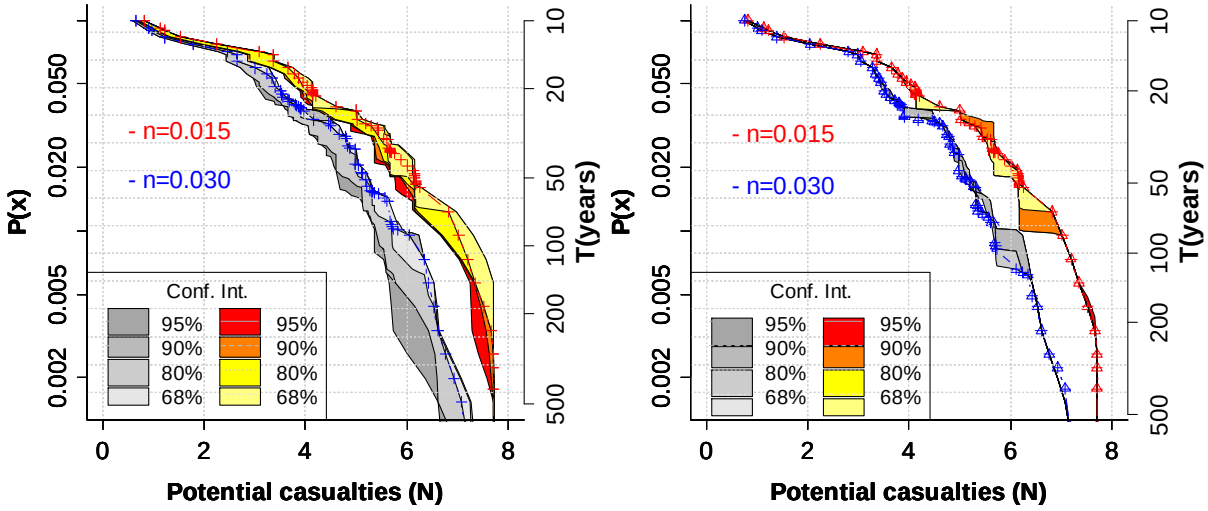

Figure 4.10 Potential casualties in Arenys basin. Case of sewer system + EWS, LSM (left) and MM (right)

According to the uncertainty results from Figure 4.8 to and Figure 4.10 the potential casualties for the 500 year return period could reach a total of 11.1 victims in the “worst case”, decreasing

to 7.7 victims if a EWS is implemented or to 7.2 victims if a sewer system is also developed. This implies a mitigation of 40% in the potential casualties if structural and NSM are implemented. Likewise the risk confidence intervals exposed before, reveal that in the societal risk analysis the SUFRI methodology, in which 4 criteria are proposed to assess the vulnerability, becomes less wide the uncertainty intervals. This is because the graphs show a minimum variability, owing to the confidence intervals does not separate from the expected value in almost all the cases. The main reason for that has been documented in the flood severities of the streets (mainly S3) due to the higher velocities.

4.8.2 Potential Economic Losses

The potential economic losses have been defined in the same mode as the potential loss of life, where a cumulative probability is linked with a value of exceeding probability similar to the potential casualties.

$$1-F_D = P(D>x) = \int_x^{\infty} f_D(x) \tag{4.9}$$

The severity of the damage is assessed through the depth-damage curves commented on section 4.7.2 where the potential damage is weighted by means of the % of the possible damage according to the depth of the flow. The main sticking point in the potential economic losses assessment is found in the cost taxation (in terms of €/m²) of the structures (exposure). The adopted values should take into account direct, indirect, cost opportunity, etc., but it is difficult to enclose all those elements, so only the direct and indirect costs are considered. It is clear that other overhead such as the opportunity costs or intangibles prices like the cultural costs could exist, that might compound the problem. A typical example can be found in the churches,

national heritages buildings or libraries where the cost of the structure (in terms of concrete and steel) would not represent all the real values that the structure could have by itself. These kinds of costs are hardly measurable; however defining the cost by means of a constant per square meters appears to be reasonable. In the Arenys de Munt basin a total cost of 894.6 €/m² for residential zones and 717.2 €/m² for industrial and commercial zones has been established. In the case of complete damage (100%) the cost of losses will be equivalent to the structures flooding area multiplied by the correspondent cost (residential or industrial).

Figure 4.11, Figure 4.12 and Figure 4.13 reproduce the F-D curves for the three risk management cases considered. In this case, respect to the societal risk, there is a clear effect of the confidence interval considered.

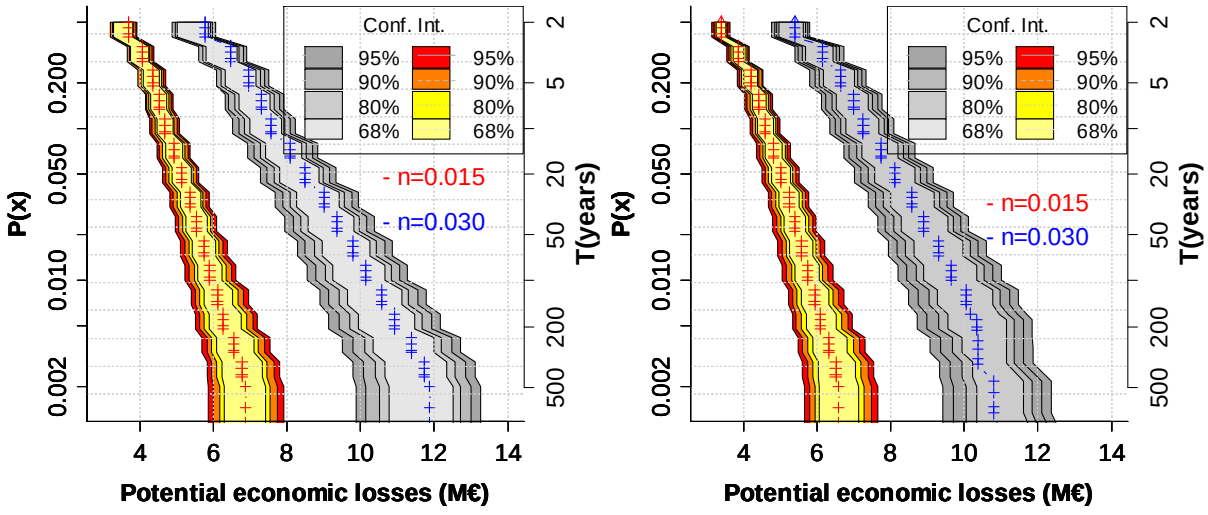

Figure 4.11 Potential economic losses in the Arenys Basin in the "worst case", LSM (left) and MM (right)

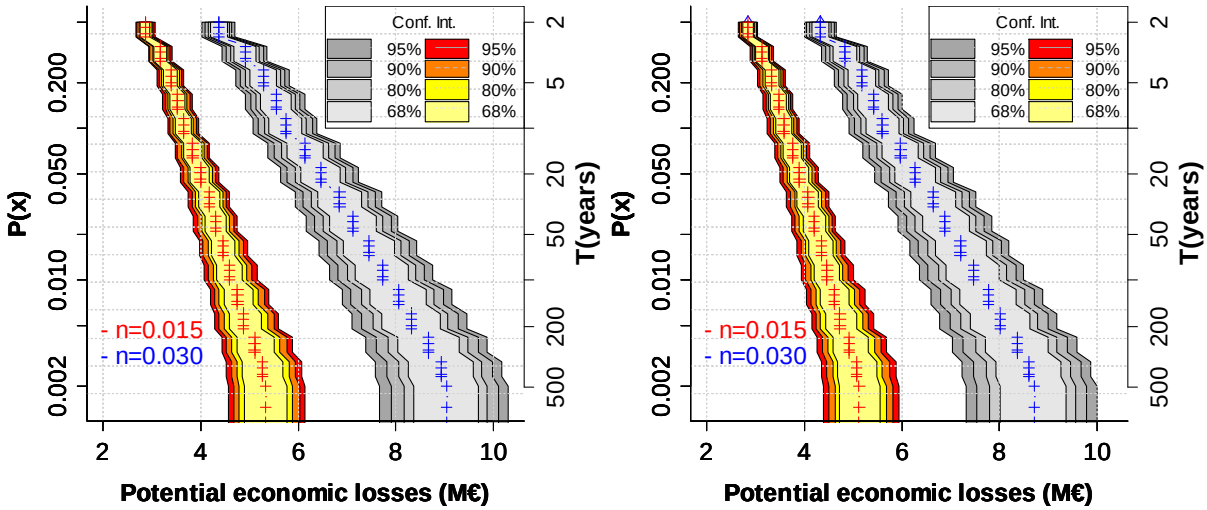

Figure 4.12 Potential casualties in the Arenys basin under EWS, LSM (left) and MM (right)

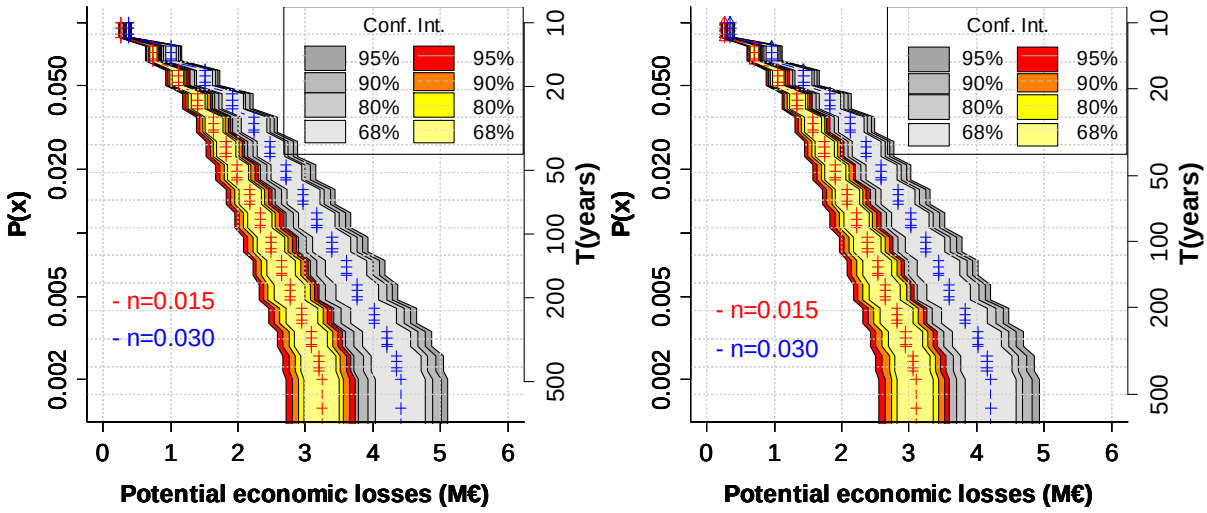

Figure 4.13 Potential economic losses. Case of sewer system + EWS, LSM (left) and MM (right)

Contrary to the societal risk, in the economic risk assessment only one vulnerability parameter was used, the depth-damage parameter. Looking at the potential economic losses (Figure 4.11 to

Figure 4.13), we observed that the confidence intervals are clearly identified as for higher confidence levels the uncertainty grows with the return period. It is clear that there is a slight difference between statistical methods (LSM and MM) under the same case. This behaviour is more evident in Figure 4.14 in which both methods are compared. The differences are very low as is shown in the right figure in which for the “worst case” and 10 year return period the potential economic losses for the LSM and MM are 4.4 M € and 4.1 M € respectively. Comparing the SM and NSM, the mitigation in the economic risk, as well as the societal risk, achieved a substantial mitigation. That falls down from 7 M€ in the "worst case" for potential economic losses until 5.4 M€ if EWS is implemented, or to 3.2 M€ if a sewer system is also developed.

4.9 Discussion

Figure 4.14 shows how the structural and non-structural measures reduce the potential risk of loss of life and economic damages. This figure does not include confidence intervals and could be considered as a synthesis of the previous results. As is discussed above, in Figure 4.8, the potential uncertainty of societal risk is limited to a narrow band. However, for economic losses, the vulnerability assessment is far from being limited, its uncertainty grows considerably for higher return periods. It is remarkable that for potential casualties and potential economic losses those figures are extremely useful tools in the decision making process: i.e. the Arenys de Munt risk curves (Figure 4.14). In this figure the different structural and NSMs, which have associated its own cost of implementation, planning characteristic and purposes are compared. The stakeholder may decide which of these measures should be implemented over any other trying to optimize their own resources.

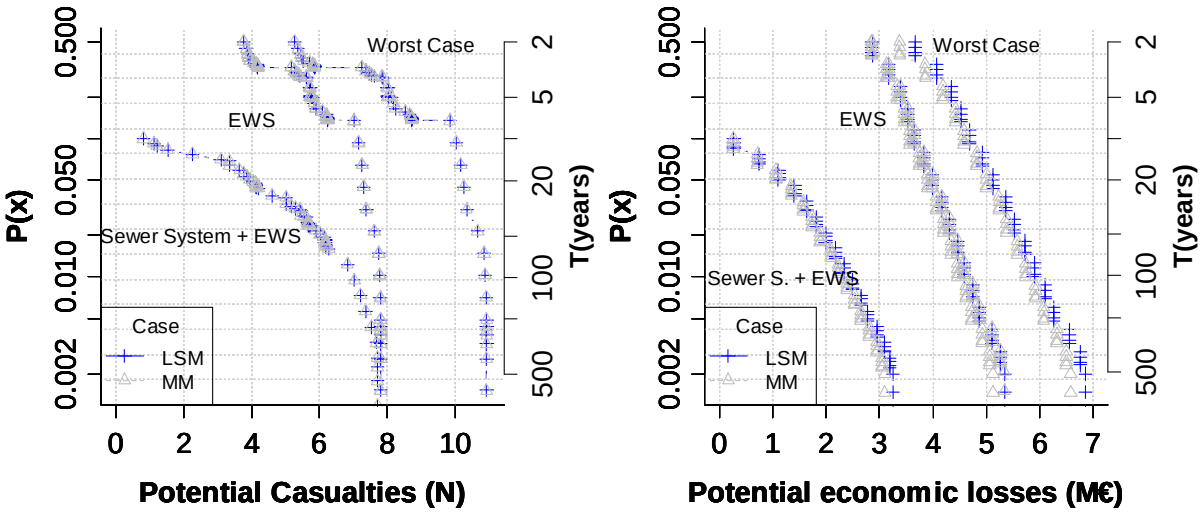

Figure 4.14 Potential casualties (left) and economic losses (right) due to pluvial flooding

In the SUFRI project different SM and NSM were analysed and an optimization method respect to the implementation cost was made. Specifically, Figure 4.14 shows that for higher return periods the mitigation of potential casualties' due to the implementation of a sewer system does not imply a better mitigation than only the EWS (Joebst et al., 2011). Whereupon, if the people in charge of the decision making process (usually stakeholders) have interest in protection from extreme events only (higher of 100 years RP), surely the sewer system would be rejected as a structural measure, which would be a wrong decision considering all the extreme events range (from low return periods to high return periods) in order to consider also minor floods (<5 years). To quantify risk and support the decision-making process, numerical parameters can be derived from the potential risk curves (F-N, F-D) such as the Expected Annual Damage (EAD). As the EAD name suggests, it is the value of expected losses in any one year, due to any flood event. In Jonkman et al, (2002), the EAD has been defined as follows:

$$EAD(D) = \int_0^{\infty} x \cdot f_D(x)\, dx \tag{4.10}$$

In which $f_D(x)$ is the probability density function of the economical losses per year and x is the losses (or damage) of this event. For every confidence interval an EAD value is computed. Figure 4.15 shows that the EAD in the experimental basin varies from 3.5 M€/year (Manning=0.030) to 2.6 M€/year if a EWS is implemented or less than 0.12 M€ if a sewer system is also operative. The horizontal axis refers to the confidence interval value. Concerning the uncertainty it can be seen that as the Manning coefficient increases the uncertainty increases, too, which means that for the same case study, i.e. the *"worst case"* and n=0.030, the upper interval of 95% of confidence is equal to 3.7 M € / year, and the same case but with a manning of n=0.015 the EAD is equal to 2.3M € / year, This means that if the real Manning is located between 0.015 and 0.030, the EAD will be between 2.3 and 3.7 M€/year respectively.

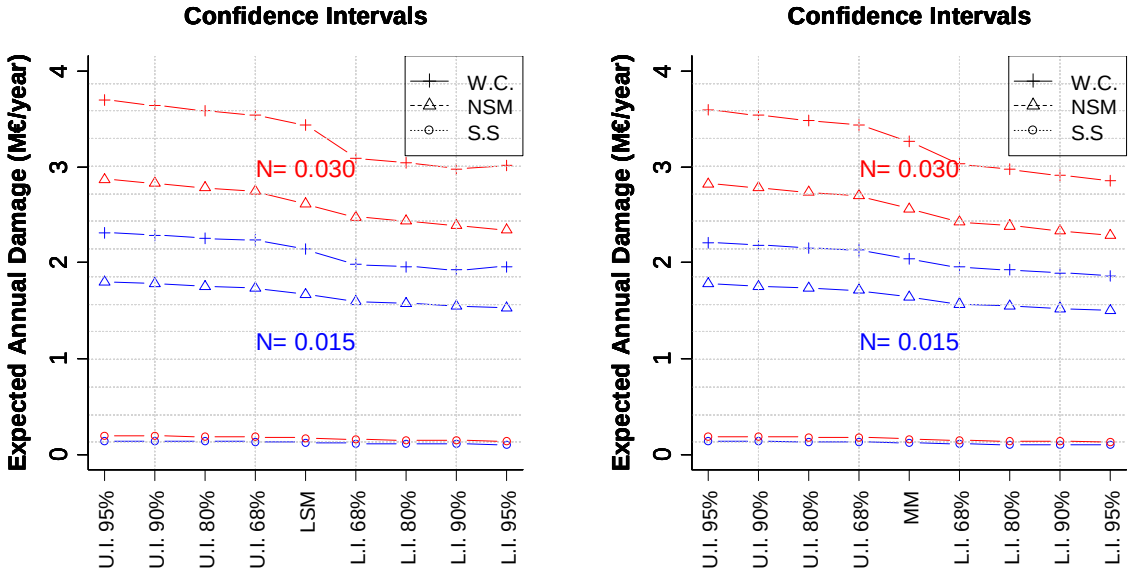

Figure 4.15 Expected Annual Damage due to pluvial flooding LSM (Left) and MM (Right)

From the above figure it can be seen that the EAD helps to quantify the economic benefits of some measures development. However, it has nothing to do with the return period by which you need to plan and design your structural measures. Due to the fact that often these measures are planned in terms of a specific return period which obviously has the sense of assuming certain levels of risk. Thus, in agreement with the idea that you can never achieve a complete mitigation of a natural hazard, it is necessary to optimize the resources of the municipality with regard to the monetary cost of the chosen return period design of the corresponding structural measure, in order to mitigate the risk as much as possible. In this paper we propose a new value to cope with the optimal design return period. It is the Optimal Expected Annual Damage (OEAD) and is defined as the maximum value of the function $m(x) = x \cdot f_D(x)$, that represents the probability density of an event times its own economical damage, as it is exposed in Figure 4.16, for both potential economic losses (left) and potential casualties (right).

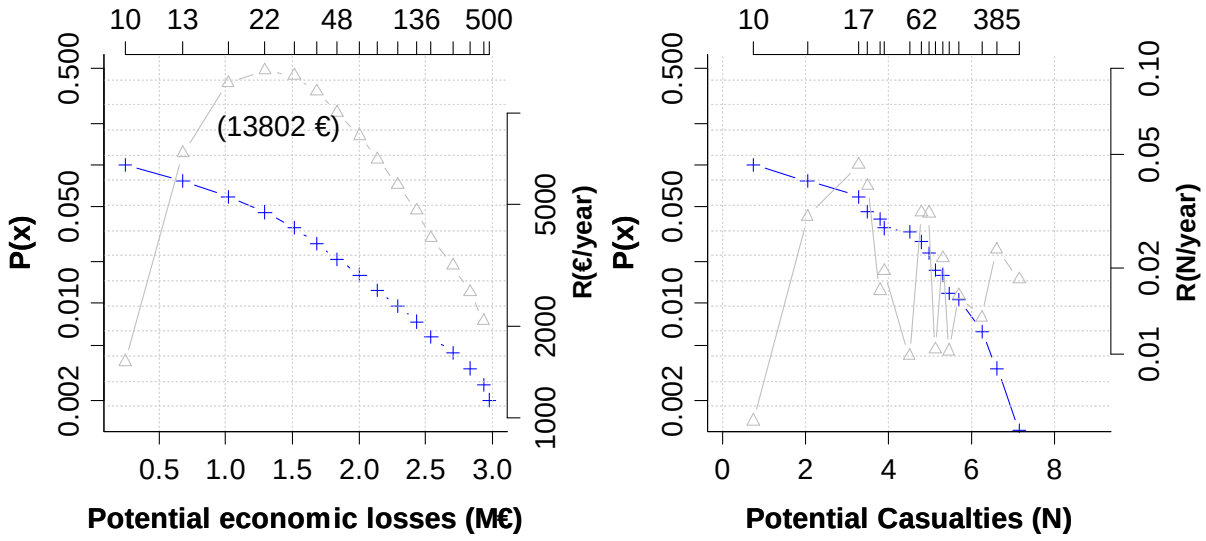

Figure 4.16 F(x) vs m(x) functions (blue and grey respectively) and their equivalent for the potential casualties, 68% Confidence interval, "sewer system + EWS" case, Manning=0.03

The total area under the curve of Figure 4.16 (left) is the EAD. The maximum value obtained in this graph is the OEAD, specifically for one of the confidence intervals (UI 67%) for the WC+SS+EWS and a Manning coefficient of 0.03, it is 13800 €/year just for a 22 year return period. Figure 4.16 (left) gives an idea of the quantitative economical mitigation effect that a measure could bring for a fixed return period. For every return period it could establish the effective mitigation which a measure could leave, i.e. if a structural measure like a flooding diversion area is planned for 22 year return period (in Figure 4.16), the mitigation obtained will be proportional to the area of the EAD reduction until the return period considered (around 31% as shown in Figure 4.17). In Figure 4.17 the EAD mitigation percentage is shown and it can be used to evaluate the mitigation percentage for the desired return period.

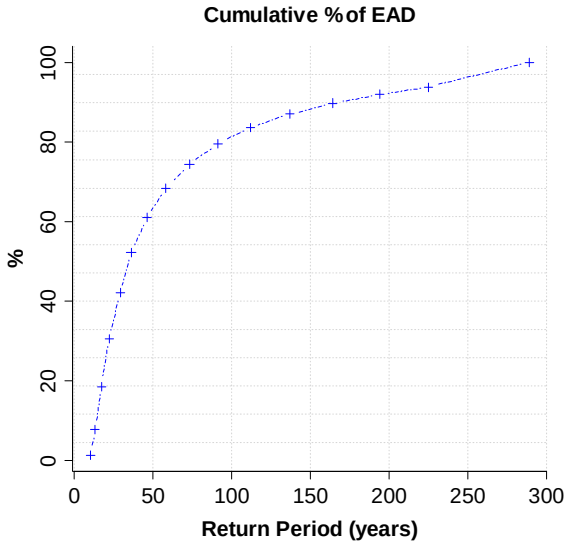

Figure 4.17 Percentage of the EAD in the figure 16 (left) example

Generally, in Catalonia the sewer systems are designed for the 10 year return period, thus, it is clear that the residual risk is high. The same graph can be made for the potential casualties (Figure 4.16 right), however, it should be noted that the curve does not reach a single peak in fact 4 peaks can be observed. This behaviour corresponds to the temporal discretization, since in the exposure calculation four discretizations have been set (day / night and winter / summer time windows season). In Figure 4.18 the different OEAD cases studies are shown, also the confidence intervals for the extreme Manning values and different cases are presented.

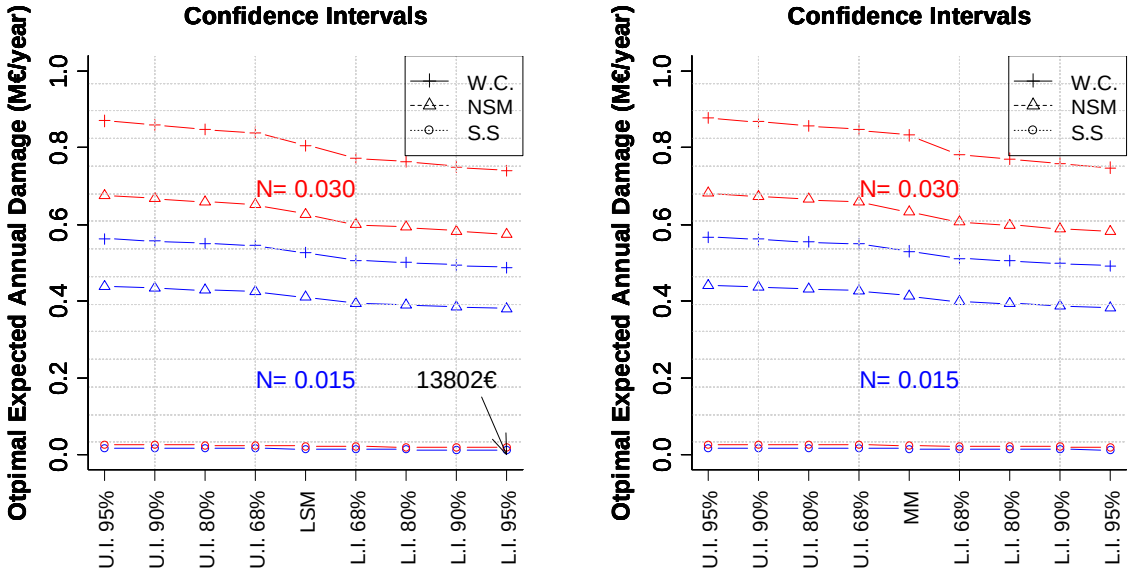

Figure 4.18 Optimal Expected Annual Damage (OEAD) due to pluvial events in Arenys de Munt

4.10 Summary

Flood risk management focusing on non-structural measures is a promising field for the mitigation of disaster consequences. Large structural measure investments have been made in recent years by entities and governments, the residual risk mitigation by non-structural measures

may be one of the ways to follow in the coming years. In the present paper an exhaustive uncertainty analysis related to the residual risk assessment by structural and non-structural measures can improve the information available for decision-making entities in charge of disaster control management. Some conclusions for the Arenys de Munt case study are listed below:

1. Regarding the cases handled for the potential economic losses it is noted that uncertainty (both hydraulic and hydrological) for the 500 year return period, the values for the "worst case" oscillates from 5.8 to 13.2 M €, from 4.5 to 10.5 M € if a NSM is implemented, and from 2.7 to 5.2 M € if a NSM + a sewer system are operative. Although the dispersion decreases for lower return periods, in general terms the values are very high (more than 50 % above its average). So uncertainty analysis in these kinds of studies could be a good tool for the decision making process.
2. In the case of potential casualties, it has been noted that for high Manning coefficients the risk is reduced. High Manning values reduce the mean flow velocity along the streets and the drag forces. In the case of potential economic losses the risk is increased by increasing the Manning coefficient, it conduces to high water levels that increase the risk of damage. From this it can be concluded that in case of potential casualties, a low Manning would be better for the risk assessment and in the counter part for the potential economic losses the highest Manning values should be taken. The statistical method used differs very little in terms of the final results, however in Figure 4.11 (comparing Left and Right), Figure 4.12 (comparing Left and right) or Figure 4.13 (comparing left and right) a variation around 5% can be seen.

3. In the literature no document exists about the influence on the risk assessment due to the use of one, two or more vulnerability parameters in the vulnerability assessment. In the societal risk assessment, the vulnerability discretization adopted in the present methodology, appears to reduce the uncertainty, because the confidence interval bands are almost identical to the expected value. This behaviour could be associated with the higher slopes present in the basin, which leads to higher velocities, therefore the vulnerability criteria including the velocity always falls into the worst scenario (severity S3) and it does not represent an improvement on the results in terms of uncertainty.
4. As it happens with the risk assessment, the EAD varies significantly according to the uncertainty analysis. In the example illustrated in section 4.9, for the "Worst Case" with n=0.030 and n=0.015 the dispersion oscillates around the 30% mark (3.7 to 2.3 M€/year), showing that this parameter is also significantly affected by the uncertainty. On the other hand, the proposed Optimal Expected Annual Damage OEAD altogether with the cumulative percentage of the EAD mitigated (Figure 4.17) could be assumed as a decision making value for the planning of structural measures. This is because most of the time the design criteria are subjectively imposed and with those parameters a mitigation level can be reached if a specific return period is chosen. Evidently any developed tool that improves the optimization of resources will help in risk management planning.
5. Risk assessment in terms of potential economic losses and casualties for 3 cases are exposed in this document. It is clear that both of them are reduced by NSM implementation and in the case of an EWS + sewer system implementation. Moreover the economic risk reduction by EWS implementation is more significant than in societal risk.

This is because a few hours of lead time could represent a significant reduction in economic losses. This reduction could even be up to 90 % of the initial value taking into account the EWS plus drainage system measures.

Chapter 5: New drought risk assessment methodology focused on meteorological drought

Over the last years great efforts have been made in order to quantify the impacts of drought for human and the environment. Risk management is a relative new science that brings opportunities to stakeholders for a better management in drought emergency events. Due to the fact that it is very hard to make one specific definition of the drought phenomena, monitoring and prediction is a very complicated process. The present chapter shows a new methodology concerning the meteorological drought phenomenon related to the potential economic losses on agricultural crops. The approach herein developed (GITS group) uses the Self-Calibrated Palmer Drought Severity index (SC-PDSI) proposed by Wells et al. (2004). This divides the phenological development of the planting process in two stages (Sowing and harvesting) and makes a statistic analysis according to these two stages. To calibrate the losses, annual data series of crop yielding and production of several rainfed crops in the Llobregat Basin were selected in order to assess the potential economic losses due to meteorological drought events.

5.1 Introduction

The work presented in this chapter is the result of the European research project, MEDDMAN of which the principal scope was to “develop and confront common and transnational methodologies for combating drought within the Mediterranean region”. As a product of this project a new methodology has been developed for drought risk assessment. To apply the aforementioned methodology, the Llobregat basin was selected as a test case study.

As described in subsection 1.3, research has mostly been conducted in quantitative hazard assessment and qualitative drought risk assessment. This means that in most drought studies the probability of a particular consequence related to a particular drought event (the quantitative risk), has not been assessed in a numerical way. On the other hand, risk analysis is nowadays mainly focused on the development of numerical indexes, which is how several meteorological and hydrological drought indices are observed such as: PDSI, (Palmer W., 1956), SPI (McKee, T.B.; N.J. Doesken; and J. Kleist. 1993), MAM, BFI (Institute of Hydrology, 1980), SC-PDSI (Wells et al., 2004), SWSI (Shafer and Dezman, 1982), Threshold level method (Tallaksen and Van Lanen, 2004), CMI (Palmer, 1968), RDI (Tsakiris, 2004), SPEI (Vicente-Serrano S. et al., 2010). These indices are designed to identify drought events and until a certain degree, they quantify the intensity of a drought event. This means that this directly relates to what is known in risk management science as “Hazard Assessment”. In order to have a complete risk assessment, a “vulnerability analysis” has to be done. This means, to quantify how the intensity of a particular event, affects the analysed variables (humans, crops, animals etc.). The difficulty in assessing the “drought vulnerability” is that it is not always known what type of drought (in terms of intensity) gives which related impact. This is a consequence of the different variables that are involved in the development of a drought event (as explained in subsection 1.3). Sometimes not all the information is available to consider all the involved variables, whereas it can be the case that simple models with less parameter give better results. The key point is to choose and select the variables that are the main representation of the problem. The present methodology considers the assessment of the hazard through the SC-PDSI (Wells et al., 2004), as explained in section 1.3.5. The vulnerability is assessed through the calibration of losses for 2 summarized phenological stages for different types of crops (representing all the available crops in Catalonia)

that are produced in the Llobregat basin. The interaction of the selected variables for the present methodology is explained from section 5.3.2 to section 5.4.

5.2 Case Study

The Llobregat River originates in Castellar de n'Hug, located in the high - central part of Catalonia in the east of Spain. The experimental basin has a catchment of 4900 km² (Figure 5.1) with a main tributary of 165 km length. This catchment is characterized by the Mediterranean torrential regimes which includes low precipitation during most of the year (especially in June-August and December to February), but with intense rainfall episodes which mainly occur in the months of October, November, April and May.

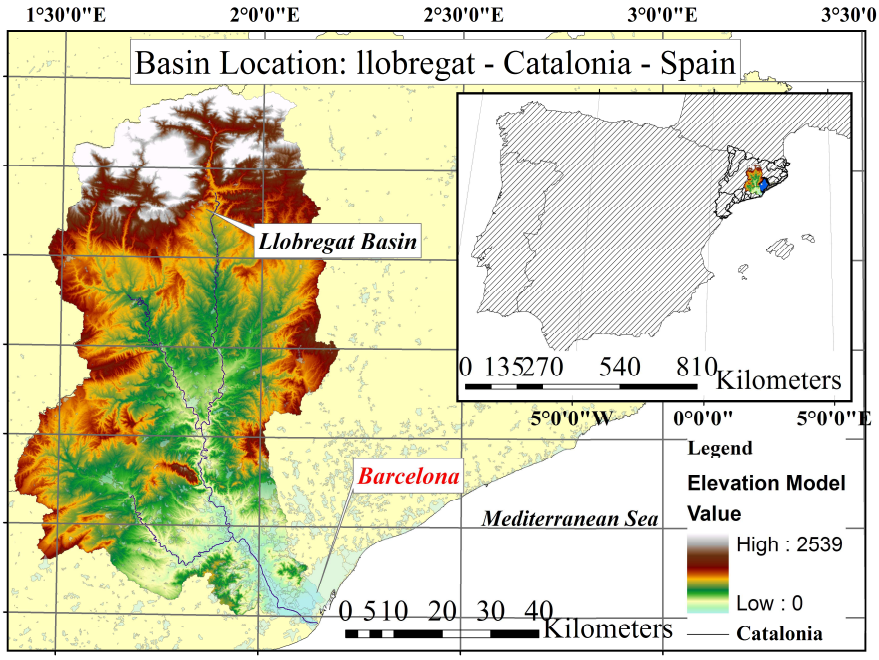

Figure 5.1 Location of the Llobregat basin and elevation map

Some studies illustrate that Llobregat River is showing a significant decrease in his discharge flow, mainly by the climatic drift due to climate change and climate variability (Catalan (1997); Marcé et al., 2012; MOP, 1996). Changes in the land cover and the forestation of large areas in the region are other important factors that influence the reduction of discharge. The metropolitan zone of Barcelona is one of the most densely populated zones in the Mediterranean region, which result in a high susceptibility to droughts. The experimental basin is located in the region of Catalonia, covering different geopolitical subdivision called Comarcas (Figure 5.2). There is statistical data available of production in tons of crops per area (Ha) and cropping efficiency (Ton/Ha), discretized per type of crop (e.g. tomato, peach, lettuce etc.) from the Ministry of Agricultural of Catalonia, this data is divided over the geopolitical subdivisions. These statistics are used to calibrate the present model and assess the potential losses when a drought event occurs. In the length of this data series (approx. 16 years record), two drought events have been detected and will be further explained in subchapter 5.4.

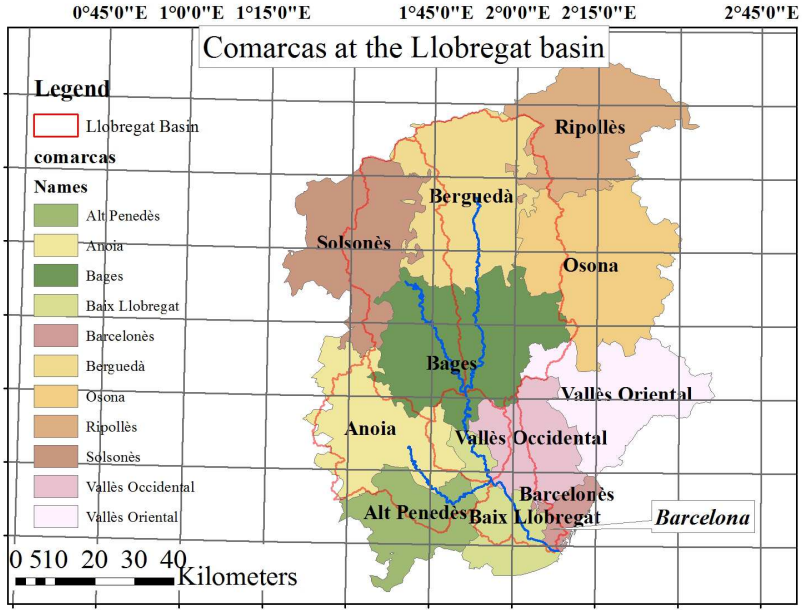

Figure 5.2 Geopolitical subdivision of Llobregat basin, to which 11 Comarcas belongs to the case study

5.3 Drought risk assessment methodology

Historically, human have been cultivating food according to the climatic characteristics of the region they settled in, according to the dietary habits of the regional population. However, nowadays the food requirement of the population forces to produce different types of crops in the arable land areas (Figure 5.3). This is possible because of technological developments, such as irrigation and sprinkling, which have made possible that some originally unfeasible food crops can be grown in water deficitary areas. An example is rice, which requires large amounts of water and because of irrigation it is possible to grow this in dry areas such as Spain. The construction of large reservoirs, like dams, can attenuate the effect of hydrological drought and subsequently irrigated crops. However this does not mean that drought cannot affect crops in irrigable areas, but the temporary extension which is required to develop drought effects are longer than in areas of rainfed crops (RC).

Figure 5.3 Example of rainfed crops (left) and irrigable crops (right).

5.3.1 Methodology structure

In the following diagram the methodology structure for the drought risk assessment is shown:

Figure 5.4 Methodology structure flow diagram

For the Llobregat basin, according to previous diagram, the next steps were implemented:

1. Historical series of SC-PDSI are obtained for all the 31 hydrometeorological stations in the basin (section 5.3.2).
2. Spatial interpolation is performed with the Ordinary Kriging method per month for every year of the data series (section 5.3.2). A total of 1128 SC-PDSI raster's have been obtained (94 years multiplied by 12 months). The followed procedure for index calculation is explained in section 1.3.5.

3. From “el Calendario de Pajes” the bands or intervals for every type of crop have been selected (section 5.3.4). Extracting the SC-PDSI in those months for the same intervals months.
4. From the statistics of crops, and the classification displayed in Table 5.2, the production (in tons) is aggregated per region or block (Comarcas) and over cells. To perform the analysis by cell, the land use map is correlated with the types of crops (section 5.3.6).
5. From the intervals selected for each type of crop (SC-PDSI in the selected months), a statistical fitness is made to obtain extreme values return periods for all 31 hydrometeorological stations (section 5.3.5), as illustrated in Table 5.6. Once return periods are found, a spatial interpolation through ordinary Kriging is done again, to have equivalent return periods in all the points in the basin for the SC-PDSI return periods.
6. A comparison between the SC-PDSI and statistical fitness has to be done in order to determine (or in every block), which return period is related to each cell (section 5.3.7).
7. From the hydrometeorological information, and specifically, from the SC-PDSI data series selected per block or Cell (step 6), the years of normal weather conditions can be found, this means, the years that have values of SC-PDSI close to 0. These years are chosen as the years in which the crop production should be "normal" or averaged (section 5.3.7).
8. From the statistical analysis of crop production two periods of drought were identified in the basin. The years 2000/2001 and 2005/2006 were the years with a low crop yield. With step 6 it is possible to determine the return periods of each event, and in step 7 it is determined which are the normal years of production related to the normal conditions.

Thus, comparing production statistics for those dry years with respect to the production of normal years, the economic losses from each event can be found (section 5.3.7).

9. In the last steps risk curves are constructed with the related return periods of the events and economic losses (section 5.4).

5.3.2 Hazard assessment

In section 1.3.5 the Palmer index has been described, which is an index that makes a hydrological balance to determine the water deficit in terms of inches of water, considering in the water balance the evapotranspiration of the place (Thornwhite formula), soil properties (in terms of AWC) and the implicit history in the same data series (autoregressive AR model). The value of the index itself is a measure of how much water is needed to develop normal conditions within the basin (Figure 5.5). This is equivalent to saying that it gives an intensity of the phenomenon, implicitly in the same index.

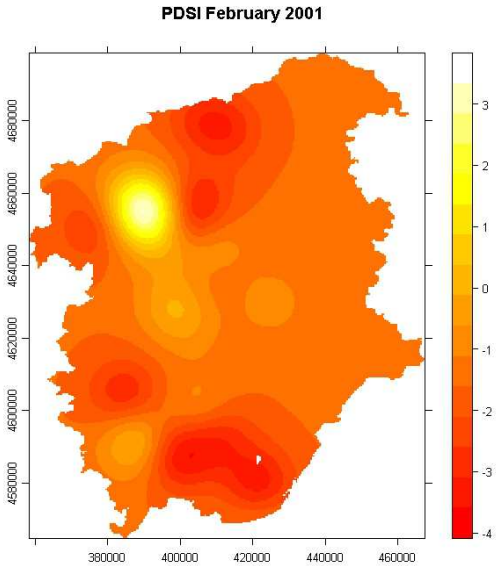

Figure 5.5 SC-PDSI (mean of -1.66 inches) in a deficitary state behaviour

The first problem of the drought risk assessment in the Llobregat basin lies in the fact that we do not have hydrometeorological station information for all the cropped areas, instead of this only punctual information is available, whereas the crop information is spatially distributed. For a complete assessment the index values have to be evaluated for the entire basin.

Although it is not the main research objective in the present document, several interpolation techniques have been compared in order to establish the one that represents the spatial information related to the SC-PDSI method best. Concisely, the techniques considered were: simple kriging, ordinary kriging, universal kriging (sometimes called external drift kriging) and inverse distance weighted (IDW). The spatial interpolation methods are briefly explained below and results are shown in Figure 5.6 to Figure 5.7.

All kriging techniques follow the next equation (Samper F., 1996; Velasco, 2009):

$$Z^*(u) - m(u) = \sum_{\alpha=1}^{n(u)} \lambda_\alpha \left[Z(u_\alpha) - m(u_\alpha) \right] \tag{5.1}$$

Where: u and u_α are location vectors for estimation point and neighbouring data points, indexed by α, $n(u)$ is the number of data points in local neighbouring areas, used for estimation of $Z^*(u)$, $m(u)$ and $m(u_\alpha)$ are expected values (means) of $Z^*(u)$ and $Z(u_\alpha)$, λ_α kriging weight assigned to datum $Z(u_\alpha)$ for estimation location u; same datum will receive different weight for different estimation location. Depending on the behaviour of the mean $m(u)$ and variance $\left[Z(u_\alpha) - m(u_\alpha) \right]$, the most used kriging methods are:

- Stationary variable with known mean and covariance (simple Kriging)

- Stationary variable with unknown mean and covariance (ordinary Kriging)
- Non stationary variable (universal Kriging)

The secret of the technique raises in the determination of the weighting factors in terms of the variogram or semivariogram (Samper F., 1996; Velasco, 2009):

$$\gamma^*(h) = \frac{1}{2N(h)} \sum_{i=1}^{N(h)} \left[Z(x_i + h) - Z(x_i) \right]^2 \tag{5.2}$$

Where: $N(h)$ is a pair of points in the spaced distance h and $Z(x_i)$ the value of the random variable. To determine an optimal fitted variogram, several theoretical variograms are available: Gaussian, Exponential or Spherical variogram. The Inverse Distance Weighted (IDW) method follows the next equation:

$$\hat{y}(x) = \left\{ \sum_{i=1}^{N} \lambda_i y(x_i) \right. \tag{5.3}$$

Where $\lambda_i = d_i^2 / \sum_i^n d_i^2$, d_i is the distance at point i, y are the values at position x_i and $\hat{y}(x)$ is an unknown value. For the drought methodology development, several statistical packages have contributed in the open source code R. To do this, the sp, hydroTSM and raster package are used. Working with these packages allows us to represent graphically spatial information and takes advantage of the statistical computational power of the R program. With the present drought model a package has been developed which can be loaded into the R program webpage.

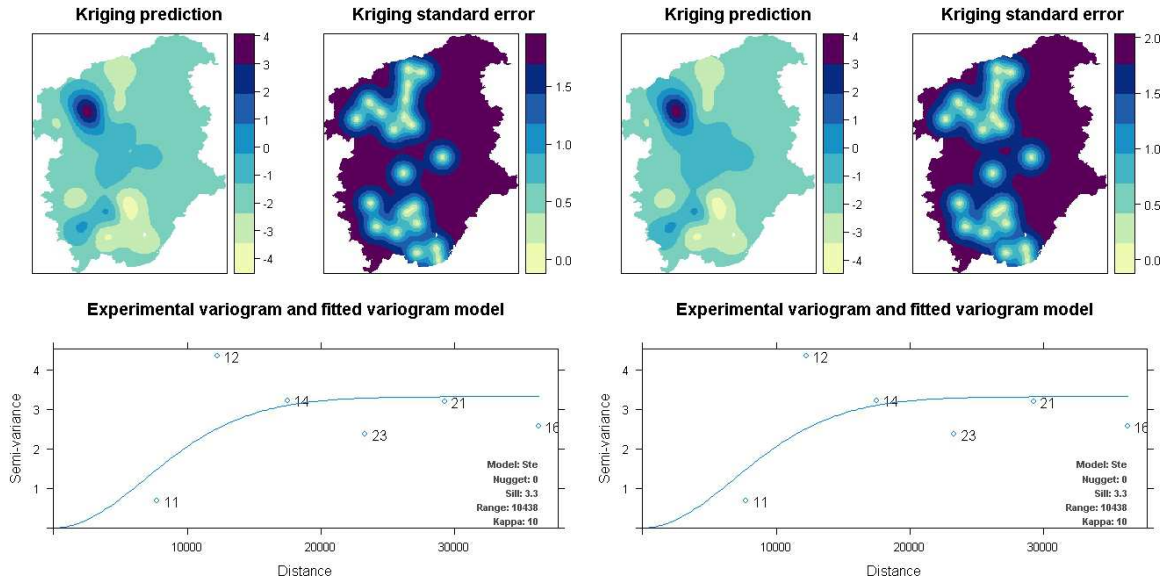

Figure 5.6 Simple (left) and Ordinary Kriging (right) for the SC-PDSI (January 2001), figures generated through package hydroTSM in R.

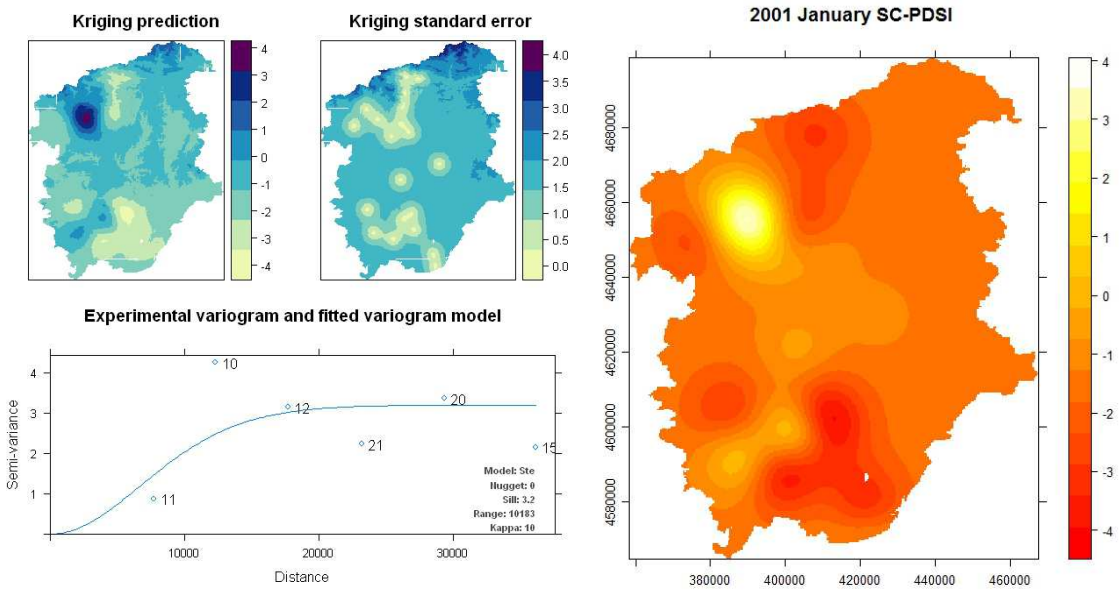

Figure 5.7 Universal Kriging (left) and IDW (right) for the SC-PDSI (January 2001), figure generated through package hydroTSM in R

From Figure 5.6 and Figure 5.7 it can be observed that it is possible to interpolate the SC-PDSI for all points inside a mesh for the basin, overcoming the limitation of the hydrometeorological station availability. To decide which is the best technique for SC-PDSI spatial interpolations a cross-validation technique has been applied (as explained in Appendix B), in which known data was artificially removed (SC-PDSI) and the kriging and IDW methods where applied in order to compare the original values against the generated ones.

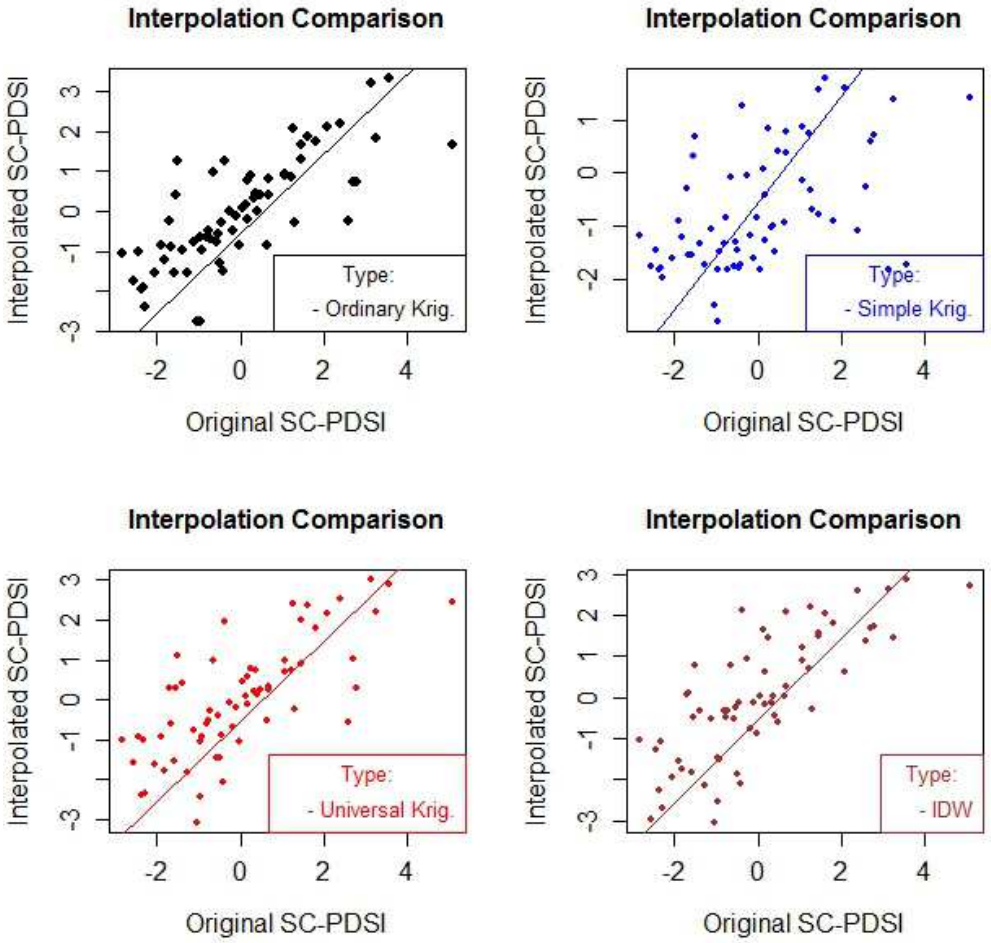

Figure 5.8 SC-PDSI in the Naves (INM135) station, for January‘s dates from 1942 until 2006 (65 values)

In general, all the considered spatial interpolation techniques preserve a tendency, but nevertheless there is huge data dispersion. This is a characteristic that is often found in hydrometeorological data series, due to implicit random behaviour in data. In Table 5.1, it is shown that the best technique, with the best fitness to Figure 5.8 (Naves station), is the Ordinary Kriging Technique, which is the reason why this is selected as the spatial interpolation technique for the SC-PDSI.

Table 5.1 Efficiency criteria's indexes of data dispersion/correlation (station INM135)

Type\coefficient	Pearson Coefficient (R)	Pearson Coefficient (R^2)	Nash-Sutcliffe Efficiency Coefficient	RMSE
Ordinary Kriging	0.784	0.615	0.507	1.062
Simple Kriging	0.511	0.261	-1.156	1.636
Universal Kriging	0.740	0.548	0.347	1.144
IDW	0.773	0.598	0.371	1.069

Although as illustrated below, statistics of crops are available since 1992 in all the geopolitical subdivision, and thanks to the Kriging technique it is possible to have the SC-PDSI indices from 1913 in the same regions or in a better resolution (cell resolution). However, it is worth mentioning that obviously the Kriging technique depends on the amount of known points in the watershed (Samper F., 1996), which were in this case sufficient.

5.3.3 Meteorological drought affectation over rainfed crops (Vulnerability)

In previous chapters it is described that drought can affect different levels and different ways of the development of a plant. This is a consequence of different conditions in the basin (as temperature, rainfall, soil moisture etc.) and types of plants, which all have their implicit particular condition to resist drought. As mentioned before the phenological development of

plants has been subdivided in two stages (see Figure 5.9): The time interval in which the plant is sowed and the season in which it is harvested, and will be explained further in section 5.3.5.

Figure 5.9 Phenological stages for fruit plants according to Urbino Vallejo (2010)

Related to the type of crops, in the Llobregat basin, for the specific case study two types of crops have been classified following the classification of the Catalonian Ministry of Agricultural, in those that have a Herbaceous origin and those that have a Woody origin (see Table 5.2).

Table 5.2 Crops types available from Catalonian Ministry of Agricultural

Herbaceous	• Forage plants: corn, alfalfa, sorghum etc..
	• Cereals: barley, wheat, oat, corn, rye etc..
	• Vegetables: lettuce, tomato, onion, chard etc
	• Leguminous: beans, carob, chickpea etc..
	• Industrial: canem, linen, sunflower etc..
	• Tubers: different kind of potatoes.
Woody	• Tree fruits: apple, apricot, peach, cherry, plum etc..
	• Olives: table and oil olives.
	• Grapes: table and wine grapes.
	• Other trees: cane, locust, cafe etc..

Further, the potential economic losses in the classified crops will be displayed according the previous table.

5.3.4 Sowing and harvesting season:

In section 1.3, it is shown that plants and generally vegetation have different water requirements, according to different variables, like: seasonality, type of the plant and plant transpiration, etc., which are summarized in the phenological curves (see Figure 1.12). The two herein considered stages attempt to reflect in which time of the phenological development, the partial or total loss of the plant occurs (which results in either minimization of growth or even death) and consequently the crop loss due to a drought event with a correlated intensity (SC-PDSI index value). Evidently in terms of accuracy, most discretization would probably drive to better results, but in order to simplify the problem, and make the present model operative these two stages have been considered in the methodology. To consider these phenological stages, an extensive research for every single crop in the case study has been made, to determine the months in which a particular type of crop is sowed and in which months those are harvested. The sowing season is defined as the time interval in which the plant is sowed until the inflorescence emerges. The harvesting season is considered from the moment of flowering until the senescence (see Figure 5.9). Nevertheless, it is important to remember that not all the plants have the same phenological stages but in general terms these are the usual intervals.

From the experience of farmers in almost every country calendars have been developed in which the right moment to start a crop and to harvest the production is suggested. In the Llobregat basin this calendar is known as *"El Calendario del Pajes"*. This calendar is mainly made for people who are not familiar with crops, making some recommendations about which are the better months for sowing and harvesting. Finally, is important to say that this calendar varies from place to place but is approximately the same from year to year according to the moon calendar.

Table 5.3 Capture of "El Calendario del Pajes".

Crop	January	February	March	April	May	June	July	August	September	October	November	December
Chard	Harvesting											
Celery	Sowing									Harvesting		
Basil		Sowing				Harvesting						
Eggplant		Sowing					Harvesting					
Strawberry			Harvesting			Sowing						
Brocoli								Sow.	Harvesting			
Pumpkin			Sowing		Harvesting							
Onion					Harvesting			Sowing				

In Table 5.3, it is shown how different plants have different crop time intervals. The way this affect a crop can be explained in an example; if a drought occurs between August and January the strawberry crop will not be affected, because this has sowing and harvesting season in June and July and from February to May respectively. This is the reason why it is important to consider these interval/stages into the present analysis.

5.3.5 Statistical distribution fitness according to the sowing and harvesting phenological stages:

There is a long tradition of using statistical methods based on extreme value theory to estimate the return period or the cumulative probability (Table 5.4) of extreme events like flooding or drought (Gumbel, 2012). For drought conditions the cumulative probability and return period is linked as follow:

$$F\left(x_S\right)=\frac{1}{T\left(x_S\right)} \quad \therefore \quad F\left(x_H\right)=\frac{1}{T\left(x_H\right)} \tag{5.4}$$

Where F and T are the cumulative probability and return period respectively for potential damage (also called consequences) in the sowing and harvesting season (x_S, x_H). A total of 19

statistical distributions have been implemented in R language in order to have a wide range of distribution functions to fit the SC-PDSI (Table 5.4). The present model is able to select the SC-PDSI from the data series from the intervals stages, as explained in the section 5.3.5 and summarized in the example of Table 5.6, it can fit several distribution functions depending on the type of interval to consider. The model has included the Kolmogorov–Smirnov test to determine which of the 19 distributions fits the indices better for the particular hydrometeorological station and stage interval (see example Table 5.5).

Table 5.4 Cumulative and density statistical distribution function implemented in R

Distribution	f(x)	F(x)	Distribution	f(x)	F(x)
Gumbel	yes	yes	Exponential	Yes	yes
Gamma	yes	yes	Reversed Gumbel	Yes	yes
Cauchy	yes	yes	Lambda Distribution	Yes	yes
Kappa	yes	yes	Generalized Normal	Yes	yes
Normal	yes	yes	Generalized Pareto	Yes	yes
Pearson III	yes	yes	Truncated Exponential	Yes	yes
Rayleigh	yes	yes	Log Normal 3 parameters	Yes	yes
Rice	yes	yes	Generalized Extremes Values	Yes	yes
Wakeby	yes	yes	Generalized Logistic Distribution	Yes	yes
Weibull	yes	yes			

Table 5.5 Kolmogorov – Smirnov test for Begues station and September/March crop time interval

Distribution	K-S (D)	p-value	Distribution	K-S (D)	p-value
Cauchy	0.1138	0.0690	Pearson III	0.0436	0.9660
Exponential	0.1641	0.0018	Rayleigh	0.0839	0.3188
Generalized Logistic Distribution	0.0530	0.8586	Rice	0.999	2.20E-16
Generalized Normal	0.0437	0.9660	Wakeby	0.0472	0.9339
Generalized Pareto	0.0870	0.2785	Kappa	0.0511	0.8859
Normal	0.0444	0.9599			

Table 5.6 SC-PDSI return periods for Begues station for best statistical function in Table 5.5 (PeIII)

Return Period (Years)	F(x)	SC-PDSI	Condition
500	0.002	-5.98	Drought Condition
200	0.005	-5.35	
100	0.01	-4.83	
50	0.02	-4.26	
20	0.05	-3.40	
10	0.1	-2.65	
2	0.5	0.02	Drought Or Wet
10	0.9	2.68	Wet Condition
20	0.95	3.43	
50	0.98	4.28	
100	0.99	4.84	
200	0.995	5.35	
500	0.998	5.98	

5.3.6 Crop production and land uses in the study area:

Another factor that complicates the drought risk assessment relies on the fact that the place where a particular crop type is placed is unknown. Although, the Ordinary Kriging helps to interpolate the SC-PDSI inside the basin, it is not recommended in this case. To manage this problem two strategies are used: 1) a land soil use map is disposed, to relate a type of crop to each pixel/cell value. 2) From the statistics, the production is available per Comarca (11 in total), which will be referred to as “block” discretization when the production is summarize over these subdivisions.

For the Llobregat basin a land use map from CREAF (4th version) is available, in which a total of 255 types of land use are discretized (see Figure 5.10). This map is available in raster format with a pixel resolution of 30x30 m, nevertheless the used resolution is 400x400 m, mainly

because the size of the mesh for the Kriging interpolation methods in R does not allow working with higher resolutions. The crop identification in the cells strategy has been done according to the land uses in the appendix A. An example of this is displayed in (Table 5.7).

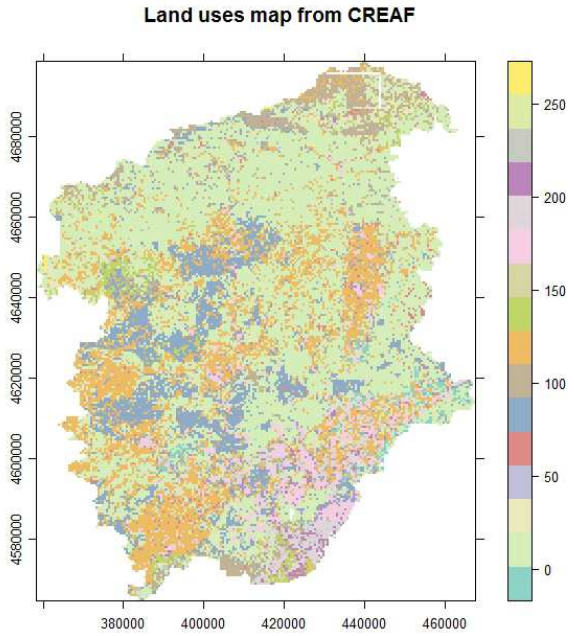

Figure 5.10 Land uses in which all pixel values are related with types of crops

Table 5.7 Relation of crop types and CREAF land uses (Table 5.2) for the first five more usual pixels in the 400x400 m resolution.

Number of pixels	CREAF Code	CREAF Description	Crop Type:
8342	124	Bushes	Herbaceous crops
7211	5	Pine forest (> = 20% cc)	No crop
6376	3	Red Pine forest (> = 20% cc)	No crop
3702	4	Holm oak (> = 20% cc)	No crop
3449	9	Pubescent oak (> = 20% cc)	No crop
2585	19	Vineyard	Vineyard crop

5.3.7 Block and Cell statistical index comparison and production condition identification

According to the strategies previously mentioned, the crop location and their respective weather conditions are identified. To do this a comparison between the statistical fitness and SC-PDSI

should be done. This means identified in the monthly spatial distributed SC-PDSI raster's (section 5.3.2), which return period correspond for each cell/block discretization according to the specific crop phenological stages. An example for celery crop is given in Figure 5.11 and Figure 5.12, which has a sowing season in January-June. The SC/PDSI for April of 2001 is approx. -2.3 for almost all the blocks (Comarcas), and if we compare this to the related return period (for that particular crop band interval), this shows that Anoia and Alt Penedès were experiencing a drought event of almost 10 year return period (Table 5.8); Vallès Occidental, Baix Llobregat and Barcelonès a return period higher than 10 year return period and Berguedà, Ripollès, Solsonès, Osona, Bages, Vallès Oriental a lower return period event. This means that if a celery crop has been sowed in Anoia, in April 2001 it could experience a drought event with a higher return period than 10 year return period.

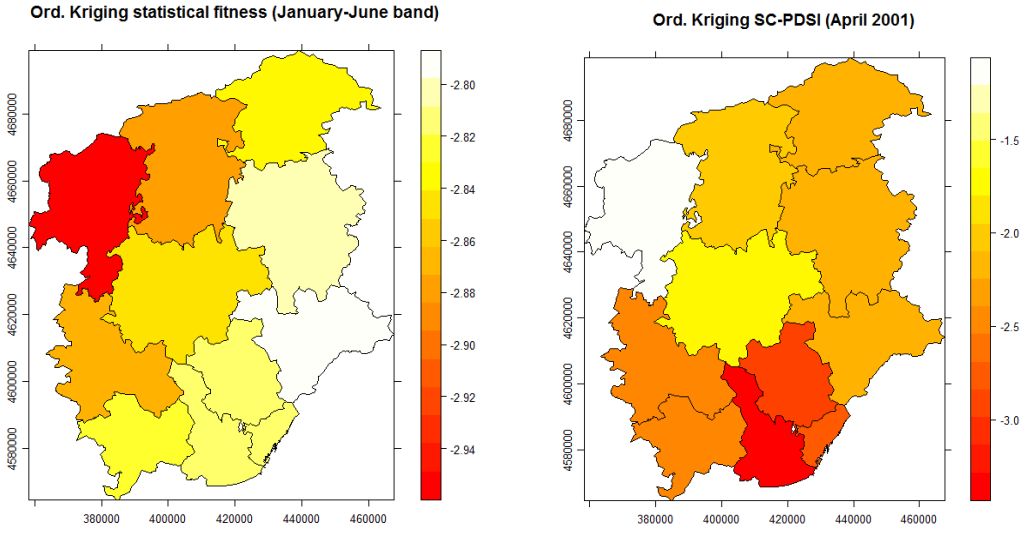

Figure 5.11 Statistical fitness of 10 year return period for the particular celery crop band interval (left) and SC-PDSI in April 2001 for Block discretization

The model considers 13 return periods, as displayed in Table 5.6: 500, 200, 100, 50 and 10 year of drought condition 2 year return period representing the normal condition and 10, 20, 50, 100, 200 and 500 for wet condition. Operatively the return period were marked as -500, -200, -100, -50, -10 and 2, 10, 20, 50, 100, 200 and 500, to differentiate between dry and wet conditions.

Table 5.8 Comparison of SC-PDSI for 2001 and the related return period for celery crop (block discr.)

Comarca	ID Code	Area (km²)	T (10 years)	SC-PDSI
Berguedà	14	1184.84	-2.670	-2.044
Ripollès	31	956.62	-2.664	-2.246
Solsonès	35	1001.24	-2.719	-1.209
Osona	24	1260.25	-2.663	-2.111
Bages	7	1299.09	-2.668	-1.666
Vallès Oriental	41	850.98	-2.666	-2.128
Anoia	6	866.31	-2.652	-2.509
Vallès Occidental	40	583.13	-2.662	-2.935
Alt Penedès	3	592.69	-2.653	-2.530
Barcelonès	13	145.75	-2.650	-2.795
Baix Llobregat	11	485.99	-2.648	-3.288

In the same way, a comparison between cells is done considering the CREAF land uses raster, which give us the location of the crop type in the basin (see Table 5.9 and Figure 5.12). The raster in the 400x400 m resolution has 335 rows and 273 columns and represents 91455 mesh cells, which means that a search algorithm has been developed.

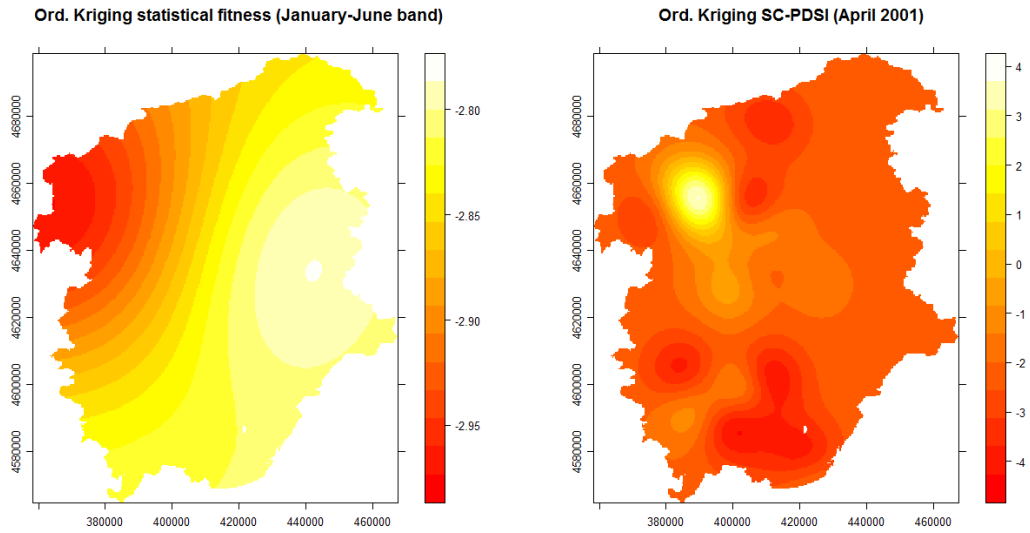

Figure 5.12 Statistical fitness for selected band (left) and SC-PDSI in April 2001 for cell/raster discretization

Table 5.9 Comparison of SC-PDSI for 2001 and the related return period for celery crop (cells discr.). Celery crop belong to vegetables classification (Table 5.7), which has a CREAF code equal to 124

Cell position from CREAF raster	T (10 years)	SC-PDSI (April 2001)
78140	-2.830	-2.614
72395	-2.843	-2.907
86884	-2.820	-2.951
71024	-2.847	-3.086
69105	-2.854	-3.154
78664	-2.832	-2.878
67593	-2.809	-3.263
65713	-2.802	-2.952

In the previous table the SC-PDSI index and return periods are displayed. A total of 8342 cells, from 91455 cells were identified as pixel with a value of 124 in the land uses raster. At same time this code is the value for the herbaceous classification (Table 5.7) which includes the vegetables crops and subsequently the celery crop. The behaviour of Figure 5.13 in which the values are almost constant, as displayed in Table 5.10, is originated from the constant statistical fitness for all hydrometeorological stations.

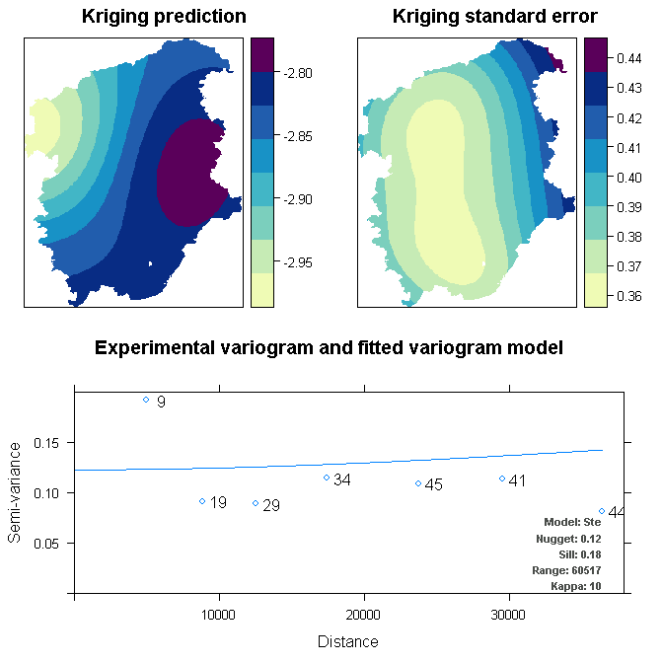

Figure 5.13 Ordinary Kriging for 10 year return period in January-June band

Table 5.10 Hydrometeorological stations and SC-PDSI return period for January-June interval

Station Name	Comarca	T (10 years)	Station Name	Comarca	T (10 years)
Aeroport	Baixllobregat	-2.958	Sant Quintí	AltPenedès	-2.82
Begues	Baixllobregat	-2.669	Caserres	Berguedà	-3.377
Gèlida	AltPenedès	-3.019	Fígols	Berguedà	-3.219
Sant Feliu	Baixllobregat	-2.636	La Pobla de Lillet	Berguedà	-2.914
Bagà	Berguedà	-2.845	Puig-Reig	Berguedà	-2.253
Igualada	Anoia	-2.966	Viver i Serrateix	Berguedà	-3.1
Piera	Anoia	-2.57	Busa	Solsonès	-3.102
Berga	Berguedà	-2.349	Naves	Solsonès	-3.428
Balsareny	Bages	-2.449	Riner	Solsonès	-3.161
Callús	Bages	-2.872	Sant Llorenç	Solsonès	-2.402
Manresa	Bages	-2.644	Solsona	Solsonès	-3.246
Moià	Bages	-2.809	Santa Maria	Anoia	-2.578
Corbera	Baixllobregat	-3.11	Esparreguera	Baixllobregat	-2.891
Cornellà	Baixllobregat	-3.048	Sant Sadurní	AltPenedès	-3.101
Olesa	Baixllobregat	-3.101	Martorell	Baixllobregat	-2.703
Sant Boi	Baixllobregat	-2.244			

Production condition identification:

The comparison of the cell and block return periods against the SC-PDSI will help fundamentally to three main effects: 1) to identify the drought events, 2) to relate annual exceedance probabilities, and 3) to find the normal production condition.

From statistics of crop production, some variables were summarized in order to identify what part of the production comes from rainfed areas and which from irrigated ones. To continue with the example of celery (classified in the Vegetables type of crop), the rainfed production was assessed through the total production and the irrigated production (Table 5.11 and Table 5.12). The crop rainfed efficiency was assessed through the total production, the rainfed and irrigated production and their corresponding areas.

Table 5.11 Statistics of vegetable crop type in the block discretization

Year	Comarca	Rainfed Area (ha)	Irrigated Area (ha)	Total Area (ha)	Crop Rai. Eff. (kg/ha)	Crop Irr. Eff. (kg/ha)	Total Prod. (tons)	Rain. Prod. (ton)
1995	Bergueda	168	180	348	8264	18987	4806	1388
1995	Ripolles	2122	10010	12132	8783	21757	236421	18637
1995	Solsones	0	12	12	NA	24333	292	0
1995	Osona	192	54	246	8810	20639	2806	1692
1995	Bages	274	1088	1362	8526	18921	22922	2336
1995	Valles oriental	30	1248	1278	12439	25582	32300	373
1995	Anoia	96	336	432	7696	19804	7393	739
1995	Valles occidental	70	750	820	9840	22074	17244	689
1995	Alt penedes	582	130	712	7637	19295	6953	4445
1995	Barcelones	0	318	318	NA	24557	7809	0
1995	Baix llobregat	678	5858	6536	10153	22724	140001	6884

Table 5.12 Statistics of vegetable crop type in the cell discretization for example of vegetable crop type

Year	CREAF Code	Rainfed Area (ha)	Irrigated Area (ha)	Total Area (ha)	Crop Rai. Eff. (kg/ha)	Crop Irr. Eff. (kg/ha)	Total Prod. (tons)	Rain. Prod. (ton)
1995	124	4212	19984	24196	8828	22106	478947	37182
1996	124	5622	29028	34650	9621	21949	691225	54090
1997	124	6808	38022	44830	9140	21820	891877	62222
1998	124	7984	47050	55034	8931	21587	1086993	71304
1999	124	9192	55276	64468	8936	21438	1267125	82144
2000	124	10326	63040	73366	8496	21456	1440308	87726
2001	124	11354	70219	81573	8604	21455	1604248	97692
2002	124	12296	77288	89584	9066	21222	1751650	111480
2003	124	13172	84524	97696	8746	21298	1915391	115204
2004	124	14216	91422	105638	8797	21448	2085850	125062
2005	124	15074	97926	113000	8505	21311	2215084	128212
2006	124	16390	103824	120214	8513	21239	2344635	139534
2007	124	17436	110317	127753	8542	21259	2494129	148947
2008	124	352	2402	2754	7582	18628	47414	2669
2009	124	17288.3	109723	127011	7864	20989	2438881	135963
2010	124	15563	101998	117544	5987	20964	2231419	93169

Considering that the value of the normal production condition should be located between the return periods -10 (dry condition) and 10 year (wet condition). The normal production condition is found in the year where the SC-PDSI (in the cells or blocks) had a value correlating to the period of 0 year return period. To detect the drought events, the model found those years which have a SC-PDSI with very high drought return periods (-∞), and considering the crop efficiency. Finally, the annual exceedance probability is found with the related return period. In Table 5.13 and Table 5.14 the examples for vegetables crop categories in cell and block discretization are shown.

Table 5.13 Drought events detection in the cell discretization for vegetables crop category

Year	T (years)	Efficiency (kg/ha)	Production (tons)
1998	-1	8930	71304
2001	-5.1051	8604	97694
2005	-13.23	8505	128212

Table 5.14 Drought events detections in blocks for vegetables crop category

Year	T (years)	Efficiency (kg/ha)	Production (tons)
1998	-1	8963	77772
2000	-6.69	8549	93056
2006	-7.56	8546	163689

Once the events and their related probability are found, some potential loss curves are proposed and will be explained in the following subsection.

5.4 Analysis of results

To obtain potential economic losses results the statistics of crop production from the ministry of agriculture has been disposed. In this statistical data there are missing values in the data series, which means that not for every crop type there are an equal number of values. In fact mostly in all type of crops only 11 years of data was available during the length of the SC-PDSI data series (1913-2006). In these 11 years only 2 events of drought were detected (2000/2001 and 2005/2006), which is a limitation for the present model calibration. Nevertheless, the following results are encouraging, because it demonstrates coherence with the conceptual behaviour of drought events over rainfed crops. The first curve that can be obtained from data exposed in Table 5.13 and Table 5.14 is the potential loss of production (in tons). In Figure 5.14 (left and right) the results for the nine crops that have been categorized are displayed. In the left figure, it

can be noticed that the curves have a monotonic decreasing behaviour and, for some type of crops, the losses are increasing faster in lower return periods. This is a first conclusion that could be extracted from this model. The rate of the increase of damage is really high for very low return periods, and probably, which means that the 100% damage will be reached faster. The right curve, instead, displays a behaviour which seems to be strange for some type of crops in a first instance: for the episodes with a return period of around 10 years the assessed damage through the model for industrial, leguminous and tubers show less damage than the episodes with a return period of around 5 years. Even though these events with a return period of around 10 years were more intense (a severe drought), the curves do not show an increase of losses because the cropped areas (exposure) in both events have not been taken into account. This gives the idea that the event with a 5 years return period, corresponding to the event in 2000, has more damage.

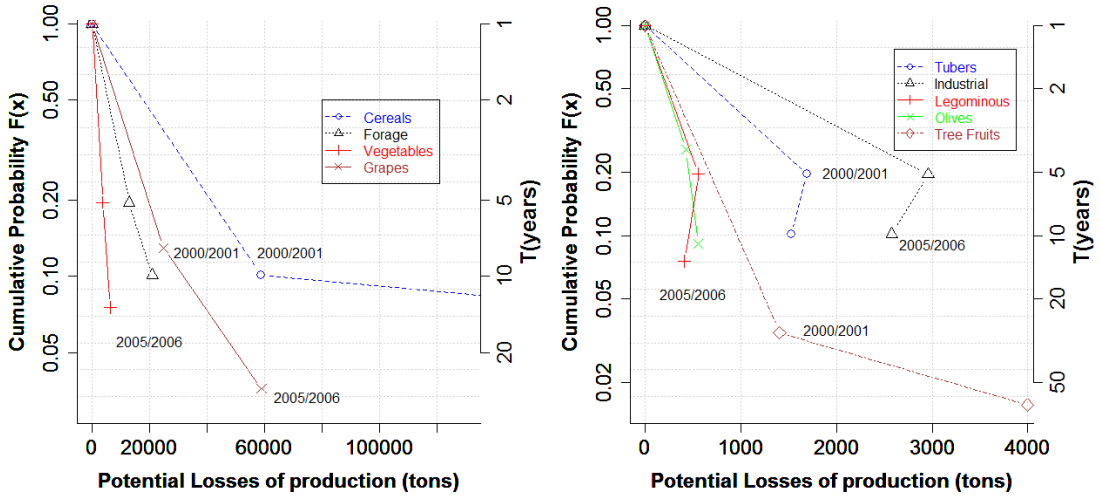

Figure 5.14 Potential crop production losses in cell discretization

One variable which is usually displayed in flood risk assessment is the potential economic losses, which is done using the potential production losses and actual costs of the specific crop in euros

(€). This is shown in Figure 5.15, which summarize 40.13 M€ and 55.84 M€ for the 2000/2001 and 2005/2006 events respectively. The curves that have been made for the Llobregat basin have been built considering official prices in Catalonia in 2015. Nevertheless, these curves show the same effect as in the last curves as they show the difference of the cropped area and related economic effects.

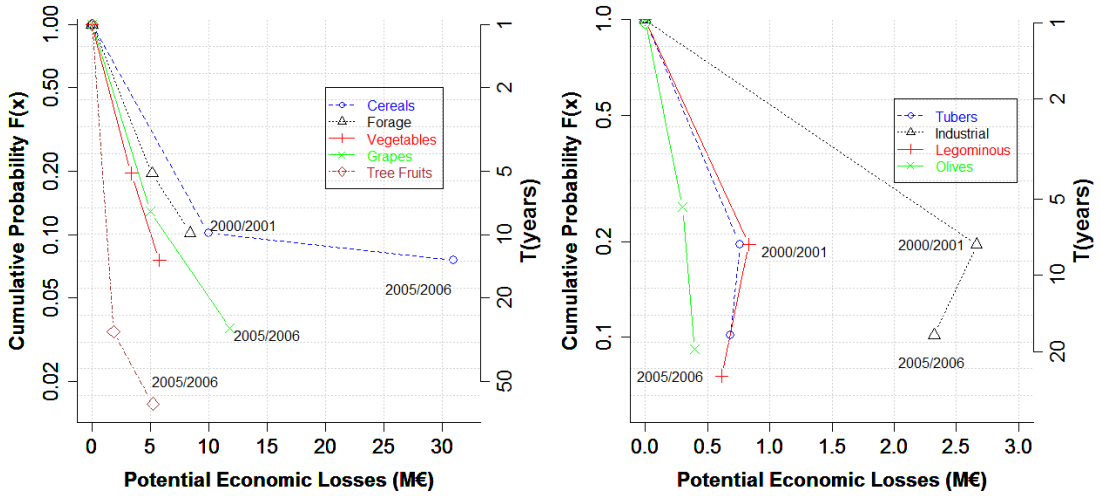

Figure 5.15 Potential economic losses in block discretization

So on, the best strategy to avoid the influence of the effect of the change in the cropping area, is to divide the potential production losses by the cropping area during each presented drought event (see Figure 5.17). This means that the potential production losses are relative to the cropped area each year.

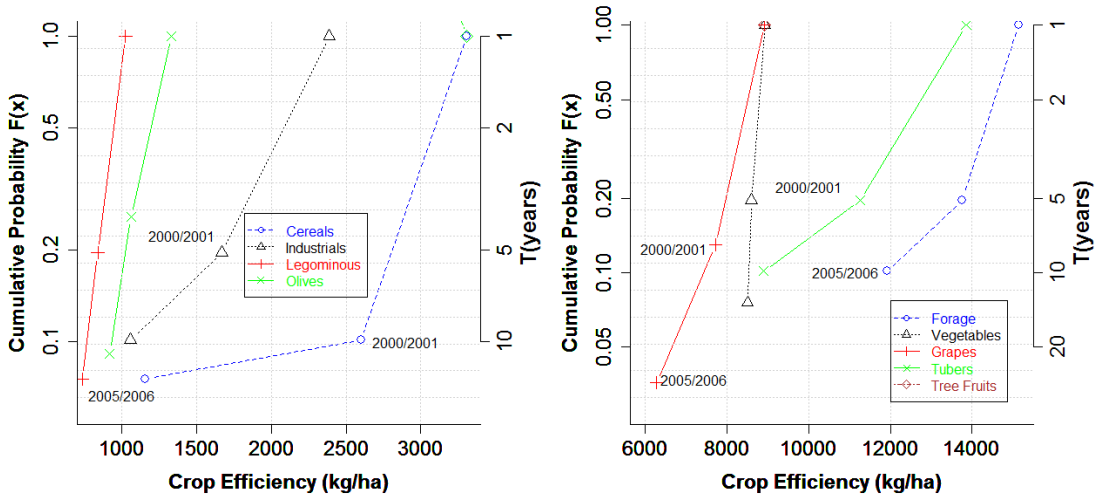

Figure 5.16 Potential crop efficiency losses in cell discretization

Equally as in the cell discretization, the displayed curves can be obtained for block discretization (see Figure 5.17 to Figure 5.19), as done with Figure 5.14 to Figure 5.16.

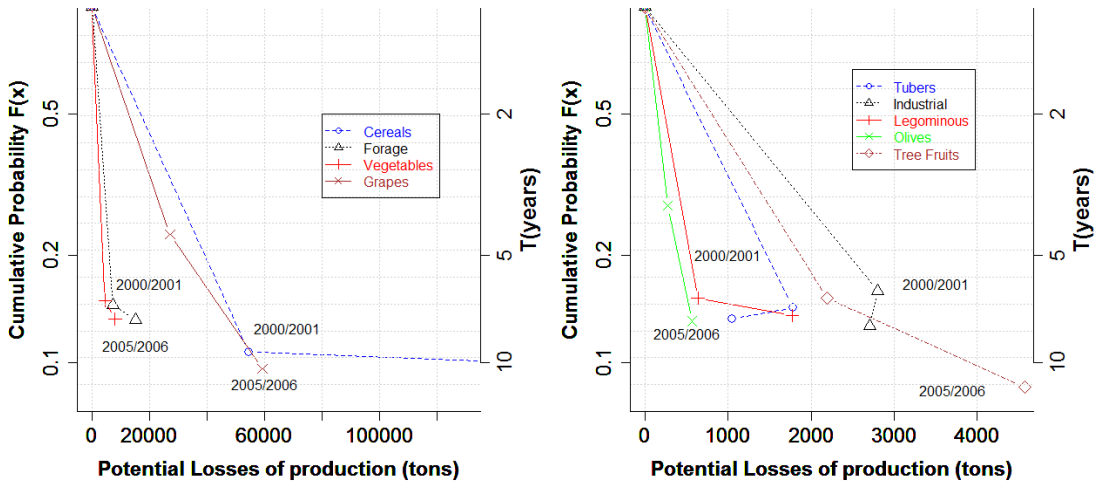

Figure 5.17 Potential crop production losses for block discretization

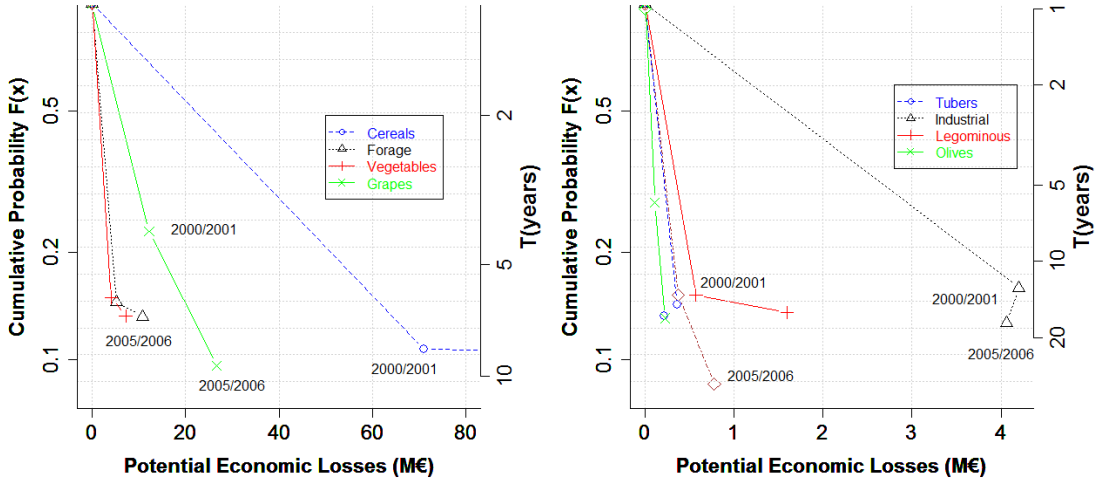

Figure 5.18 Potential economic losses for block discretization

From the previous figures is it remarkable that even if the model detects the same drought events, the same return periods are not related. These conclusions could already be extracted in the beginning from Table 5.13 and Table 5.14. This is because the spatial discretization makes that the different SC-PDSI and consequently different return periods are assigned to these events. The potential crop efficiency loss curves, which are shown in Figure 5.19, display several slopes according to the crop type characterization. This means that the steeper slopes, represent a lower sensitivity of crop type to drought events, and lower slopes mean a higher sensitivity to drought events.

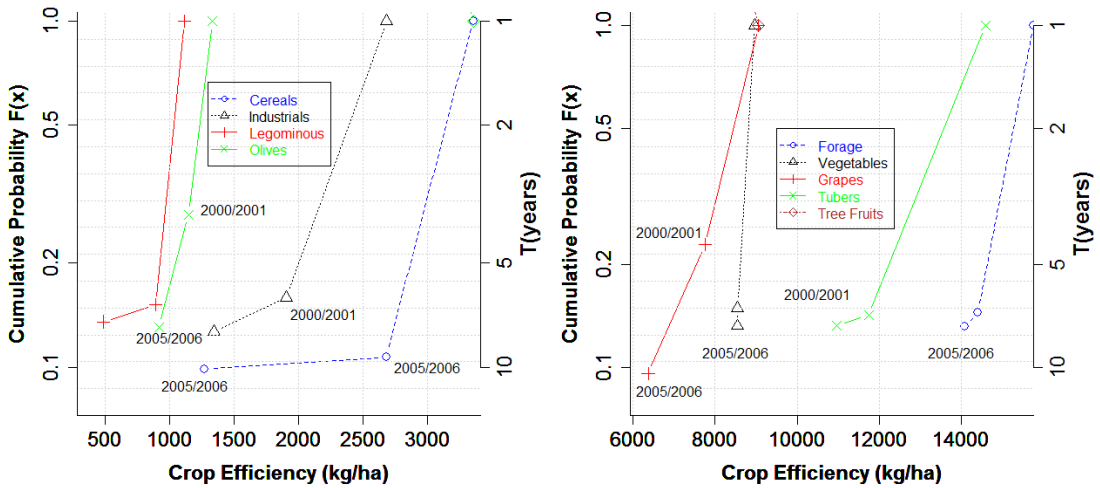

Figure 5.19 Potential crop efficiency losses in block discretization

5.5 Summary

Although this model has some limitations in the accuracy of the results, it is remarkable that it is one of the few tools for quantitative risk assessment that relates to the exceedance probability of an event and its possible consequences. Also some curves which may help to managers in the drought risk management process have been proposed. Below, some conclusions about the proposed agricultural drought risk assessment model over rainfed crops are listed:

1. In this thesis a new methodology for quantitative risk assessment for drought has been developed. For this, the SC-PDSI model was used linking potential losses in rainfed crops, with a return period in terms of cumulative frequency probability.

2. The curves of potential production losses, potential economic losses, and most significantly, the potential loss of crop efficiency have been proposed for crops, oriented to the decision-making process.
3. Regarding the vulnerability of crops, the methodology shows that a classification of several kinds of crops, with characteristic bands (or intervals), can help to simplify and relate the damage to rainfed crops.
4. Although, obviously the model does not detect all periods of drought, it does for those of substantial magnitude and duration: i.e., for periods of severe drought, it can detect these events and assign related return periods. The proposed methodology can identify normal production years (the months / years of SC-PDSI close to 0), and quantify potential losses (of production, economy and efficiency). Part of this limitation can be related to the behaviour of the SC-PDSI model, which has been extensively criticized, as exposed in section 1.3.
5. On the curves which are shown, it is to mention that for economic losses (M€), and loss of production (in tons), some graphs show inflection points, which for higher return periods displays minor damages (or losses). This is mainly because of the exposure which is represented by the area of crop, which is not constant in time. Considering the fact that the presented model is based on real production and areas of rainfed crops (for calibration), and that the related events are the ones with a higher return period with minor damage, the “potential loss of crop efficiency curves” seems to be a better tool for the decision making process in drought management than economic or production losses curves.

6. The proposed curve for the potential crop efficiency losses, implicitly illustrates many features of drought events; First of all, the same curves shows that different types of cultivation (olives, vegetables, grapes) have different slopes, which shows the sensitivity of the crops. For example, this is shown in Figure 5.19, where the slope of the potential crop efficiency loss curve for olives is much higher than for cereals, because an olive tree is a lot more resistant to drought than cereals crops. Secondly, a very interesting feature is the asymptotic behaviour of the curve which gives up to 100% damage for lower return periods. This is exactly the opposite behaviour of the curves for potential economic losses in flood events, in which, higher return periods can have high potential damage. Thirdly, all detected events fall in the 2000/2001 and 2005/2006 years, but these curves show that the same event does not have the same associated return period in every crop type. This is because the same event affects every crop type differently.
7. Finally, the potential economic losses for the events of 2000/2001 and 2005/2006 were approximately 40.13 M€ and 55.84 M€ respectively.

Chapter 6: Conclusions

In the present thesis two perspectives for risk management of flood and drought events were proposed: in case of flood events, a methodology has been developed to include the implementation of non-structural measures in the risk assessment process. In case of drought events, a new methodology to relate the meteorological drought with potential losses in rainfed crops is suggested.

The implementation of non-structural measures has been identified as a feasible way to reduce flood risk in basins in which structural measures have been exhaustively applied. By implementing the non-structural measures in the flood risk assessment, more mitigation can be achieved. In drought risk assessment, few quantitative models are available to relate potential losses in rainfed crops with the return period of the events. Chapter 3 and 4 describe the implementation of non-structural measures (methodology and uncertainty analysis) and Chapter 5 the drought risk model implementation. The following conclusion can be extracted from these chapters.

6.1 Methodology for optimization of non-structural measures in pluvial flooding residual risk mitigation; The Arenys de Munt basin

1. A methodology for the inclusion of the NSMs in the risk assessment process has been developed. The case study focussed on pluvial flooding with as the experimental basin the Arenys de Munt in Catalonia. In this methodology, eight steps were proposed in order

to optimize the use of resources (mainly in terms of money), and focusses on the process of implementation of NSMs. As any risk study, some hypotheses had to be imposed in societal and economic risk assessment: people at risk had to be estimated; an analysis was carried out considering a worst case event in which urban drainage systems and gutters collapsed; the reduction due to the implementation of several NSMs was applied (see section 3.11).

2. About the Arenys de Munt case study, the 500.000 € per year considered in the present study for flood risk management would be an excessive and "fictitious" amount, because many of the resources planned for NSMs implementation already exist. This means that the real cost of the NSM implementation will be less. If we subtract the corresponding money from the implemented NSMs from NSMs to implement, the final real cost for flood risk is reduced to 33.000 €/year, around 3.89 € per capita (8484 inhabitants). On the other hand, the Expected Annual Damage (EAD), obtained from the F-€ curve set out in Figure 3.10 (potential economical losses), is equal to 119.383 €/year. Thus we can conclude that the NSMs investment in the basin is below the amount that can be lost annually.
3. For the inclusion of the NSMs in the risk assessment process, risk reduction coefficients were developed. These coefficients are valid for the particular case study and cannot directly apply over other basins. The coefficients that have been denoted in Chapter 3, show that different combinations of NSMs brings different results in risk mitigation. Furthermore, focussing all the resources on one NSM does not necessary mean more mitigation. This is because the NSMs have implicit restrictions. To understand this, it can be idealized the classical example of a painter painting a wall, in when another painter

helps, the speed will be double, but if the quantity of painters tend to infinite, this does not mean that the time to finish the work will tend to 0. There is a point in which adding more workers will not increase the speed due to space restriction. More research should be done about the mitigation coefficients, to increase the amount of knowledge about the behaviour of the NSMs which subsequently will lead to better risk management.

4. In Arenys the Munt a worksheet for the action forces (agencies) and the population is presented with the role to be developed by each agency in case of flood emergency (communication, mobilization actions etc.).

6.2 Uncertainty in Pluvial Residual Risk Assessment due to Flash Floods

1. An uncertainty analysis was developed in order to analyse the possible variation in the results due to hydrologic, hydraulic and statistical distribution uncertainty. Evidently, there are more uncertainty sources which have not been included, but in order to see the behaviour in the risk assessment process, an analysis has been done after the implementation of NSMs.
2. In the potential casualties' assessment, there is not any document about the influence of using one, two or more vulnerability parameters on risk assessment. The analysis that has been done shows that the vulnerability discretization that is adopted in the present methodology appears to reduce the uncertainty, because the confidence interval bands are almost identical to the expected value (see Figure 4.8). This behaviour could be associated with the higher slopes that are present in the basin, which leads to higher flow velocities. Therefore the vulnerability criteria including velocity always end up in the

worst scenario (severity S4) and it does not necessary represent an improvement on the results in terms of uncertainty. In terms of potential economical damages, confidence interval bands were obtained after including the hydrologic (9 confidence intervals), hydraulic (2 Manning coefficient) and statistical uncertainty (moments and least square methods).

3. About the cases handled for the potential economic losses it is noted that both uncertainty values (hydraulic and hydrological) for a 500 years return period, and the "worst case", oscillate from respectively 5.8 to 13.2 M € and from 4.5 to 10.5 M € if a NSM is implemented and from 2.7 to 5.2 M € if a NSM and a sewer system are operative. Although the dispersion decreases for low return periods, the values are very high in general. Low differences between moments and least square method have been observed in the statistical uncertainty. Including an uncertainty analysis in this kind of studies would provide a helpful tool in the decision making process.
4. It has been noted that the risk of potential casualties is reduced for high Manning coefficients. High Manning's coefficient values reduce the mean flow velocity along the streets and the drag forces. The risk of potential economic losses is increased by increasing the Manning coefficient because this leads to have high water levels that increase the risk damage. Therefore, in case of potential casualties, a low Manning coefficient would be better for the risk assessment. In the counterpart, for the potential economic losses, the highest Manning values should be taken. The statistical method used, differs very little in the final results. However, when comparing left and right sides of Figure 4.11, Figure 4.12 or Figure 4.13 a variation of around 5%, can be seen.

5. The EAD confidence intervals vary significantly according to the uncertainty analysis, as well as potential economical losses. In the example exposed in section 4.9, for the "Worst Case" and n=0.030 and n=0.015, the dispersion oscillates around the 30% (3.7 to 2.3 M€/year), showing that also this parameter is significantly affected by the uncertainty. On the other hand, the proposed Optimal Expected Annual Damage OEAD altogether with the cumulative percentage of the EAD mitigated (Figure 4.17) could be assumed as a decision making value for the planning of structural measures. This is because the design criteria are subjectively imposed many times and with those parameters a mitigation level for a specific return period can be established. Evidently, any developed tool that improves the optimization of resources will help in the risk management planning.
6. Risk assessment in terms of potential economical losses and casualties for 3 cases are exposed in this document. It is clearly reduced by the implementation of NSM and in case of an EWS (Early Warning System) and the implementation of a sewer system. Moreover the economic risk reduction by the implementation of a EWS system is more significant than in societal risk. This is because a few hours of lead time could represent significant economic loss reduction. This reduction could even be up to 90 % of the initial value taking into account the EWS plus drainage system measures.

6.3 New drought risk assessment methodology focused on meteorological drought

1. A new methodology for quantitative risk assessment relating meteorological drought and potential losses in rainfed crops has been developed. The model uses the SC-PDSI in

order to monitoring the meteorological drought conditions, with crop related statistics to link potential losses in rainfed crops, with the related return period.

2. Although the model has some limitations, it is remarkable that it is one of the few tools for quantitative drought risk assessment.
3. Three curves for the decision making process have been proposed; potential production losses, potential economic losses, and most significantly, the potential loss of crop efficiency curve. Even though mitigation measures have not been researched for drought events (structural or non-structural measures), the model and concisely these curves can be a good tool for risk managers when measures will be proposed to be implemented
4. The vulnerability assessment for rainfed crops has been one of the key points in the present model. The methodology shows that a classification of several kinds of crops, with a characteristic bands (or intervals) related to the phenological stages (harvesting and sowing), can help to simplify and relate the damage to rainfed crops.
5. The model does not detect all periods of drought, and the experience of the modeller is required for filtering the information and to detect those of substantial magnitude and duration. Nevertheless, once curves of risk are built, the potential economic losses can be found through the drought condition monitoring (SC-PDSI). This means that the model can work for monitoring and forecast conditions.
6. Inflection points in economic losses (M€), and loss of production (tons) have been detected. This is mainly because the exposure (of crops) is not constant in time, doing that for higher return periods less damages are observed for some crop types. For this reason the potential loss of crop efficiency curves seems to be a good tool for the decision making process in drought management.

7. The proposed curve for potential crop efficiency losses, illustrates three main characteristics under drought events; First, different types of crops (olives, vegetables, grapes etc.) have different slopes, which shows the implicit sensitivity of the particular crop to drought events. For example, in Figure 5.19, where the slope of the potential crop efficiency loss curve for olives is much higher than for cereals. This is because the olive is more resistant to drought than cereals crops. Secondly, a very interesting feature is the asymptotic behaviour of the curve which gives up to 100% damage for low return periods. This is exactly the opposite behaviour of the curves for potential economic losses in flood events, in which, higher return periods can have high potential damage. Thirdly, all detected events fall in the 2000/2001 and 2005/2006 years, but these curves show that the same event does not have the same associated return period in every crop type. This is because the same event affects every crop type differently.
8. Finally, for the Llobregat basin case study, potential economic losses for the events of 2000/2001 and 2005/2006 were approximately 40.13 M€ and 55.84 M€ respectively M€ in the geopolitical subdivision called "Comarcas" of the Llobregat basin. In which in almost all cases the event of 2005/2006 was much more intense but the exposition of rainfed crops (cropped area) was less than the event of 2000/2001, leaving relative less damages for the 2005/2006 event.

6.4 Future works

Without a doubt, risk management is a science which can help in disaster consequence mitigation. Nevertheless, nowadays there is still some a lack of knowledge in around topics that

makes this science inaccurate. As a result of the present research some future fields of work are listed below:

1. A future research line is to track and follow the implemented NSMs in a basin, where economic losses and human casualties occurred after the implementation of the measures. These basins can be used to calibrate the mitigation coefficients of the NSMs. Additionally, NSMs combinations are unique for each basin making that these measures cannot be applied equally from one place to another. However, each time these measures are executed, the mitigation coefficients can be corrected or modified when subjected to flood events.
2. There are several sources of uncertainty; not only the hydraulic, hydrology and statistical distribution uncertainty could affect the risk assessment, but also vulnerability assessment uncertainty, with the depth – damages curves or the rates of casualties can include huge variability. So on, more research in the vulnerability assessment should be done.
3. The developed drought methodology has been applied to the Llobregat basin crop data, however, in order to gain reliability, other applications with different crop information and weather characteristics should be performed. The results for potential economic losses should be compared against data that is available at insurance companies or from official governmental data.

Bibliography

Allen, C. D., Macalady, A. K., Chenchouni, H., Bachelet, D., McDowell, N., Vennetier, M., Kitzberger, T., Rigling, A., Breshears, D. D., Hogg, E., Gonzales, P., Fensham, R., Zhang, Z., Castro, J., Demidova, N., Lim, J., Allard, G., Running, S., Semerci, A., and Cobb, N. 2010. "A global overview of drought and heat-induced tree mortality reveals emerging climate change risks for forests." Forest Ecology and Management no. 259 (4):660-684.

Andjelkovic, I. 2001. Guidelines on NSMs in urban flood management. Paris: UNESCO.

Arnell, N. W. 1989. "Expected annual damages and uncertainties in flood frequency estimation." Journal of Water Resources Planning and Management no. 115 (1):94-107.

AUDACIOUS. 2008. Building Knowledge for Climate Change Adaptable Urban Drainage - Addressing Change In Intensity, Occurrence And Uncertainty of Stormwater (Summary Report). United Kingdom.

Ballard, J. G. 1965. The drought. London: Cape.

Barriendos, M., and Pomés, J. 1993. Floods and Hydric Resources. Mataró.

Berga, L. 1995. "La problemática de las inundaciones en Catalunya." El agua en Catalunya, edited by: Berga, L:237-256.

Beven, K. 2011. "Distributed Models and Uncertainty in Flood Risk Management." In Flood Risk Sciences and Management, edited by John Wiley and Sons. London.

Beven, K., and Binley, A. M. 1992. "The future of distributed models: model calibration and uncertainty prediction." Hydrological Processes. no. 6:279-298.

Castro, F., Tudela, A., and Sebastià, M. 2003. "Modeling moisture content in shrubs to predict fire risk in Catalonia (Spain)." Agricultural and Forest Meteorology no. 116 (1):49-59.

Catalan, L. 1997. Estudio hidrológico del Río Llobregat. Barcelona.

CEDEX. 2007. Cuencas Internas de Cataluña. Madrid.

Climate Communication Center. 2014. Predicted changes in global crop productivity http://www.climatecommunication.org/affects/food-production/.

Coleman, M. E., and Marks, H. M. 1999. "Qualitative and quantitative risk assessment." Journal of Food Control.

COST 731. 2010. Propagation of uncertainty in advanced Meteohydrological forecast systems. In Framework Programmes (FP6), edited by COST initiative: EUROPE UNION.

CREAF. 2009. Mapa de Usos del Sol.

CRUE. 2009. Synthesis Report: Risk Assessment and Risk Management Effectiveness and Efficiency of Non-structural Flood Risk Management Measures. edited by Crue Era-Net funding initiative: Europe union.

Custodio, E., Cacho, F., and Peláez, M. D. 1976. Problemática de la intrusión marina en los acuíferos del Delta del Llobregat. Paper read at II Asamblea Nacional de Geodesia y Geofísica, at Madrid.

Chiatante, D., Iorio, A. D., Sciandra, S., Scippa, G. S., and Mazzoleni, S. 2006. "Effect of drought and fire on the root development in Quercus pubescens Willd. and Fraxinus ornus L. seedlings." Environmental and experimental botany no. 56 (2):190-197.

Chow, V. T. 2000. Hidráulica de Canales Abiertos. Bogotá, Colombia.: McGraw Hill.

Dasgupta, R. 2007. Disaster management and rehabilitation: Mittal Publications.

DEFRA. 2010. Surface Water Management Plan, Technical Guidance. edited by Department for Environmental Food and Rural Afairs. United Kingdom.

Díaz, M. A., Bateman, A., and Medina, V. 2008. Estudio de la sequía hidrológica y meteorológica en la cuenca del río llobregat. Paper read at XXIII Congreso Latinoamericano de Hidráulica, at Cartagena de Indias, Colombia.

Dixon, G. R., and Trevor, M. L. 2009. "Chapter 17 - The Impact of Climate and Global Change on Crop Production." In Climate Change, 307-324. Amsterdam: Elsevier.

Drobyshev, I., Niklasson, M., and Linderholm, H. W. 2012. "Forest fire activity in Sweden: Climatic controls and geographical patterns in 20th century." Agricultural and Forest Meteorology no. 154:174-186.

Drobyshev, I., Niklasson, M., Linderholm, H. W., Seftigen, K., Hickler, T., and Eggertsson, O. 2011. "Reconstruction of a regional drought index in southern Sweden since AD 1750." The Holocene no. 21 (4):667-679.

Drunasky, N., and Struve, D. K. 2005. "Quercus macrocarpa and Q. prinus physiological responses to drought stress and their potencial for urban forestry." Urban Forestry & Urban Greening no. 4 (1):13-22.

Dueñas, C. 2010. Discussion Table. Paper read at proceedings of the challenges and opportunities about the Flood Directive.

Escuder-Bueno, I., Castillo-Rodríguez, J., Zechner, S., Jöbstl, C., Perales-Momparler, S., and Petaccia, G. 2012. "A quantitative flood risk analysis methodology for urban areas with integration of social research data." Natural Hazards and Earth System Science no. 12 (9):2843-2863.

Escuder, I., Morales, A., Castillo, J., and Perales, S. 2010. Workpackage 3 on the Sustainable Strategies of Urban Flood Risk Management with non-structural measures to cope with the residual risk (SUFRI).

Escuder, I., Morales, A., Castillo, J., and Perales, S. 2011. SUFRI Methodology for pluvial and river flooding risk assessment in urban areas to inform decision-making. Valencia.

European Parliament. 2007. "Directive 2007/60/EC of the European parliament and of the council of 23 October 2007 on the assessment and management of flood risks." Official Journal of the European Union no. L 288/31.

EWASE. 2008. Final Report Effectiveness and Efficiency of non-structural Flood Risk Management Measures. edited by Crue Era-Net: EWASE.

Faber, R. 2006. Flood risk analysis: Residual risks and uncertainties in an Austrian context, University of Natural Resources and Applied Life Sciences, Vienna, Austria.

Feyen, L., Dankers, R., Bódis, K., Salamon, P., and Barredo, J. I. 2012. "Fluvial flood risk in Europe in present and future climates." *Climatic change* no. 112 (1):47-62.

Fleig, A. 2004. Hydrological drought – A comparative study using daily discharge series from around the world, Instituto de Hidrología, , Universidad de Freiburg, Freiburg, Alemania.

Forman, R. 2004. Mosaico territorial para la región metropolitana de Barcelona. Barcelona.

Forn i Salvà, F. 2002. Dear Stream: Geographic – Historic study of the Arenys de Mar stream. Arenys de Mar, Spain.

Fuchs, S., Spachinger, K., Dorner, W., Rochman, J., and Serrhini, K. 2009. "Evaluating cartographic design in flood risk mapping." Environmental Hazards no. 8 (1):52-70.

Gallart, F. 1991. "Estudi geomorfològic de la conca d'Òdena. Estr 2." Revista d`Arquelog. Prehis. i Història Antiga.

Ganatsas, P., Antonis, M., and Marianthi, T. 2011. "Development of an adapted empirical drought index to the Mediterranean conditions for use in forestry." Agricultural and forest meteorology no. 151 (2):241-250.

Gifu, D., Dima, I. C., and Teodorescu, M. 2014. "New communication approaches vs. traditional communication." International Letters of Social and Humanistic Sciences (20):46-55.

Gumbel, E. J. 2012. Statistics of extremes: Courier Corporation.

Haiganoush, P. K., and Westerling, A. L. 2007. "Statistical model for forecasting monthly large wildfire events in western United States." Journal of Applied Meteorology and Climatology no. 46 (7):1020-1030.

HEC. 1989. "Expected Annual Flood Damage." In CPD-30 user manual, edited by Davis. U.S.A.

Heddinghaus, T., and Sabol, P. 1991. A review of the Palmer Drought Severity Index and where do we go from here? Paper read at Applied Climatology.

Hinckley, T., Dougherty, P., Lassoie, J., Roberts, J., and Teskey, R. 1979. "A severe drought: impact on tree growth, phenology, net photosynthetic rate and water relations." American Midland Naturalist:307-316.

Hisdal, H., and Tallaksen, L. M. 2003. "Estimation of regional meteorological and hydrological drought characteristics: a case study for Denmark." Journal of Hydrology no. 281 (3):230-247.

Hsiao, T. C., and Acevedo, E. 1974. "Plant responses to water deficits, water-use efficiency, and drought resistance." Agricultural Meteorology no. 14:59-84.

Hu, Q. S., and Willson, G. D. 2000. "Effects of temperature anomalies on the Palmer Drought Severity Index in the central United States."

IAEM. 2007. Principles of Emergency Management Supplement. International Association of Emergency Managers.

Ibarra, M. 2009. Comunicación para la Gestión del Riesgo o del Riesgo de Gestionar Estratégicamente la Comunicación. Paper read at XIII Encuentro Latinoamericano, at La Habana, Cuba.

ICC. 2002. Mapa de la Geología en el Maresme. Barcelona, Spain: (Instituto Cartográfico de Cataluña).

Iglesias, A., Cancelliere, A., Cubillo, F., Garrote, L., and Wilhite, D. A. 2009. Coping with drought risk in agriculture and water supply systems. The Netherlands: Springer.

Institute of Hydrology. 1980. Low flow studies report. Institute of Hydrology. Wallingford, UK.

INUNCAT. 2010. Catalonia Special Flooding Plan. edited by INUNCAT. Barcelona, Spain.

Jha, A. K., Bloch, R., and Lamond, J. 2012. Cities and flooding: a guide to integrated urban flood risk management for the 21st century: World Bank Publications.

Jobstl, C., Zechner, S., Knoblauch, H., and Pohl, R. 2011. SUFRI – Sustainable Strategies of Urban Flood Risk Management with non-structural measures to cope with the residual risk. Graz.

Jonkman, S. N. 2007. "Loss of life estimation in flood risk assessment." Civil engineering faculty.

Jonkman, S. N., Van Gelder, P. H., and Vrijling, J. 2003. "An overview of quantitative risk measures for loss of life and economic damage." Journal of Hazardous Materials no. 99 (1):1-30.

Keetch, J. J., and Byram, G. M. 1968. A drought index for forest fire control. In Res. Paper SE-38. Southeeastern Forest Experiment Station, U.S.: Department of Agriculture, Forest Service.

Kerstin S. 2002. Hydrological Drought – a Study Across Europe, Instituto de Hidrología, Universidad Albert Ludwigs Freiburg, Polonia

Kolen, B., Maaskant, B., Helsloot, I., and Thonus, B. 2008. EvacuAid: probabilistic evacuation model to determine expected loss of life for different strategies for mass evacuation: The Authors.

Kron, W. 2002. Flood risk = hazard x exposure x vulnerability. Paper read at International Symposium on Flood Defense

Liedloff, A., and Cook, G. 2007. "Modelling the effects of rainfall variability and fire on tree populations in an Australian tropical savanna with the FLAMES simulation model." Ecological Modelling no. 201 (3):269-282.

Luna, E. M. 2009. Community development as an approach to reducing risks among flashflood-affected families in Albay, Philippines. Disaster Studies Working Paper 24.

Llistosella, X., and Pàmies, M. 2003. Arenys de Munt Land Planning

Mak, J. 2008. Modelling the evacuation process in case of flooding: an application of a dynamic traffic model, a comparison to existing models and an optimization of the evacuation process. edited by in FLOODSite.

Manzano, M. 1986. Estudio sedimentológico del prodelta holoceno del Llobregat, Universidad de Barcelona, Barcelona.

Marcé, R., Honey-Rosés, J., Manzano, A., Moragas, L., Catllar, B., and Sabater, S. 2012. "The Llobregat River Basin: A paradigm of impaired rivers under climate change threats." In The Llobregat, 1-26. Springer.

Mckee T., D. N., Kleist J. 1993. The relationship of drought frequency and duration to time scales Paper read at Eight Conference on Applies Climatology, at California, United States.

Min, S.-K., Zhang, X., Zwiers, F. W., and Hegerl, G. C. 2011. "Human contribution to more-intense precipitation extremes." Nature no. 470 (7334):378-381.

Moneo, M. 2008. Drought and climate change impacts on water resources: management alternatives, Technical University of Madrid, Madrid, Spain.

MOP. 1996. Estudio de los recursos hidráulicos totales de las cuencas de los ríos Besós y Bajo Llobregat. edited by Ministerio de Obras Públicas. Barcelona: CASPO-SGOP.

N.R.C.S. 1998. Soil Quiality Resource Concerns: Available Water Capacity. edited by Soil Quality Information Sheet: USDA information sheet.

Nania, L. 1999. Metodología numérico-experimental para el análisis del riesgo asociado a la escorrentía pluvial en una red de calles, E.T.S. Ingenieros de Caminos Canales y Puertos de Barcelona, Universitat Politècnica de Catalunya, Barcelona, España.

Newton, R., Funkhouser, E., Fong, F., and Tauer, C. 1991. "Molecular and physiological genetics of drought tolerance in forest species." Forest Ecology and Management no. 43 (3):225-250.

Nishat, A., Nishat, B., and Abdullah Khan, M. F. 2011. "A Strategic View of Land Management Planning in Bangladesh." In Flood Risk Sciences and Management, edited by John Wiley and Sons. London, United Kingdom.

NOAA. 2014. "Billion-Dollar Weather and Climate Disasters."

Palmer, W. C. 1965. RESEARCH PAPER NO. 45. Meteorological Drought. Washington D.C.: Office of Climatology, U.S. Weather Bureau.

Palmer, W. C. 1968. "Keeping track of crop moisture conditions, nationwide: The new crop moisture index."

Paté-Cornell, M. E. 1996. "Uncertainties in risk analysis: Six levels of treatment." Reliability Engineering & System Safety no. 54 (2):95-111.

Pearce, L. 2003. "Disaster management and community planning, and public participation: how to achieve sustainable hazard mitigation." Natural hazards no. 28 (2-3):211-228.

Pender, G., and Faulkner, H. 2011. Flood Risk Sciences and Management. London, United Kingdom.

Piperno, A., and Sierra, P. 2007. Estrategias desde el ordenamiento territorial para la prevención y mitigación de inundaciones. Paper read at International meeting about risk Management, at Montevideo.

Pitt, M. 2008. "The Pitt Review: Learning lessons from the 2007 floods." London: Cabinet Office.

Quarantelli, E. L. 1988. "Disaster crisis management: A summary of research findings." Journal of management studies no. 25 (4):373-385.

Quintero, F., Sempere-Torres, D., Berenguer, M., and Baltas, E. 2011. "A scenario-incorporating analysis of the propagation of uncertainty to flash flood simulations." Journal of Hydrology no. 460â€“461 (0):90-102.

Rot, A. 2008. IT risk assessment: quantitative and qualitative approach. Paper read at World Congress on Engineering and Computer Science.

Ruiz-Gonzales, A. D. 2004. La predicción de la humedad en los restos forestales combustibles: Aplicación a masas arboladas en Galicia, Universidad Politécnica de Madrid, Madrid, Spain.

Samper F., C. J. 1996. Geoestadística, aplicaciones a la hidrología subterranea. Edited by Centro Internacional de Métodos Numéricos (CIMNE). Vol. 1. Barcelona - Spain: Centro Internacional de Métodos Numéricos (CIMNE)

Sayers, P., Wallis, M., Simm, J., Baxter, G., and Andryszewski, T. 2011. "Towards the Next Generation of Risk-Based Asset Management Tools." In Flood Risk Sciences and Management, edited by John Wiley and Sons. Pender G. and Faulkner H.

Sempere Torres, D., Sánchez-Diezma Guijarro, R., Berenguer Ferrer, M., Pascual Berghaenel, R., and Zawadzki, I. 2003. "Improving radar rainfall measurement stability using mountain returns in real time."

Shafer, B. A., and Dezman, L. E. 1982. Development of a Surface Water Supply Index (SWSI) to assess the severity of drought conditions in snowpack runoff areas. Paper read at Proceedings of the Western Snow Conference.

Sole Sabarris, L. 1963. Ensayo de interpretación del Cuaternario Barcelonés. Barcelona.

Stahl, K. 2002. Hydrological drought-a study across Europe, Universitätsbibliothek Freiburg, Poland.

Stambaugh, M. C., Guyette, R. P., McMurry, E. R., Cook, E. R., Meko, D. M., and Lupo, A. R. 2011. "Drought duration and frequency in the US Corn Belt during the last millennium (AD 992–2004)." Agricultural and forest meteorology no. 151 (2):154-162.

Tallaksen, L. M., and Van Lanen, H. A. 2004. "Hydrological drought, processes and estimation methods for streamflow and groundwater". Ámsterdam: ELSEVIER.

Tapsell, S. 2011. "Chapter 20: Socio-Psychological Dimensions of Flood Risk Management." In Flood Risk Sciences and Management, edited by John Wiley and Sons. London, United Kingdom: Pender G., Faulkner H.

Thampapillai, D. J., and Musgrave, W. F. 1985. "Flood damage mitigation: a review of structural and nonstructural measures and alternative decision frameworks." Water Resources Research no. 21 (4):411-424.

Trenberth, K., Smith, L., Qian, T., Dai, A., and Fasullo, J. 2007. "Estimates of the global water budget and its annual cycle using observational and model data." Journal of Hydrometeorology no. 8 (4):758-769.

Tsakiris, G. 2004. Meteorological Drought Assessment. In Report for the European Research Project MEDROPLAN (Mediterranean Drought Preparedness and Mitigation Planning). Zaragoza, Spain.

Urbino Vallejo, V. 2010. Fenología y vida de las plantas. Universidad de Lleida.

USACE. 2006. Coastal Engineering Manual. Vicksburg, USA.: U.S. Army Corps of Engineers.

Van der Molen, M. K., Dolman, A. J., Ciais, P., Eglin, T., Gobron, N., Law, B. E., Meir, P., Peters, W., Phillips, O. L., Reichstein, M., Chen, T., Dekker, S. C., Doubková, M., Friedl, M. A., Jung, M., van den Hurk, B. J. J. M., de Jeu, R. A. M., Kruijt, B., Ohta, T., Rebel, K. T., Plummer, S., Seneviratne, S. I., Sitch, S., Teuling, A. J., van der Werf, G. R., and Wang, G. 2011. "Drought and ecosystem carbon cycling." Agricultural and Forest Meteorology no. 151 (7):765-773. doi: http://dx.doi.org/10.1016/j.agrformet.2011.01.018.

Velasco, C. 2009. Optimal estimation of rainfall fields for hydrological purposes in real time, Technical University of Catalonia, Barcelona, Spain.

Vicente-Serrano, S. M., Beguería, S., and López-Moreno, J. I. 2010. "A Multiscalar Drought Index Sensitive to Global Warming: The Standardized Precipitation Evapotranspiration Index." Journal of Climate no. 23 (7):1696-1718. doi: 10.1175/2009JCLI2909.1.

Vicente-Serrano, S. M., Cuadrat-Prats, J. M., and Romo, A. 2006. "Early prediction of crop production using drought indices at different time-scales and remote sensing data: application in the Ebro Valley (north-east Spain)." International Journal of Remote Sensing no. 27 (3):511-518.

Wells, N., Goddard, S., and Hayes, M. J. 2004. "A self-calibrating Palmer drought severity index." Journal of Climate no. 17 (12):2335-2351.

West, C., and Council, C. 2013. "Flood Risk Assessments."

Wheater, H., Beven, K., Hall, J., Pender, G., Butler, D., Calver, A., Djordjevic, S., Evans, E., Makropoulos, C., O'Connell, E., Penning-Rowsell, E., Saul, A., Surendran, S., Townend, I., and Watkinson, A. 2007. Broad Scale Modelling for Planning and Policy. In Technical Report FD2118. London, United Kingdom: Department for Environment, Food and Rural Affairs - DEFRA.

Wilhite, D. A. 2000. "Drought as a natural hazard : Concepts and definitions." Drought, A global assessment no. 1:3-18.

Zambrano, M. 2010. On the effects of hydrological uncertainty in assessing the impacts of climate impacts of climate change on water resources, Trento University, Italy.

Appendices

Appendix A Llobregat geologic and land uses labels

Table A.1 Label of the Geological Formations (ICC, 2002)

Dig. Cod	Description	Dig. Cod	Description	Dig. Cod	Description	Dig. Cod	Description
Q2E	Clays	Q3A	Sands	Q2D	Gravels	P67C	Gaps (La torre)
P67A	Conglomerates	P5E	Pebbles (Beuda)	C1A	Carbonated Gaps	J1C1	Dolomites (Garraf)
P7H	Pebbles (Noguera)	Q3F	Silts (valley bottom)	N3C	Sandstones (Selva)	COA	Microconglomerates
K4D	Bioclastic limestone	N1A	limestone esculloses	N1B	bioclastic limestones	C2A	Bioclastic Calcareous
P16A	Pebbles (Valldeperes)	Q2A	Lacustrine silts (Olot)	Q2C	Travertines (Banyoles)	GRDA	Granodiorites biotíties
N2C	Shales and sandstones	Q3D	Gravels, sands and clays	P7B	Sandstones, marls, limestones	N2E	Conglomerates (Cerdenya)
P5D	locally dark Marls with chalk	ST2	Volcanic Tuffs and Magma	N2D	Conglomerates, sandstones	P16B	Limestones (Forest in Borras)
P8L	Pebbles (Barbastro, Balaguer)	Q3E	Silts (coluvial and fluvioglaciers)	Q3G	Gravels, sandstones and lutites	K3E	Sandstones and conglomerates
P7D	Limestones (Tossa de Montbuy)	OB	Volcanic materials and porfirites	K5P1B	Limestones lake levels and lignite	C4A	Marlstones and marl-calcareous
P8F	Limestones (Tarrega, Castelldans)	N1C	Silts, clays and loams bioclastics	Q1D	Conglomerates, sands and lutites	P6B	Blue marl (Banyoles, Mesh, Ainsa)
C12	No differentiable calcareous stones	P7A	Blue marls and sandstones (Even Vic)	N2A	Siliceous and bioclastic sandstones	P2	Limestones with alveolina (Cadi Orpí)
P6E	Limestones with nummulites (Tavertet)	N1H	Gaps, conglomerates and sandstones	DSC	Grey Mudstones, nodules and pelites	P7G	Potassium and sodium salts (Cardona)
Q2F	Conglomerates, sandstones and lutites	N1F	Shales, sandstones and conglomerates	P8I	Sandstones and shales (Fraga, Solsona)	P7C	Local sandstones (Santa Marta Chico)
P7E	Sandstones with glauconite (Puigsacalm)	K5P1A	Conglomerates, sandstones and red clays	P6C	Sandstones and gray marls (Cuvet, Barcons)	P16E	Shales and red conglomerates (Romagats)
P5A	Turbidites (Campdevànol), gypsum ceiling	P3B	Marls, red clays and limestones (Corones)	P4D	Marl, and margocalcàries gaps (Armàncies)	P23	Chalks and marls with interbedded limestones
P8H	Red shales, sandstones and limestones (Flix)	N3E	Conglomerates, sandstones and shales (Cerdenya)	J13	Dolomites, limestones and calcareous marls (Bonansa)	P6F	Conglomerates and sandstones (Campany Bellmunt)
P67B	Sandstones and shales (Montserrat, St.	P16D	Red shales, conglomerates and breccias	P4E	Limestones with nummulites and assilines (Rock	P8J	Conglomerates, sandstones and shales (Solsona Margalef)

	Llorenþ Munt)		(Carmen, Cairo)		Terrades)		
P8K	Massive conglomerates (San Llorenþ Morunys, Montsant)	P7F	Sandstones, conglomerates, marls and lignites(Sossa, Vilada)	P	Conglomerates, sandstones, shales and acid tuffs (Peranera)	DCO	Pelites and limestones, calcareous pelites multicolored carbonates
S	Ampelitiques slates locally calcareous, lidites and radiolarites	P16C	Sandstones, conglomerates and red shales (La Pobla de Claramunt)	P8G	Shales, sandstones, limestones and locally dolomitic marls and gypsum	N3A	Marine sediments: shales, marls, sandstones, conglomerates and breccias
Q3B	Shales with organic matter and peat (filled wetlands, abandoned channels)			CAA	Lydite with phosphates and calcareous nodules. Turbidites, sandstones, pelites and conglomerates		

Table A.2 Label of land uses (CREAF)

Dig. Cod.	Description	Dig. Cod.	Description	Dig. Cod.	Description	Dig. Cod.	Description
202	Jails	1	Roads	205	Farms	84	Stones
218	Resorts	124	Bushes	209	Streams	73	Airports
105	Railroads	19	Vineyard	85	Widenings	147	Campsites
142	Urban Parks	231	Cemeteries	70	Sport zones	173	Olive forests
187	Town center	69	Golf Courses	127	Burned areas	152	Greenhouses
103	Urbanizations	25	Industrial zone	108	Road parklands	188	Other buildings
48	Cultural centres	138	Isolated houses	97	Beaches (5-20% cc)	233	Pine Plantations
148	Urban reservoirs	113	Natural channels	190	Religious centres	185	Non citrus Orchard
6	Beech (> = 20% cc)	12	Buffer strip of oak	87	Artificial Channels	226	Recreational Par.
186	Poplar Plantations	193	Isolated Industries	177	Terraced vineyards	134	Banana Plant.
101	Holm oak (5-20% cc)	216	Fir tree (> = 20% cc)	128	Railway greenzones	33	Car service areas
180	Crop transformations	118	Red pine plantations	192	Tree forests (5-20% cc)	4	Holm oak (> = 20% cc)
64	Single Family Houses	194	Thermal power plants	230	Regeneration Pinnace	107	Reservoirs (dams etc.)
37	Health care structures	82	Black pine plantations	68	Educational structures	184	Tree Forests (> = 20% cc)
189	White pine plantations	207	Unbuilt urban soils	52	Bushes for firewall uses	119	Meadows and grasslands
11	Mineral extractions zone	227	Family garden	15	Deciduous riparian forests	7	Sewer system plants
191	Lakes and inland lakes	223	Pine plantations	88	Electricity infrastructures	129	Administrative buildings
28	Pubescent oak (5-20% cc)	126	Motorways and highways	117	Regeneration of oak leaves	83	Riparian scrub formations
143	Buffer strip of white pine	178	Abandoned crops - forests	229	Industrial zones (irregular)	125	Arrhenatherion meadows
157	Barns from agricultural use	156	Abandoned fields - scrubs	198	Stones in steep slopes	23	Plowing agricultural zones

71	Naked soils for firewall uses	9	Pubescent oak (> = 20% cc)	141	Other deciduous (5-20% cc)	93	Regeneration of white pines
132	Colonies and isolated towns	135	Agricultural water reservoirs	45	Telecommunication towers	104	Other deciduous (> = 20% cc)
22	Shopping centres and offices	151	Sewage and water treatment plants	44	Scrub slices from everywhere	214	Olive plant. on terraces
41	Other crops on irrigated zones	26	Other arable crops on terraces	222	Vegetation of inland wetlands	120	Anthropogenical soil erosion
80	Regeneration of pubescent oak	17	Urban areas under construction	183	Earthworks and soil movements	181	Regeneration of evergreen oaks
3	Red pine forest (>=20% cc)	20	Red pine forest (5-20% cc)	66	Plantations of non-native conifers	114	Non-citrus fruit in irrigated zones
111	Large oak leaf forest (> = 20% cc)	31	Black pine forest (5-20% cc)	27	Pine forest(5-20% cc)	94	Whtie pine forest (5-20% cc)
5	Pine forest (> = 20% cc)	212	Stone pine Forest (5-20% cc)	86	White pine forest (> = 20% cc)	78	Tiny oak leaf forest (5-20% cc)
89	Stone pine forest (> = 20% cc)	95	Mediterranean pine forest (> = 20% cc)	201	Tiny oak leaf forest (> = 20% cc)	42	Non-citric fruit plantations on terraces
179	Black pine forest (> = 20% cc)	182	Meadows and high mountain grasslands	219	Meadows and grasslands for firewall uses	215	Abandoned fields - meadows in forest areas
217	Meadows and grasslands from everywhere	211	Abandoned vineyards - meadows in agricultural areas	106	Abandoned olive plants - meadows in agricultural areas	203	Other arable crops abandoned - meadows in agricultural areas
206	Abandoned non citric fruit zones - meadows in agricultural areas	199	Other abandoned herb crops - grassland in agricultural areas on terraces	224	Other non-irrigated arable crops watered abandoned - meadows in agricultural areas		

Appendix B (The Llobregat and Arenys de Munt data quality control analysis)

According to subchapter 2.4, in which the quality control has been defined in order to improve the input data for the developed methodologies, the following drawbacks in the hydrometeorological series of precipitation, river flow discharge and temperature data series were observed:

1. The length of the data time series for different locations is variable because the data were lost, were not valid or simply were not registered for that time instant.
2. Different seasons show significant changes of orders of magnitude for the variable values. This behaviour is described in subchapter 2.4.
3. The EDA has shown unusual data such as high discharge flow values without any perceptible rainfall in the basin, or without correlation with other stations. (These kinds of errors were few and occasional).
4. There are some time intervals in the series which illustrate constant flow discharge.

The analysis conducted for the drought and flood risk assessment implies assessing some indexes and hydrologic parameters that univocally depend on the quality and length of the hydrometeorological data series. In order to fulfil this requirement, it was decided to complete as much as possible the missing values. The criteria established to correct the missing values, sudden jumps and the periods of constant discharge in the data series are:

a. The rainfall data series have not been completed and their length has been taken as an indicator of where the discharge flow and temperature data series need to be

completed (for this geographical location), ensuring the same length and number of elements.

b. The errors defined in section 2.4 for a maximum of 15 consecutive days in a temperature or discharge flow data series have been corrected by removing the wrong data and running the interpolation program.
c. No more than 36 days (or data) for hydrologic year in the series (10% of the data) were interpolated, in order to not include artificial behaviours in the analysis.
d. Errors longer than 15 consecutive days were removed from the analysis.
e. The elimination of an entire season depends on the start and the end of the hydrologic year.

B.1 Interpolation of the temperature data series

There are different methods to complete hydrological series, from physical models to probabilistic models simulations. A good "meteorological drought" analysis requires long enough precipitation and temperature data series to fulfil some requirements implicit in the applied methods.

The temperature data series behaviour (spatially speaking) is less random than the rainfall data series. In fact, the measured temperature in two towns with 2 km of separation could be practically the same. However, if in one of them the pluviometers are registering rainfall, it does not imply that the other one will be measuring rainfall too. Consequently, it is possible to affirm that depending on the precision and scale of the required data, an extrapolation can be run to

complete missing data or outliers. This extrapolation would be inconceivable for precipitation data.

The procedure executed includes the following steps:

i. Construct a correlation matrix between all temperature stations for each time interval.
ii. All stations which have a counterpart in the series data are marked. This means, which stations have the same day, month and year a temperature value of the missing value in the station to complete. Otherwise, it ignores the series of this station.
iii. Choose the stations with a correlation higher than 0.9 to interpolate the series to complete. Additionally, limit to a distance of 50 km, the maximum distance between stations.
iv. The last step is the extrapolation of data using a linear equation (1.12). This equation is easily deduced from the ideal gas equation, using atmospheric pressure.

Assuming that there is not a very high variation in height (less than 4000 m) and without taking into account variations in atmospheric pressure between stations, a linear expression for the correction of the temperatures is obtained. If the pressure variable is included, the following procedure has to be done:

Figure B.1 Free body diagram of an atmospheric layer in static equilibrium

From Figure B.1, if a balance of forces is made, the following expressions are derived:

$$\sum F_y = \left[-P\left(y+dy\right)+P\left(y\right)\right]A - mg\left(n_m A dy\right) = 0 \tag{B.1}$$

$$\frac{P\left(y+dy\right)-P\left(y\right)}{dy} = -n_m mg \tag{B.2}$$

$$\frac{dP}{dy} = -n_m mg \tag{B.3}$$

Where: $P=$ analysed layer pressure; $dy=$ elevation increment; $n_m = \frac{N_m}{V_l} =$ number of molecules per unit volume; $m=$ mass of the considered layer and $g=$ constant of gravity. Following, if it is considered that the ideal gas equation is satisfied:

$$PV_l = N_m kT \tag{B.4}$$

$$P = n_m kT \tag{B.5}$$

Where: $N_m =$ number of molecules; $k=$ Boltzmann constant; $V_l =$ layer volume and $T=$ temperature. Solving (B.3) with (B.5) the following equation is obtained:

$$\frac{dP}{dy} = -P\frac{mg}{kT} \tag{B.6}$$

Integrating along the height and pressure:

$$\int_{P_0}^{P} \frac{dp}{P} = -\frac{mg}{kT} \int_{0}^{y} dy \tag{B.7}$$

$$P = P_0 . e^{-\frac{mgy}{kT}} \tag{B.8}$$

And if it is supposed that temperature decreases lineally (the lineal atmosphere hypothesis):

$$T = T_0 - ay \tag{B.9}$$

$$\int_{P_0}^{P} \frac{dp}{P} = -\frac{mg}{k} \int_{0}^{y} \frac{dy}{(T_0 - ay)} \tag{B.10}$$

$$P = P_0 \left(\frac{T_0 - ay}{T_0} \right)^{\frac{mg}{ka}} \tag{B.11}$$

From equation (B.11) with the pressure and temperature you can adjust the constant a, which is the height correction constant. Generally, in the case studies little spatial atmospheric pressure information was available. For this reason, the lineal atmosphere hypothesis has been taken in the places and years without information. The equation (B.12) was obtained for the Llobregat case study:

$$T_e = T_0 - 0.0117 * y \tag{B.12}$$

Where: $T_e =$ temperature in the station without data (Data series to complete); $T_0 =$ temperature in the station with available data and $y =$ elevation difference between both stations. The verification of this method was performed by cross validation, in which random data are removed for a given year in a real data series, and then, using the methods described above, they are extrapolated. At the end, the generated values are compared with the original data. The correlation matrix of the generated data with respect to the real data, shows that the method

reproduce properly the temperature fields. Table B.1 and Table B.2 display the real temperatures and the generated ones for Bagà station.

Table B.1 Six random years of real temperature data in Bagà station

Temperature in Fahrenheit (Bagà)												
Year	Jan	Feb	Mar	Apr	May	Jun	Jul	Aug	Sep	Oct	Nov	Dec
1990	40.3	48.7	48.7	47.1	59.1	64.0	72.2	71.7	65.7	55.9	43.3	35.6
1991	38.3	38.0	47.7	46.4	51.6	63.5	72.2	75.0	66.7	51.6	43.9	41.1
1992	38.0	41.8	45.9	51.9	59.7	57.6	69.0	71.5	62.9	51.4	50.4	42.2
1993	42.0	41.2	45.5	50.2	56.8	66.0	68.2	70.6	61.7	52.0	44.2	40.8
1994	40.4	44.0	53.0	50.0	59.4	67.6	76.6	76.1	63.4	56.9	52.2	44.2
1995	42.7	48.0	48.0	53.6	58.5	62.3	72.5	69.8	60.2	60.4	49.8	44.0

Table B.2 Extrapolation of 6 years of temperature data in Bagà station

Temperature in Fahrenheit (Bagà)												
Year	Jan	Feb	Mar	Apr	May	Jun	Jul	Aug	Sep	Oct	Nov	Dec
1990	39.8	47.5	47.7	48.5	57.8	63.1	69.3	69.1	63.9	55.0	44.5	36.9
1991	39.0	39.4	47.7	47.4	51.4	62.3	68.6	70.1	63.8	50.8	43.8	40.1
1992	35.8	40.3	45.3	49.9	57.5	57.4	66.0	68.6	61.1	50.8	47.4	40.3
1993	39.3	40.4	44.4	49.6	55.8	63.5	66.3	68.3	59.8	50.6	44.0	40.9
1994	39.5	41.8	49.1	48.8	57.7	64.8	71.7	71.2	60.7	54.2	49.2	41.4
1995	39.7	44.7	45.1	50.0	56.1	60.2	68.6	66.6	58.1	56.7	46.9	42.5

Table B.3 Month correlation matrix between real data and extrapolated values

Correlation matrix between real and extrapolated data series (Bagà Station)													
	Year	Jan	Feb	Mar	Apr	May	Jun	Jul	Aug	Sep	Oct	Nov	Dec
Year	1.00	0.62	0.17	0.24	0.80	0.31	0.19	0.25	-0.16	-0.85	0.57	0.70	0.85
Jan	0.15	0.67	0.40	0.43	-0.29	-0.17	0.81	0.48	0.08	0.04	0.57	-0.35	-0.19
Feb	-0.12	0.44	0.94	0.26	-0.01	0.49	0.10	0.27	-0.35	-0.02	0.69	-0.14	-0.51
Mar	-0.28	-0.36	0.02	0.84	-0.61	-0.11	0.47	0.83	0.87	0.69	0.14	0.07	-0.11
Apr	0.60	0.47	0.36	-0.32	0.91	0.70	-0.36	-0.40	-0.72	-0.91	0.26	0.50	0.36
May	0.18	0.25	0.66	0.26	0.43	0.98	-0.03	0.09	-0.26	-0.39	0.35	0.46	-0.07
Jun	-0.02	0.34	0.04	0.57	-0.53	-0.18	0.98	0.51	0.48	0.28	0.15	-0.30	-0.20
Jul	0.16	0.12	0.34	0.97	-0.26	0.09	0.64	0.98	0.66	0.28	0.59	0.27	0.12
Aug	-0.34	-0.55	-0.40	0.62	-0.64	-0.21	0.45	0.54	0.94	0.69	-0.32	0.04	-0.04
Sep	-0.93	-0.68	-0.22	0.08	-0.92	-0.41	0.00	0.09	0.48	0.98	-0.46	-0.58	-0.70
Oct	0.37	0.57	0.90	0.52	0.30	0.47	0.18	0.58	-0.19	-0.29	0.97	0.29	0.04
Nov	0.60	0.00	0.26	0.60	0.60	0.66	-0.05	0.53	0.25	-0.40	0.44	0.97	0.67
Dec	0.91	0.36	-0.21	0.06	0.71	-0.01	0.04	0.10	-0.05	-0.72	0.28	0.63	0.95

In Table B.3 the displayed correlation values are very high. With this, it can be concluded that the generated values can be accepted.

B.2 Flow discharge data extrapolation:

In order to homogenize the flow discharge data series, an algorithm has been developed, which completes the missing flow discharge values in the data series. To perform this extrapolation, it follows almost all the steps of the previous criteria. A maximum of 15 consecutive and not more than 36 data values per year are extrapolated. The daily data is chosen as the smallest time scale because the information used before the 1996 year are available only in this format. For dates after the 1996 year 5 minutes data resolution is available.

The algorithm for discharge flow extrapolation is quite similar to the temperature method. The main difference consists in not taking into account the station elevation correction that is performed in the temperature algorithm. As well, the correlation range that exists between the station to complete and the station with the discharge flow can be lower than 0.9. Otherwise, this would be a very strict criterion for the discharge flow interpolation.

The procedure that follows the algorithm for extrapolation of discharge flow values is defined as follows:

1. To establish a correlation matrix for the values of flow in the series for all available stations.
2. All the stations that have a data series value for the same day, month and year of the station to complete are identified. the rest are ignored.
3. The stations with the best correlation value with respect to the incomplete one are chosen.
4. For each hydrological year, no more than 15 data series values and no more than 36 values per hydrologic year are extrapolated.
5. The extrapolated values for each of the 6 series with the highest correlation with the station to be interpolated are assessed with the equation (B.13) . Note: A total number of 6 stations to interpolate the values over the incomplete data series were chosen, without following any specific law/rule.
6. Finally, the extrapolated value is the average of the 6 discharge flow values described in the equation (B.14).

$$Q_i^{c|j} = Q_{i-1}^c + \left(Q_{i-1}^c - Q_{i-2}^c\right) / \left(Q_{i-1}^j - Q_{i-2}^j\right) * \left(Q_i^j - Q_{i-1}^j\right) \quad \text{(B.13)}$$

$$Q_i^c = \left(Q_i^{c|1} + Q_i^{c|2} + Q_i^{c|3} + Q_i^{c|4} + Q_i^{c|5} + Q_i^{c|6}\right)/6 \quad \text{(B.14)}$$

Where: $Q_i^{c|j} =$ extrapolated discharge flow due to the j correlated station; $Q_i^c =$ discharge flow in the station to complete in the i time position and $Q_i^j =$ discharge flow from the station which has the j higher correlation position value in the i time position. This equation shows that the flow discharge assessment of a data series requires a minimum of two values. These correspond to the $i-1$ and $i-2$ interval. When there are no gaps left in the series, the values to extrapolate

start to depend on the previously generated values. The proposed algorithm is a smoothing stochastic model which consists in a linear extrapolation method (Pena D. 2005).

Appendix C Integral Scale

An important characteristic of the PDSI index is its self-recursiveness, because the present value of the index depends on its past, as is shown in equation (C.1). This means that it preserves the history implicit in the data series behaviour, which makes it conceptually considered as an autoregressive model of order 1. As an autoregressive model, it is possible to find with the integral scale theory the number of significant past intervals which affect the present value of the index. To find the number of time intervals, proceed as follows:

From Palmer index:

$$X_{i+1} = aX_i + bZ_i \tag{C.1}$$

Where X_i (the present PDSI index) is known as the stochastic variable and Z_i is the innovation on the stochastic model. Developing from past time intervals:

$$X_i = aX_{i-1} + bZ_{i-1} \tag{C.2}$$

$$X_{i-1} = aX_{i-2} + bZ_{i-2} \tag{C.3}$$

From (C.2) in (C.1):

$$X_{i+1} = a\left(aX_{i-1} + bZ_{i-1}\right) + bZ_i \tag{C.4}$$

$$X_{i+1} = a^2 X_{i-1} + b\left(aZ_{i-1} + Z_i\right) \tag{C.5}$$

From (C.3) in (C.5):

$$X_{i+1} = a^2\left(aX_{i-2} + bZ_{i-2}\right) + b\left(aZ_{i-1} + Z_i\right) \tag{C.6}$$

$$X_{i+1} = a^3 X_{i-2} + b\left(a^2 Z_{i-2} + aZ_{i-1} + Z_i\right) \tag{C.7}$$

This leads to:

$$X_{i+1} = a^n X_{i-(n-1)} + b\left(Z_i + aZ_{i-1} + a^2 Z_{i-2} \ldots a^{n-1} Z_{i-(n-1)}\right) \tag{C.8}$$

If n is very big enough and $a < 1$:

$$X_{i+1} = b\left(Z_i + aZ_{i-1} + a^2 Z_{i-2} \ldots a^{n-1} Z_{i-(n-1)}\right) \quad \text{(C.9)}$$

$$X_{i+1} = b\sum_{j=0}^{j=n-1} a^j Z_{i-j} \quad \text{(C.10)}$$

The previous expression shows that the present PDSI index value is recursively influenced by past information in terms of a^n and b coefficients. If a^n and b coefficients are plotted (Figure C.) with respect to each PDSI innovation value (Z), it can be noted that distant innovations Z_{i-j} have less weighted influences in the present innovation value Z_i.

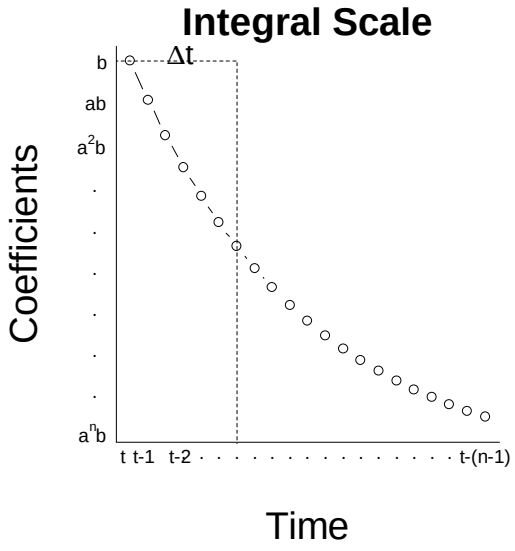

Figure C.1. Integral scale of Palmer index coefficients

In the previous graph, the interval width (Δt), which has to accumulate an area under the curve in Figure C.1 equal to the integral of the function defined in (C.10), depends on the number of intervals to be considered. If the original values of Palmer index are replaced in equation (C.10) with $b = 1/3$ and $a = 0.897$, the same area tends to an asymptotical. In Figure C.2 (left and right)

the asymptotic behaviour can be observed, and the function $f(n) = a^n n = 0.897^n n$ reaches its maximum at 9.19.

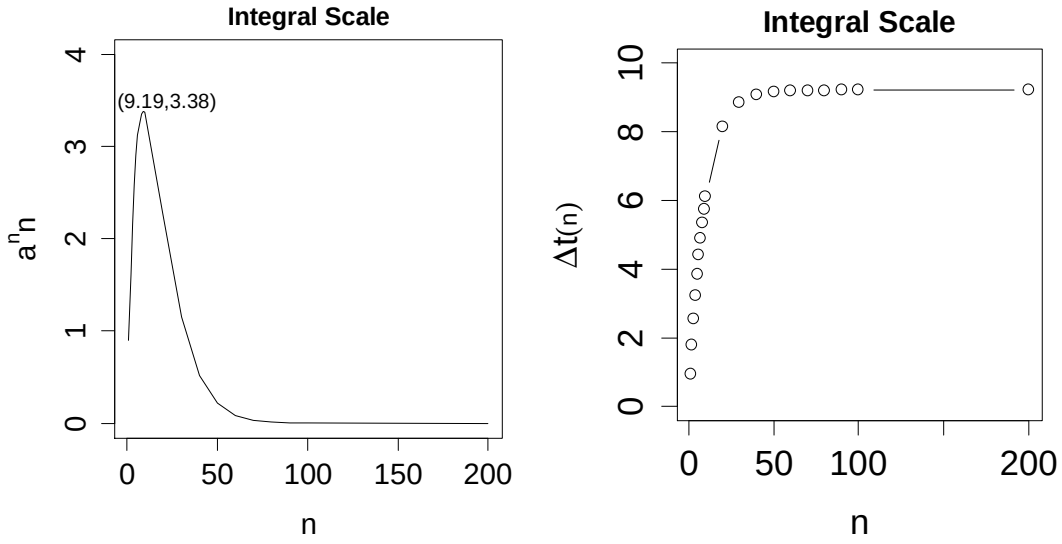

Figure C.2 Interval width Δt by which the a^n and b coefficients will no longer influence the present value

Table C.1 Interval width Δt values of Figure C. (right)

N	Δt	N	Δt
1	0.94756718	20	8.15346467
2	1.79753494	30	8.84686715
3	2.55995602	40	9.08070231
4	3.24384773	50	9.15955822
5	3.8572986	60	9.18615069
6	4.40756402	70	9.19511843
7	4.90115211	80	9.19814261
8	5.34390062	90	9.19916245
9	5.74104604	100	9.19950637
10	6.09728548	200	9.19968136

From Table C.1 it can be concluded that a total of 9.2 previous step intervals have a significant weight on the present innovation index Z_i and, consequently, on the index value X_i.

Appendix D Hydrologic water balance in the PDSI

The PDSI index is defined in terms of its past values and the new weather condition, which in stochastic models is known as innovations, and which W. Palmer called the moisture anomaly (Z), and it is assessed as follow:

$$Z_i = d_i K_i \tag{D.1}$$

Where $Z_i =$ current moisture anomaly; $d_i =$ moisture departure for a particular month ($P - \hat{P}$) and $K_i =$ climatic characteristic factor. If there exists any precipitation deficiency in equation (D.1), the Z_i variable will have negative values and, consequently, the PDSI index X_i (defined in subchapter 1.3.5) will tend to a negative value too.

D.1 Climatic characteristic factor (K):

Initially, the Palmer index was derived from data in some U.S. regions. Later, Wayne Palmer proposed a corrective factor in his index in order to make it operational and to be able to apply his index in different regions than the original one. This coefficient is recognized as the climatic characteristic factor K .

$$K_i = \frac{17.67}{\sum_{j=1}^{12} \overline{D_j} K'_j} K'_j \tag{D.2}$$

Where $K_i =$ current climatic factor; $K'_j =$ climatic characteristic weighting factor computed for each month of the year and $\overline{D_j} =$ monthly mean of the absolute values of d .

K'_j is assessed through the following equation:

$$K'_i = 1.5 \log_{10} \left[\frac{\frac{\overline{PET}_i + \overline{R}_i + \overline{RO}_i}{\overline{P}_i + \overline{L}_i} + 2.8}{\overline{D}_i} \right] + 0.5 \qquad \text{(D.3)}$$

Where $\overline{PET}_i =$ mean potential evapotranspiration; $\overline{R}_i =$ mean recharge of subsoil layers (2 discretised layers); $\overline{RO}_i =$ mean runoff; $\overline{P}_i =$ mean precipitation; $\overline{L}_i =$ mean losses in both layers and $\overline{D}_i =$ mean absolute values of d_i. In the previous equations it can be observed that the climatic factor K is defined in terms of the particular history of the station location, making an average until the final time step i (current date of calculation).

D.2 The moisture departure (d):

The moisture deficiency or excess is the balance between the atmospheric water demand and supply, assessed with equation (D.4).

$$d = P - \hat{P} \qquad \text{(D.4)}$$

Where $P =$ precipitation and $\hat{P} =$ CAFEC precipitation (Climatically Appropriate for Existing Conditions). In other words, d is the relation between the precipitation and the required atmospheric water demand. $\hat{P}$ can be assessed through the following expression:

$$\hat{P} = \alpha_i . PET_i + \beta_i . PR_i + \gamma_i . PRO_i - \delta_i . PL_i \qquad \text{(D.5)}$$

The i subscript refers to the specific month of the year (if monthly scale is analysed), and coefficients α_i, β_i, γ_i and δ_i are the average between the variables used to calculate the water balance and they are assessed as follows:

$$\alpha_i = \frac{\sum_{Lon.Serie} ET_i}{\sum_{Lon.Serie} PET_i} \quad \beta_i = \frac{\sum_{Lon.Serie} R_i}{\sum_{Lon.Serie} PR_i}$$
$$\gamma_i = \frac{\sum_{Lon.Serie} RO_i}{\sum_{Lon.Serie} PRO_i} \quad \delta_i = \frac{\sum_{Lon.Serie} L_i}{\sum_{Lon.Serie} PL_i} \tag{D.6}$$

To assess the variables exposed in Table 1.2 (PET, PR, PRO, RO, L, Ss, Su, PL, ET and R_c) 4 input data are used: the precipitation data series, the temperature data series, the station latitude to make a spatial correction with the geographic position in the evapotranspiration and, finally, the AWC. To assess the potential evapotranspiration (PET), Palmer recommends the Thornwhite method. The potential variables are calculated with the following expressions:

$$PR = AWC - (Su + Ss) \tag{D.7}$$
$$PRO = AWC - PR = AWC - (AWC - (Su + Ss)) = Su + Ss \tag{D.8}$$
$$PET = Thornwhite\ Method \tag{D.9}$$

The potential losses (PL) depend on the potential evapotranspiration, which leads to 2 different options:

1. If the moisture present in the superficial subsoil layer (Ss) is enough to cover the potential evapotranspiration of the atmosphere $Ss >= PET$:

$$PL = PET \quad \text{(D.10)}$$

2. If the moisture present in the superficial subsoil layer (Ss) is not enough to cover the potential evapotranspiration of the atmosphere $Ss < PET$ (only a fraction of the moisture in the under-layer is lost):

$$PL = \left(\left(PET - SS \right) * Su / AWC \right) + Ss \quad \text{(D.11)}$$

Note: This expression is restricted to the potential losses not being higher than the total moisture of the soil $Su + Ss$ defined as (PRO). If $PL > PRO \rightarrow PL = PRO$ $PL > PRO \therefore PL = PRO$.

D.3 Water balance (hydrologic model in the PDSI):

After obtaining the potential variables equations (PET, PL, PR and PRO), the current values of ET , L , R_c and RO are evaluated. These variables are assessed by means of some roles proposed by Wayne Palmer, making a balance between P , PET and the soil moisture. Here is where the 2 subsoil layer model proposed by Palmer is manifest. In the superficial layer a minimum storage 1 inches of water (moisture) is supposed, which is used when demand is higher than supply and is the first layer to be recharged when the situation is contrary. The deepest layer can store a maximum of ($AWC - 1.0$) inches of water (if the superficial layer is only storing 1.0 inches). Likewise, it is assumed that only a part of moisture in the deepest layer can be suddenly removed. Considering the possible cases in both subsoil layers, the water balance leads to different options:

1. If $P >= PET$, there exists enough precipitation to cover the atmospheric water demand:

$$ET = PET \quad \text{(D.12)}$$

$$L = 0 \tag{D.13}$$

1.1. If $(P - PET) > (1.0 - Ss)$: There is enough precipitation to recharge both layers.

$$Rs = (1.0 - Ss) \tag{D.14}$$

A. If $(P - PET - Rs) < ((AWC - 1.0) - Su)$: The available water after PET requirement and subsoil layer recharge is totally taken in the deepest layer (under-layer), thus there is no runoff.

$$Ru = (P - PET - Rs) \tag{D.15}$$

$$RO = 0 \tag{D.16}$$

B. If $(P - PET - Rs) >= ((AWC - 1.0) - Su)$: There is enough water to cover the atmospheric water demand, recharge both layers, and it will produce runoff.

$$Ru = ((AWC - 1.0) - Su) \tag{D.17}$$

$$RO = (P - PET - (Rs + Ru)) \tag{D.18}$$

Note: Total recharge is $R_c = Rs + Ru$

1.2. If $(P - PET) <= (1.0 - Ss)$: There is only enough water moisture to recharge the superficial layer.

$$R_c = (P - PET) \tag{D.19}$$

Note: $R_c = Rs$

2. If $P < PET$: There is not enough precipitation to cover the atmospheric water demand (PET) and subsoil water moisture will be lost. No runoff and recharge is expected

$$R_c = 0 \tag{D.20}$$

$$RO = 0 \tag{D.21}$$

2.1.1. If $Ss > (PET - P)$: The superficial soil layer is able to cover the part of water demand (PET) that precipitation has not covered, thus, only superficial layer will experiment losses.

$$Ls = (PET - P) \tag{D.22}$$

$$Lu = 0 \tag{D.23}$$

2.1.2. If $Ss <= (PET - P)$: The superficial soil layer is not able to cover the part of water demand (PET) that precipitation has not covered, thus, part of the under-layer moisture will be lost.

$$Ls = Ss \tag{D.24}$$

$$Lu = (PET - P - Ls) * Su / AWC \tag{D.25}$$

Note: Where the total losses in the second case are $L = Ls + Lu$, the actual evapotranspiration is assessed as the precipitation plus the moisture losses $ET = P + L$. It is important to notice that PDSI index never makes the under-layer instantaneously drier.